5-2016

In Vivo Kinome Screen Reveals Non-Canonical Cdk-Driven Metabolic Adaptation In Brain Metastasis

Frank J. Lowery III

IN VIVO KINOME SCREEN REVEALS NON-CANONICAL CDK-DRIVEN METABOLIC ADAPTATION IN BRAIN METASTASIS

by

Frank Joseph Lowery III, BS

APPROVED:

_____

Dihua Yu, MD, PhD
Advisory Professor

_____

Lee M. Ellis, MD

_____

Isaiah J. Fidler, DVM, PhD

_____

Mien-Chie Hung, PhD

_____

Pierre D. McCrea, PhD

APPROVED:

_____

Dean, Graduate School of Biomedical Sciences
The University of Texas Health Science Center at Houston

IN VIVO KINOME SCREEN REVEALS NON-CANONICAL CDK-DRIVEN METABOLIC ADAPTATION IN BRAIN METASTASIS

A

DISSERTATION

Presented to the Faculty of

The University of Texas

Health Science Center at Houston

and

The University of Texas

MD Anderson Cancer Center

Graduate School of Biomedical Sciences

in Partial Fulfillment

of the Requirements

for the Degree of

DOCTOR OF PHILOSOPHY

by

Frank Joseph Lowery III, B.S.

Houston, Texas

May, 2016

Dedication

To Mom-you are my daily inspiration. I am sorry that the work described herein did not do anything to help you, but I hope the experience I got while performing it allows me to help other mothers be there for their kids, just like you were for us.

Acknowledgements

Thank you to Dr. Dihua Yu for your mentorship and guidance throughout my doctoral training, I am thankful to have you as my tiger mom. I really appreciate the exposure to the ins and outs of the cancer research system that you have given me over the years.

To the past and present members of the Yu lab team, thank you for all of our insightful discussions regarding both science and life, as well as your technical guidance and training (and patience) so crucial for someone who came here as raw as me. Special thanks to my fellow graduate students Sunil Acharya, Tina Chang, Dr. Brian Pickering, and Dr. Sumaiyah Rehman for your commiseration; five-hour lab meetings were made more tolerable by our Chipotle-fueled discussions afterward. Finally, a great deal of gratitude goes to Yong Xia, who worked so hard in support of this project during his time in the Yu lab.

To Dr. Patrick Zhang, thank you for everything. From the first day of my rotation, I've enjoyed the privilege of working with you and getting to pick your brain on everything under the sun. From teaching me how to perform the intracarotid injection procedure to challenging my knowledge on seemingly every topic in U.S. history, our time together has been unforgettable. From one person with their head in the cloud to another, I will always appreciate our time together and the unique perspectives you have shared with me.

To my committee members, Drs. Josh Fidler, Mien-Chie Hung, Lee Ellis, and Pierre McCrea, thank you for your wisdom and guidance over the years. I especially appreciate Dr. Ellis for being my advocate even when the rest of the crowd was pretty tough, and Dr. McCrea, a philosopher in the truest sense of the word.

To the wonderful ladies of METAvivor, thank you for supporting my work the last two years. I appreciate you all for your extraordinary efforts to raise funding and awareness for metastatic

breast cancer research, all while fighting for your lives. CJ, Beth, and Leslie: I love you all and you are an inspiration.

To all my Houston friends, grad school classmates, softball and trivia teammates, and everyone else, thanks for all of our fun times together, as well as for the times that you let me lean on you when things were not going so well. Tim: thanks for everything buddy. I might have missed my chance to hang with you in college but we made up for it here. It is actually hard to imagine life if you had not come to Houston when you did; fortunately I do not have to.

To my brothers, Liam and Patrick Lowery, thank you for all of your love and support while I have been in Texas. I am sorry for being such an absentee brother for so many years and I really appreciate you for understanding and picking up my slack. You guys were there for Mom and Dad when they needed it and I was unable to be there, and I am forever grateful for that. I am so proud of you and love you both.

To my fiancée, Dr. Caitlin May, you make my coming to GSBS worthwhile since that is what it took for us to meet. Thank you for always supporting me in everything, most of all the editing of this dissertation. You are my soulmate and I have had a wonderful two (only two?) years with you. I love you and I cannot wait for the rest of our life together.

To my parents, Frank and Michele Lowery, thank you for being the most loving and supportive parents anyone could ask for. I know you are proud of me, but even better than that, I know you love me no matter what. Mom: you were the most caring mother in the world and you would have done anything for your kids. Given the hand you were dealt, you easily could have turned into a bitter me-me; you worked so hard to give us a normal childhood while fighting for your life for so many years. Have no fear; I'll never forget my divinity. I love you and I miss you, but I know you are always with me. Dad: I couldn't have picked a better role model for how to be a husband or father even if I had a say in it. You have always taken care of Mom and us kids and put us first in your life without a question. Even after seeing you pull it off, it is still incredible

how you were able to always be there for our family when you worked so hard defending our country. Whenever I waited until the last minute to do my homework, or if I did not quite master the lesson that day in math, you were always ready to stay up late until the job was done. Reflecting back on it, those times you were patient with me until the lightbulb went on and I finally got it were what gave me the confidence to know I can do anything. If you had just said ‘good enough’ before it actually was, we could have both gotten a lot more sleep, but where would I be now? I appreciate my natural talents, but I appreciate you more for teaching me to get the most out of them. Thanks to you, I know I can do anything if I want it badly enough and do it the right way. I love you and I am proud of you.

IN VIVO KINOME SCREEN REVEALS NON-CANONICAL CDK-DRIVEN METABOLIC ADAPTATION IN BRAIN METASTASIS

Frank Joseph Lowery III, BS

Advisory Professor: Dihua Yu, MD, PhD

Brain metastasis, which frequently arises from breast cancer, lung cancer, melanoma, and colorectal cancer, remains a severely unmet medical need and its incidence continues to rise while treatment options remain palliative. To better understand the biology underlying its aggressive, incurable nature, I performed an unbiased *in vivo* kinome screen to identify potential driver kinases of experimental brain metastasis in a nude xenograft model using the human breast cancer cell line MDA-MB-231. Several of the kinase pools led to decreased brain metastasis-specific survival in nude mice, shortening survival time by up to 50% relative to controls. Targeted next-generation sequencing (NGS) was performed to analyze pre- and post-injection MDA-MB-231 cells, thus identifying 31 kinases that were significantly enriched in multiple animals. To validate the clinical relevance of these potential targets, kinase expression was analyzed in a collection of 32 clinical breast cancer, lung cancer, and melanoma brain metastases by RNA sequencing (RNA-seq); all but two of the kinases were expressed in brain metastases from all three types of primary tumor. Based on its enrichment *in vivo* and high expression in brain metastasis across cancer types, I chose to focus on PCTK1 as a potential driver. PCTK1 is expressed during spermatogenesis and neuronal differentiation but reports of its roles in cancer are limited. While overexpression of PCTK1 in MDA-MB-231 cells did not affect proliferation under routine cell culture conditions, it led to a faster rate of brain metastasis

growth and thereby decreased mouse survival time by 75%. The Cancer Genome Atlas (TCGA) data analysis revealed a potential link between PCTK1 expression and glutamine metabolism and I demonstrated that the growth advantage conferred by PCTK1 was due to increased glutamine consumption by the cancer cells. Knockdown of PCTK1 in the brain metastatic HCC1954Br breast cancer cell line increased mouse survival time in an experimental brain metastasis model, indicating that PCTK1 may indeed represent a potential therapeutic target for brain metastasis. In conclusion, this study identified PCTK1 as a novel driver of brain metastasis and exposed a means of cancer cell survival in the nutrient-restricted brain.

Table of Contents

List of Illustrations

List of Tables

List of Abbreviations

18-FDG: ^{18}F-deoxyglucose

ACS: American Cancer Society

ASNS: asparagine synthetase

ATCC: American Type Culture Collection

BBB: blood-brain barrier

bFGF: basic fibroblast growth factor

BLAST: Basic Local Alignment Search Tool

BM: basement membrane

BME: Basal Medium Eagle

BSA: bovine serum albumin

CCNY: cyclin Y

CDK: cyclin-dependent kinase

cDNA: complementary DNA

CML: chronic myelogenous leukemia

COX2: prostaglandin-endoperoxide synthase 2

CRC: colorectal cancer

CSF: cerebrospinal fluid

CT: computed tomography

Ct: cycle threshold

CTC: circulating tumor cell

CUP: cancer of unknown primary

DCIS: ductal carcinoma in situ

DMEM: Dulbecco's Modified Eagle Medium

EAAT: excitatory amino acid transporter

ECL: enhanced chemiluminescence

ECM: extracellular matrix

EGFR: epidermal growth factor receptor

EOC: epithelial ovarian carcinoma

ER: estrogen receptor

F12: Ham's Nutrient Mixture F12

FACS: fluorescence-associated cell sorting

FasL: Fas ligand

FBS: fetal bovine serum

GABA: γ-aminobutyric acid

GBM: glioblastoma

gDNA: genomic DNA

GFP: green fluorescent protein

GFPT1: glucosamine-fructose-6-phosphate transaminase 1

GLS: glutaminase

H&E: hematoxylin and eosin

HBSS: Hank's Buffered Saline Solution

HER2: human epidermal growth factor receptor 2

HK2: hexokinase 2

HR: hazard ratio

IACUC: Institutional Animal Care and Usage Committee

IBC: invasive breast cancer

IFN-γ: interferon-γ

IHC: immunohistochemistry

IL-1β: interleukin-1β

i.v.: intravenous

IVIS: *In Vivo* Imaging System

LAT1: large neutral amino acid transporter 1

LGG: low-grade glioma

luc: luciferase

MMP: matrix metalloprotease

MOI: multiplicity of infection

MRI: magnetic resonance imaging

mRNA: messenger RNA

MS: mass spectrometry

mTOR: mammalian target of rapamycin

NCI: National Cancer Institute

nCPM: normalized transcript counts per million reads

NeoR: neomycin resistance

NGS: next-generation sequencing

NSF: N-ethylmaleimide-sensitive fusion protein

ORF: open reading frame

PARP: poly-ADP ribose polymerase

PBS: phosphate-buffered saline

PBST: PBS-Tween 20

PCK2: phosphoenolpyruvate carboxykinase 2

PCR: polymerase chain reaction

pCR: pathological complete response

PET: positron-emission tomography

PFKL: phosphofructokinase-liver

PFKM: phosphofructokinase-muscle

PIN: prostate intraepithelial neoplasia

pO_2: partial pressure of oxygen

PR: progesterone receptor

PVDF: polyvinyldifluoride

qPCR: quantitative PCR

RNA-seq: next-generation RNA sequencing

rpm: revolutions per minute

RT-PCR: reverse transcriptase-PCR

SDS-PAGE: sodium dodecosulfate-polyacrylamide gel electrophoresis

SEER: Surveillance, Epidemiology, and End Results database

SERM: selective estrogen receptor modulator

TBS: Tris-buffered saline

TBST: TBS-Tween 20

TCGA: The Cancer Genome Atlas

TdTomato: tandem dimer Tomato

TGF-β: transforming growth factor-β

TNBC: triple-negative breast cancer

TNF-α: tumor necrosis factor-α

TRAIL: TNF-related apoptosis-inducing ligand

USPSTF: US Preventive Services Task Force

UTMDACC: The University of Texas MD Anderson Cancer Center

UV: ultraviolet

VEGF: vascular endothelial growth factor

ZO: zona occludens

Chapter 1: Introduction

1.1 Breast Cancer

1.1.1 Breast cancer epidemiology

Breast cancer is a common and frequently deadly malignancy. In 2016, approximately 246,660 American women will be diagnosed with invasive breast cancer (IBC) and nearly 40,450 women will die of this disease. Breast cancer can occur in men as well, but the incidence and mortality rates are 100 times lower than in women (1). These statistics actually represent improvement over the last 30 years, as early detection and advances in treatment regimens have resulted in the decline of age-adjusted death rates from a peak of greater than 33 deaths per 100,000 women in 1989 to around 21 deaths per 100,000 today. However, it must not be discounted that the gains in survival rates have largely been manifested in early-stage breast cancer, while advanced breast cancer continues to be incurable.

Breast cancer incidence is similar among non-Hispanic white and black women in the United States, although there is a large disparity in mortality rates, with white women at 21.9 deaths per 100,000 and black women at 31 (1). While the reasons for this disparity are unknown, a partial explanation may come from the increased prevalence of the more lethal triple-negative breast cancer (TNBC) within this group (2). Strikingly, Asian-American, Hispanic-American, and Native American women show lower incidence of and mortality due to breast cancer than non-Hispanic white and black women in the United States, although the effect on mortality is almost entirely due to the decreased incidence. These numbers are exemplary of the importance of both genetic and environmental factors in the risk of developing breast cancer.

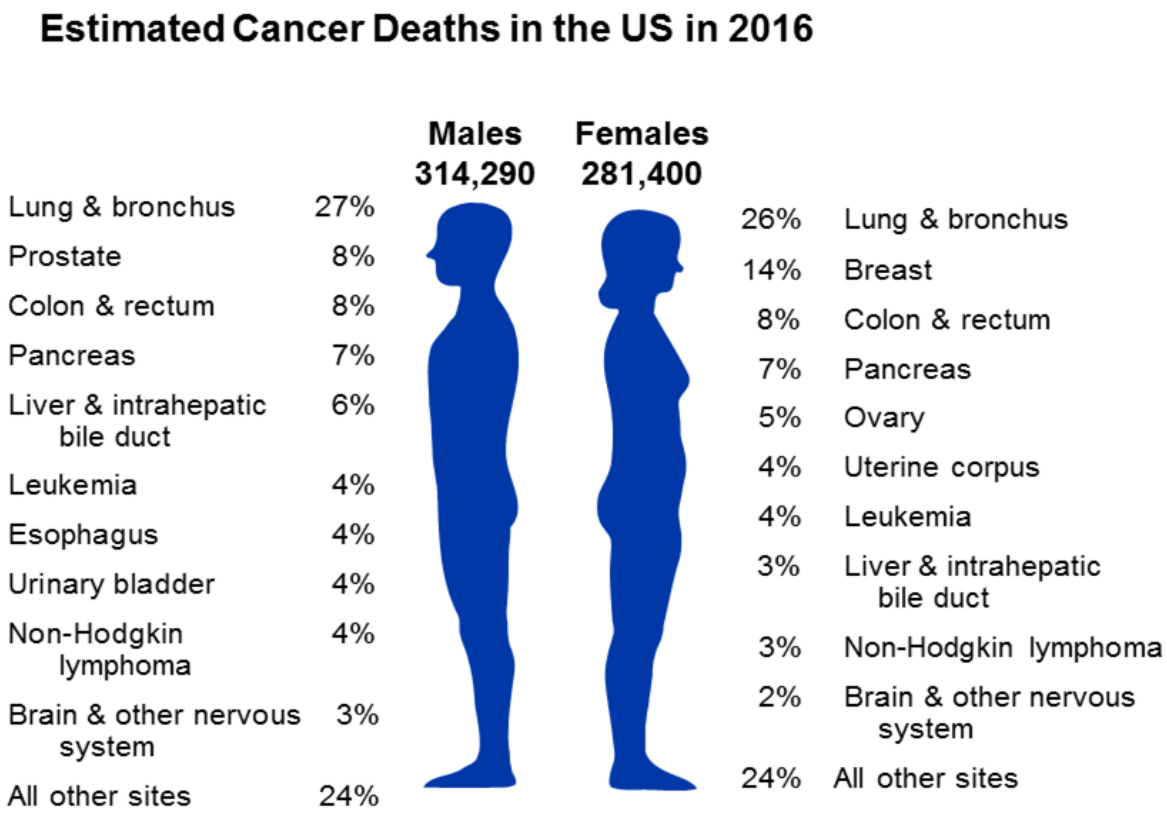

Figure 1. Estimated cancer deaths in the United States in 2016. Breast cancer is the second-leading cause of death among in the United States, behind only lung cancer. *Reprinted with permission from American Cancer Society,* Cancer Facts & Figures 2016.

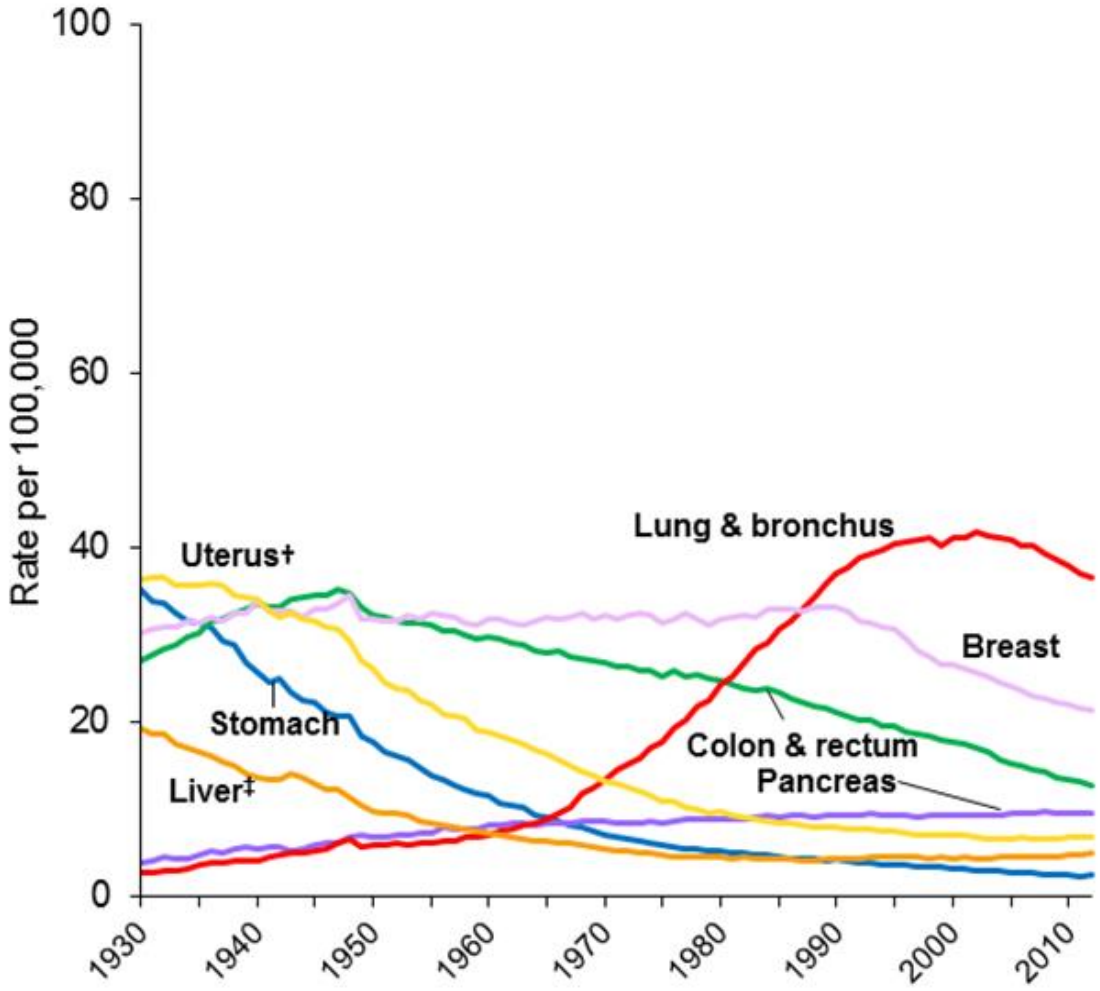

Figure 2. Trends in cancer death rates among females in the United States through 2012. Breast cancer mortality rates have declined since the early 1990s, as the advent of mammograms and targeted therapies led to earlier detection and more effective treatment. Rates are age-adjusted to the United States population in 2000. *Reprinted with permission from American Cancer Society,* Cancer Facts & Figures 2016.

Breast cancer risk rises substantially with age, as both breast cancer incidence and mortality increase after age 60 (3). This risk association with age is not exclusive, however. While younger (<40 years old) women only account for 5% of IBC diagnoses (4), breast cancer was the most common cause of cancer-related deaths in this population in 2011, according to

the latest available statistics. Additionally, breast cancer occurring before the age of 40 is more likely to be associated with genetic mutations in breast cancer susceptibility genes *BRCA1* and *BRCA2* and/or a family history of breast cancer. Therefore, while the majority of breast cancer deaths occur after the age of 50, a substantial number of life-years lost to breast cancer are from those diagnosed at earlier ages.

The differences in age-adjusted breast cancer risks have recently been the focus of a public health controversy in the United States. Namely, while mammograms have been demonstrated to enable earlier detection of breast cancer ((5)) and early detection is known to be a key predictive factor in long-term survival, two leading organizations, the American Cancer Society (ACS) and the US Preventive Services Task Force (USPSTF), have recommended that women of average risk begin regular mammography-based screening at a later age (45 or 50, respectively) instead of the previous guidelines suggesting that screening start at age 40 (6, 7). These decisions were based upon the findings that low number of cancers detected in younger women does not warrant the cost of regular screening, both in terms of health care expenses and the emotional toll of false-positive tests. It will take some time for the results of this change in policy to become apparent, but one would expect that breast cancer incidence (that is, clinically detected breast cancer) may see a decrease in the population of women under 50 years old with a possible concomitant rise in breast cancer mortality rates for the same group.

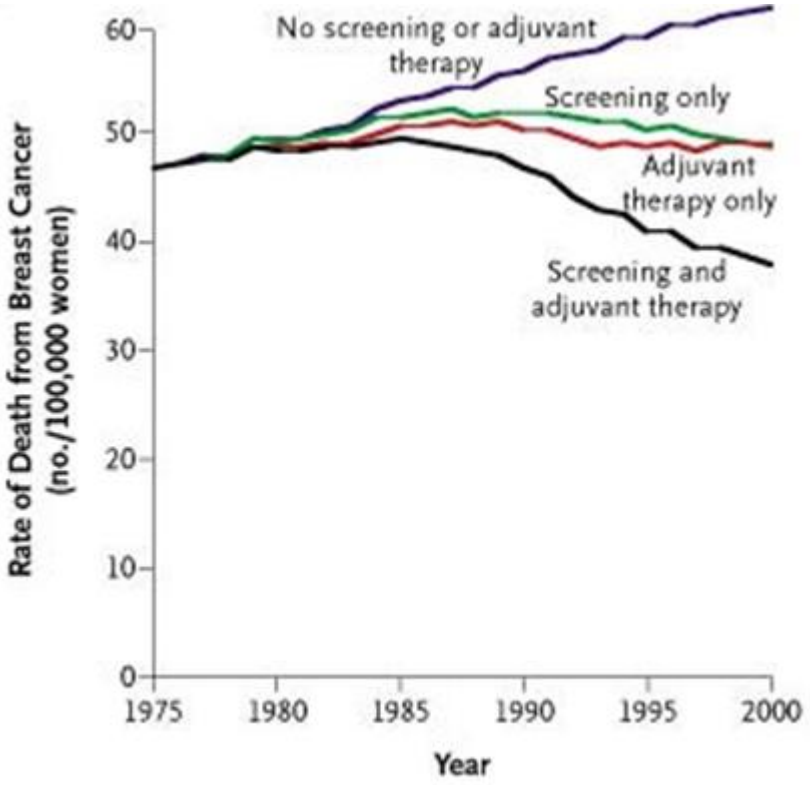

Figure 3. Screening and adjuvant therapy have both decreased the incidence of breast cancer over time. Comparison of models of breast cancer death rates among women age 30-79 with or without inclusion of mammogram and/or adjuvant therapy (tamoxifen, chemotherapy, or both) estimated the lives saved as 25 per 100,000 per year, compared to only 12 for either factor alone. Note that the population considered here is women age 30-79, so the estimated death rate from breast cancer is higher than in previous figures which included the whole female population. *Reprinted with permission from Berry DA, Cronin KA, Plevritis SK, Fryback DG, Clarke L, Zelen M, Mandelblatt JS, Yakovlev AY, Habbema JD, Feuer EJ, Intervention Cancer, & Collaborators Surveillance Modeling Network. "Effect of screening and adjuvant therapy on mortality from breast cancer."* The New England Journal of Medicine. *2005 Oct 27;353(17):1784-92.*

1.1.2 Breast cancer features and clinical characteristics

The stages of breast cancer at diagnosis, which heavily impact treatment options and prognosis, range from Stage 0 to Stage IV. This staging is determined by both the size and spread of the primary tumor. Stage 0 represents carcinoma in situ, in which cancerous cells are found in either the duct or lobe of the breast, but have not invaded into the surrounding tissue. Stage I refers to primary tumors 2 cm or smaller, and, if any tumor cells are found in the nearby lymph nodes, the clusters are 2 mm or less. Stage II encompasses tumors 0-5 cm that have spread to 1-3 axillary lymph nodes, as well as those less than 2 cm that are not detected in the lymph nodes. Stage III represents tumors of any size that have spread to more than 3 axillary lymph nodes, as well as tumors greater than 5 cm that have spread to any lymph nodes. Additionally, cancer that has spread to the skin of the breast or the chest wall is classified as Stage III. Stage IV comprises breast cancer that has spread beyond the breast and lymph nodes and metastasized to bone, lungs, liver, brain, or other organs. (3)

Table 1. Stage-specific breast cancer survival rates in women in the United States.

Stage	5-year relative survival rate
0	100%
I	100%
II	93%
III	72%
IV	22%

Adapted and reprinted with permission from American Cancer Society, Cancer Facts & Figures 2016.

Breast cancer is divided into three main clinical subtypes based on histological and pathological criteria. These subtypes, along with disease stage, dictate the standard of care. The major subtypes are luminal, basal, and HER2, which are classified according to the

expression of 3 cell surface proteins: estrogen receptor (ER), progesterone receptor (PR), and human epidermal growth factor receptor 2 (HER2) (8). General characteristics are included in Table 2.

Table 2. Clinical characteristics of breast cancer subtypes.

Molecular Subtype			
	Luminal	**HER2**	**Basal**
Gene expression pattern	High expression of hormone receptors and associated genes (luminal A>luminal B)	High expression of HER2 and other genes in amplicon Low expression of ER and associated genes	High expression of basal epithelial genes, basal cytokeratins Low expression of ER and associated genes Low expression of HER2
Clinical features	~70% of invasive breast cancers ER/PR positive Luminal B tend to be higher histological grade than luminal A Some overexpress HER2 (luminal B)	~15% of invasive breast cancers ER/PR negative More likely to be high grade and node positive	~15% of invasive breast cancers Most ER/PR/HER2 negative (‘triple negative,’ TNBC) *BRCA1* dysfunction (germline, sporadic) Particularly common in African-American women
Treatment response and outcome	Respond to endocrine therapy (but response to tamoxifen and aromatase inhibitors may be different for luminal A and luminal B). Response to chemotherapy variable (greater in luminal B than in luminal A).	Respond to trastuzumab (Herceptin) Respond to anthracycline-based chemotherapy Generally poor prognosis	No response to endocrine therapy or trastuzumab (Herceptin) Appear to be sensitive to platinum-based chemotherapy and PARP inhibitors

	Prognosis better for luminal A than luminal B.		Generally poor prognosis (but not uniformly poor)

Modified and reprinted with permission from Schnitt SJ. "Classification and prognosis of invasive breast cancer: from morphology to molecular taxonomy." Modern Pathology. *2010 May;23 Suppl 2:S60-4.*

While these molecular subtypes of breast cancer are based on a rather simplistic 3-gene signature, even advanced analysis of a large data set of tumors by The Cancer Genome Atlas (TCGA) Network, which incorporated genomic, transcriptomic, proteomic, and epigenomic signatures, failed to tangibly improve upon these classifications (9). Other recent studies in have delineated up to 10 separate subtypes (10), but this molecular gerrymandering has not yet elucidated any new actionable theme within breast cancers, and instead has only served to re-emphasize their heterogeneity. To further this point, the only genes commonly mutated in >10% of all breast cancer were in TP53, PIK3CA, and GATA3; the only other gene mutated in >10% of any subtype of breast cancer was MAP3K1 in luminal A (9).

The lack of clarity generated by these large-scale studies is likely based on the fact that the broad subtypes represent breast cancers with different cells of origin, while the narrower grouping is further subsetting the tumors beyond their originating cells (11). These narrow groupings could hold promise in terms of identifying therapeutic responders and non-responders, but it would require careful post-hoc analysis of well-designed clinical trials, and the fact that such subtyping is transcriptome-dependent would necessitate the messenger RNA (mRNA) profiling of trial subjects. However, as an example of this potential, the TCGA analysis did identify 2 smaller subsets of TNBC that did not cluster with basal-like breast cancer: claudin-low and normal-like (9, 12). Claudin-low cancer is a subtype of TNBC that proliferates more slowly than basal-like cancer (13); normal-like TNBC molecularly resembles normal breast and is negative for cytokeratins 5 and 6 and the epidermal growth factor receptor (EGFR) (14). In a

small study, normal-like TNBC had a favorable prognosis compared to basal-like (14). If such differential prognoses are true in larger trials, and immunohistochemically amenable markers are identified beyond genetic signatures, it may allow for their regular employment in clinical practice (15).

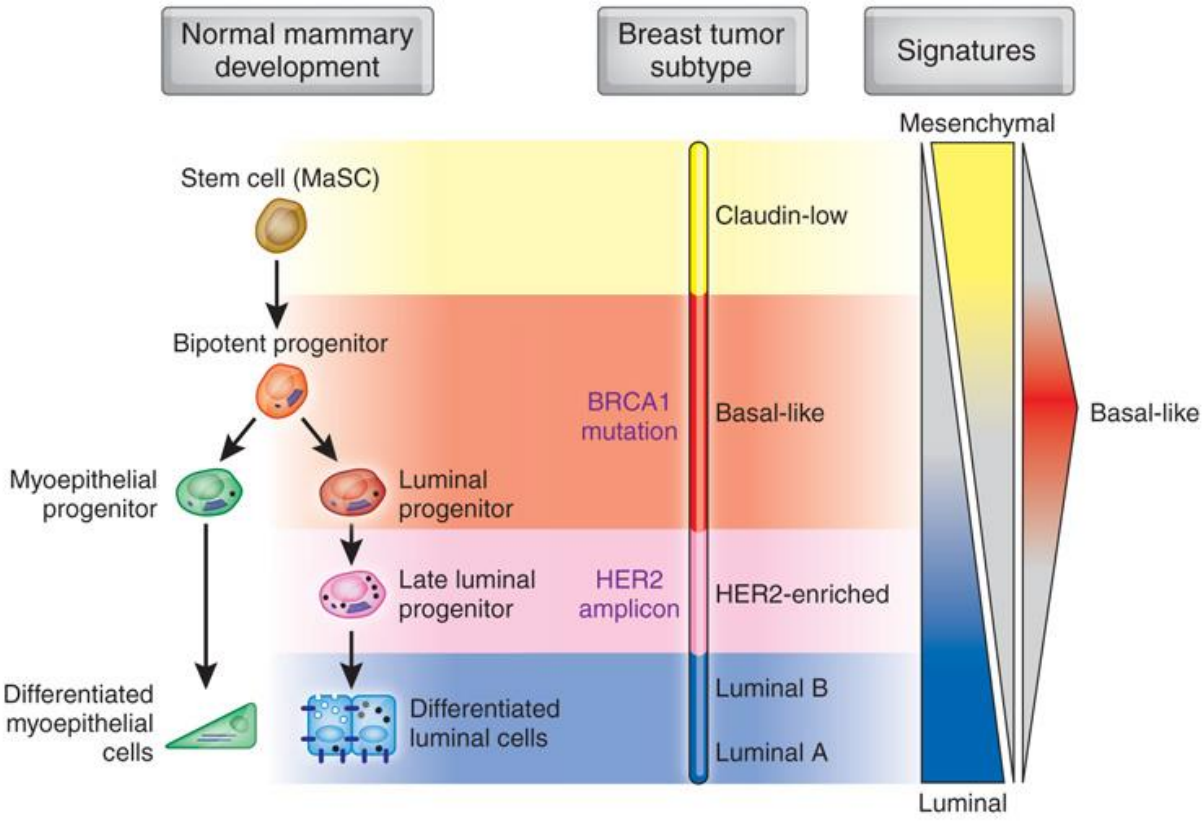

Figure 4. Breast cancer subtypes originate from cells of different stages of mammary development. (left) Subpopulations of normal breast tissue and potential cells of origin for the intrinsic subtypes of breast cancer; these cells may represent a stage of developmental arrest for a tumor with an origin earlier in the differentiation hierarchy or, alternatively, transformation of a cell type at one specific stage of development. (center) The various breast tumor subtypes molecularly compared to subpopulations from normal breast tissue. (right) The defining expression patterns of luminal, mesenchymal or claudin-low, and basal-like cells. *Reprinted with permission from Prat A & Perou CM. "Mammary development meets cancer genomics."* Nature Medicine. *2009 Aug;15(8):842-4.*

Choice of breast cancer therapy is dependent upon stage at diagnosis, subtype, and previous treatments. It can consist of surgery to excise the primary tumor and conserve the remainder of the breast in the case of small, localized tumors or extend to radical mastectomy (removal of the whole breast) with neoadjuvant or adjuvant therapy (including radiotherapy, chemotherapy, and/or targeted therapy). Radiotherapy is delivered locally in the case of early-stage breast cancer in hopes of ensuring that any residual cancer cells following surgical resection of the tumor are killed, while chemotherapy is given in an attempt to kill unseen tumor cells that may have spread to the bloodstream. Both chemotherapy and radiotherapy serve as regular means of treatment for cancers that have invaded beyond the breast, whether to the lymph nodes or to secondary organs.

In addition to these classic treatment strategies, targeted therapies may be used depending on the breast cancer subtype. Targeted therapies seek to disrupt the pro-growth or pro-survival pathways that imbue cancer cells with growth advantages, and they attempt to do so in a way that is less toxic to normal cells than chemotherapy does. For ER-positive breast cancer, endocrine therapy, either by targeting the estrogen receptor itself [as in tamoxifen, a selective estrogen receptor modulator (SERM)] or perturbing the availability of its ligands (aromatase inhibitors such as letrozole or exemestane), is frequently used in treatment at all stages. Because proteins called kinases, which activate other downstream target proteins by post-translational modification known as phosphorylation, frequently play pro-growth and pro-survival roles in cancer cell signaling, they serve as common targets of small molecule inhibitors. One such inhibitor, the cyclin-dependent kinase 4/6 (CDK4/6) inhibitor palbociclib, has recently been approved for treating advanced hormone receptor-positive breast cancer (16). HER2-overexpressing breast cancers have a number of therapeutic options targeting the receptor, including trastuzumab, pertuzumab, ado-trastuzumab emtansine (T-DM1), and lapatinib. Trastuzumab serves as the first-line therapeutic option, but the other therapies can serve as backup options in case of cancer progression. TNBC is unfortunately defined by its

lack of molecular targets for targeted therapy. However, it has exhibited higher rates of pathological complete response (pCR) following neoadjuvant chemotherapy regimens (17) that included platinum-based compounds or taxanes (18-20). Furthermore, TNBC frequently exhibits defects in DNA repair proteins BRCA1 and BRCA2, and clinical trials attempting to promote synthetic lethality by treating with inhibitors of the DNA repair protein poly-ADP ribose polymerase (PARP) are ongoing (21, 22). Despite the existence and continued development of these and other therapies, breast cancer that spreads to secondary sites remains incurable (3).

Like other cancers, genetic instability and its resulting heterogeneity are the primary reasons why it tremendously difficult to treat breast cancer. In this vein, it is quite telling that the most common mutations in breast cancer are to *TP53*, which encodes the protein p53, nicknamed the “guardian of the genome.” Loss of function of this or other tumor suppressors, such as *BRCA1* or *BRCA2*, which are frequently mutated in hereditary breast cancer, allow mutant cells that would otherwise either repair their DNA or die to instead continue proliferating, creating daughter cells that are more and more genomically unstable and phenotypically diverse. This genomic instability and its resulting biological heterogeneity make cancer cells incredibly fit when exposed to the crucibles of evolutionary selective pressure, whether they come in the form of differing tumor microenvironments throughout the body or therapeutic agents targeting distinct mechanisms of tumor growth. It is due to this fact that unless the target of a therapy is totally indispensable to cancer cells for survival, they will find a way survive without it and become resistant.

The best example of the acquired resistance phenomenon in cancer is the use of imatinib in chronic myelogenous leukemia (CML). CML arises from cancer cells with a single translocation of chromosome 9 and 22 [t(9,22)] that causes the kinase domain of Abl to be constitutively activated downstream of the breakpoint cluster region on chromosome 22 (BCR-Abl). Imatinib targets this mutation-driven cell growth and has transformed the treatment of CML, doubling its 5-year survival from 31% in the pre-imatinib era to 63% in 2011, and serving

as the best clinical example of a targeted therapy in action. However, even in this best-case scenario wherein a single gene translocation represents the driving agent of cancer, resistance still occurs through a number of mechanisms. This situation has played out similarly in breast cancer, where aromatase inhibitor treatment leads to mutations causing constitutive activation of the estrogen receptor, and where HER2 targeting in HER2+ breast cancer can lead to resistance to up to four available therapies. Cancer has thus far proved impossible to cure once it is no longer confined within the primary site, when it is no longer amenable to surgical removal. Even the best, most promising targeted therapies tried to date have ultimately fallen short in the game of molecular whack-a-mole.

1.2 Metastasis

1.2.1 Clinical background

While the vast majority of cancer funding and public attention are directed towards the treatment and prevention of primary cancer (23), the sad truth is that 90% of cancer mortality is due to metastasis, the spread of cancer to secondary organ sites (24). In primary cancers affecting organs related to reproduction (e.g., breast, ovary, or prostate), which are necessary for propagation of the species but non-vital at an organismal level, metastasis is the cause of nearly all cancer-related deaths. With few exceptions, which will be addressed later, metastatic cancer represents a terminal diagnosis; to emphasize this point, metastatic cancer patient advocates have begun referring to themselves as “lifers” (25, 26).

Metastasis is typically considered to be late event in cancer progression, but this is highly dependent upon cancer type and the associated capabilities of screening and early detection. Imaging-based methodologies, including magnetic resonance imaging (MRI), computed tomography (CT), and positron-emission tomography (27), are useful in detecting cancer earlier than was possible in the past, but limitations of these technologies mean that tumors must usually reach a diameter of at least 4-7 mm for detection (28, 29). While a 5 mm tumor seems small, a lesion of that size is expected to contain upwards of 1.25×10^7 cells (30).

Given cancer's enormous genomic instability and biological heterogeneity, 12 million cells are more than capable of proving evolutionarily fit.

Varied methods of screening and detection as well the natural history of different types of cancer are manifested in the stages at diagnosis of different cancers. For example, cancers with either screening tests available and in regular practice (breast and prostate) or relative ease of observation (melanoma) are more likely to be detected and diagnosed prior to stage IV, with only 6% of breast cancer and 4% of prostate cancer and melanoma are diagnosed at the metastatic stage. Conversely, cancer types where regular screening is either not performed or patients are diagnosed late due to symptom confusion, e.g., cancers of the esophagus, stomach, or small intestine, are often diagnosed at stage IV and carry a markedly poorer prognosis. Indeed, this is evident in a comparison of 22 primary cancer types in the National Cancer Institute's (NCI) Surveillance, Epidemiology, and End Results (SEER) database, which shows that there is a strikingly negative correlation between the percentage of patients of a given cancer type diagnosed at stage IV and 5-year survival. The fact that stage IV cancer carries a worse prognosis is unsurprising, but that such a comparison yields an R^2 value of 0.45 is almost shocking. Independent of tumor biology or therapy available for different types of primary cancer, the presence of metastasis at the time of diagnosis in a subset of patients is highly correlated with survival outcomes in the whole cohort.

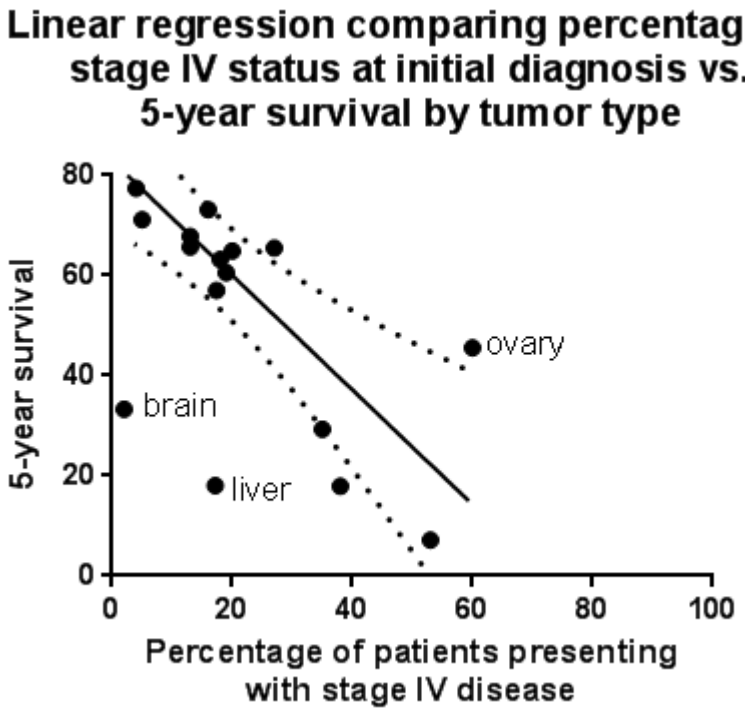

Figure 5. Negative correlation between percent of patients diagnosed with stage IV cancer and the five-year survival of all patients of that tumor type. Linear regression performed on data from SEER (SEER 18 2005-2011). Solid line represents the regression y = -0.3956x + 42.66, R^2 = 0.45. Dotted lines indicate 95% confidence interval. Tumor types representing substantial departures from the line of best fit are indicated on the plot.

One of the most sobering implications put forth by this data is the sheer level of determinism that currently exists between the presence of metastasis and the likelihood of mortality due to said metastasis. If current therapies could significantly affect the long-term survival of cancer patients with metastasis, no such linear relationship would be evident. However, metastatic cancer is typically treatment-refractory, as it is composed of tumor cells that have progressed and grown under the artificial selective pressure of chemo-, radio-, or targeted therapy and/or the natural selective pressure the microenvironment of a secondary organ. Therefore, metastasis represents a substantially different population of cancer cells than the primary tumor from which it originated.

The ending that befalls metastatic cancer patients is unimaginably painful. As the tumor cells outcompete the resident cells comprising the body's essential organ systems, patients ultimately succumb to organ failure. This failure can be brought about by metastasis to the bones, which first leads to risk of fracture due to structural erosion and later to suppression of the body's ability to maintain its hematopoietic and immune systems as the cancer cells overtake the bone marrow (31, 32). The lungs are incredibly hardy and resilient, able to allow for survival even when tumor burden reduces their capacity by up to 75% (with continuous supplemental oxygen); however, when overtaken by metastasis they eventually cannot keep up with the body's need for oxygen. Patients may die due to lack of oxygen, lung infection, or heart failure (33-35). Liver metastasis can be fatal when the liver parenchyma is replaced by tumor tissue, preventing essential metabolic functions and leading to multi-organ system failure, metabolic acidosis, renal insufficiency/renal failure, or total liver failure (36, 37). Brain metastasis carries the worst prognosis; its lethality is attributed to neurological losses of function, headache, seizure, cognitive or motor dysfunction, and coma (38, 39). In addition to directly causing death, metastasis across cancer types can also increase the risk of infection, heart failure, pain medicine overdose or other complications. Thus far, treatment is largely palliative; there is little chance of long-term survival for those diagnosed with metastatic disease. What it is it that makes this diagnosis so dramatically worse than primary cancer? What exactly is so unique about metastasis that has made it such an insurmountable challenge?

1.2.2 The biology of metastasis

One of the key concepts of metastasis was described in the seminal work "The Distribution of Secondary Growths in Cancer of the Breast" by Stephen Paget, a 19th century English surgeon (40). Paget observed the records of 735 women who had died of breast cancer, and noted a strong preponderance of metastases to the liver and lungs. He looked at a further 244 lethal cases of gynecological cancer and noted again a high proportion of liver metastases.

He examined the contemporary literature and found that metastasis to bone was also quite common, and that only specific bones were affected. He reasoned that the preferential growth of metastases at certain sites was due to interactions between the unique “seeds,” i.e., the cancer cells, and a receptive “soil,” the anatomic location of successful metastasis, not to random chance. This idea stood in stark contrast to the accepted wisdom of the time, which held that patterns of metastatic spread were due to simple patterns of vascular flow. While his work was at first rejected, Paget’s “seed and soil” hypothesis was rediscovered and validated by Dr. Isaiah Fidler in the 1970s and 80s. Fidler’s experiments demonstrated that only rare populations of cells within a tumor are capable of forming metastases (41), even when introduced directly into the circulation (42). His studies further showed that site specificity was not due to the circulation dynamics; even following the transplantation of different organs subcutaneously or intramuscularly into recipient mice prior to intravenous (i.v.) injection of tumor cells, thus normalizing the cancer cells’ access to the target, cancer cells maintained their original organ tropism (43).

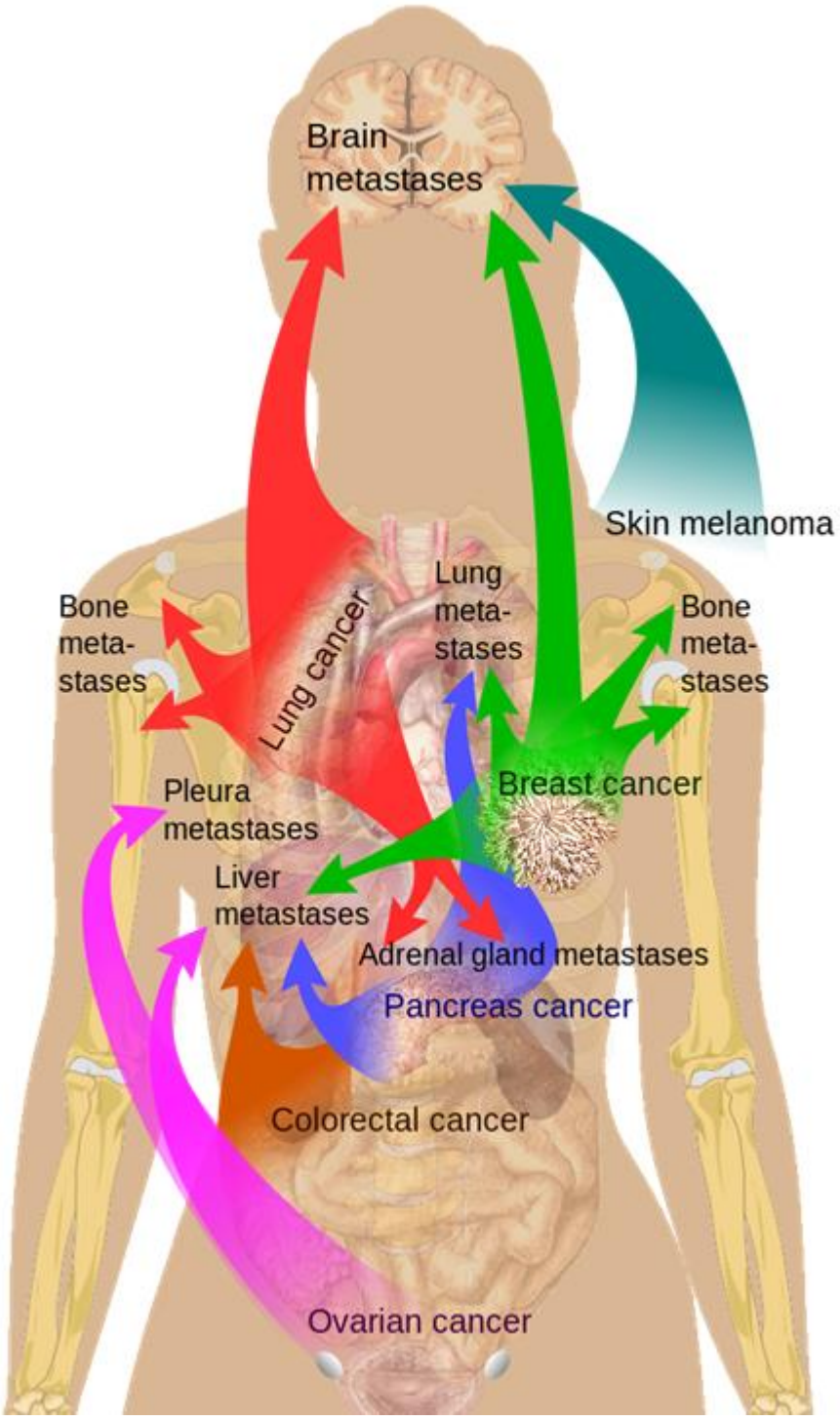

Figure 6. The seed-and-soil nature of metastatic organotropism. Some common cancer types are included with their most frequent sites of metastasis. Direction of arrows indicates spread from primary to metastatic site. *Reprinted with permission from Wikimedia Commons.*

As suggested previously, the process of metastasis represents an evolutionary challenge to potentially metastatic cancer cells. Fortunately, the degree, diversity, and number of these physical constraints on would-be metastatic cancer cells make the process tremendously inefficient. For this reason, cancer cells capable of initiating metastases have been likened to decathlon champions (44). A schematic of the steps required for the successful initiation and formation of metastases, reprinted from (44), is included as Figure 7.

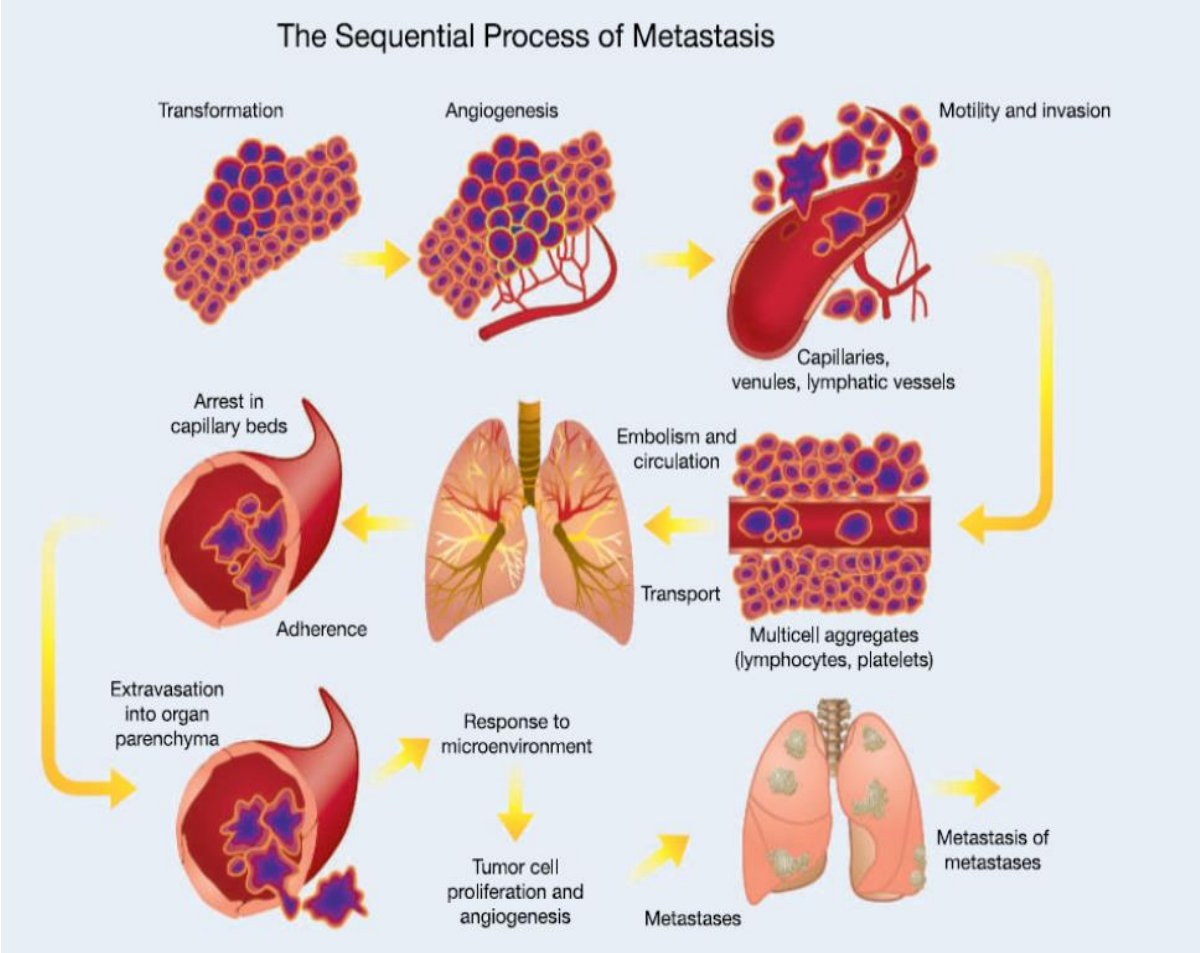

Figure 7. The metastatic cascade. Successful establishment and growth of metastasis at secondary organ sites requires that cancer cells fulfill 10 evolutionarily challenging steps. *Reprinted with permission from Talmadge JE & Fidler IJ. "AACR Centennial Series: the biology of cancer metastasis: historical perspective."* Cancer Research. *2010 Jul 15;70(14):5649-69.*

The initial steps of the metastatic cascade are common to all transformed cells that grow beyond even a few millimeters in diameter (45). Following cell transformation, cells need to obtain oxygen and nutrients to survive and meet their needs for energy consumption and biomass generation. Due to the limits of oxygen diffusion through tissue, which can be as low as 100 μm (46), any cells beyond this distance from existing blood vessels would be unable to survive and proliferate (47, 48); for this reason tumors cannot grow larger than 2-3 mm without an adequate blood supply (49). Dr. Judah Folkman first connected the presence of blood vessels around growing tumors to tumoral release of a factor that would later be identified as vascular endothelial growth factor (VEGF) (50). While the means by which tumors acquire their blood supply has proven to be more varied than simply VEGF release (51, 52), the requirement of an adequate blood supply to support tumor growth is recognized as one of cancer's hallmarks (45).

Even a well-vascularized tumor abundant in mutations does not usually pose a threat if it remains stationary and confined to its site of origin (53), with the exception being tumors that grow locally but produce deleterious effects due to their physical size interfering with normal physiological functions (54). In fact, it is the distinction between invasiveness and non-invasiveness of tumors that determines a malignant or benign diagnosis. Dr. Lance Liotta demonstrated that only malignant cancers are able to degrade their basement membrane (BM) and invade into the surrounding vasculature (55). Later studies determined that the causative agents in BM degradation and invasion were matrix metalloproteases 2 and 9 (MMP2/9) (56). As an aside, in addition the tumor classifications of benign versus malignant, a classification of "pre-malignant" refers to transformed cells that are more likely to become invasive over time given the accumulation of additional genetic aberrations. Some cancers have relatively well-characterized evolutionary courses, whereby development of additional mutations can be correlated with a progressive increase in malignancy; these characterizations are referred to as Vogelgrams, after Bert Vogelstein who first used it to describe the sequential genetic changes

and malignancy of colorectal cancer (CRC) in 1990 (57). The progression of increasing genomic mutational events corresponding with increased malignancy can be observed in CRC and cancers of the breast, prostate, esophagus, and cervix, among others, which are preceded by the premalignant lesions colorectal adenoma, carcinoma in situ [ductal carcinoma in situ (DCIS) or lobular carcinoma in situ], prostate intraepithelial neoplasia (PIN), Barrett's esophagus, and cervical dysplasia, respectively. However, detection of a pre-cancerous lesion with mutation X does not guarantee the accumulation of subsequent mutations Y and Z or subsequent progression to later stages in these diseases. This is important clinically, as overtreatment of premalignancies such as DCIS and PIN and the associated loss of quality of life is one of the main arguments against the earlier implementation of mammography for early detection of breast cancer (58) and fanatical adherence to the results of prostate specific antigen (59) screening for prostate cancer (60); the inability to determine which pre-cancers will progress to invasive cancer mirrors the lack of predictability of which invasive cancers will metastasize. Underscoring the evolution of both invasive cancer and metastasis is the fact that cancers are genetically unstable and biologically heterogeneous, making it currently impossible to predict which mutations will arise next in any tumor; even the father of the Vogelgram has deemed the genetic mutations arising during cancer progression as stochastic (61).

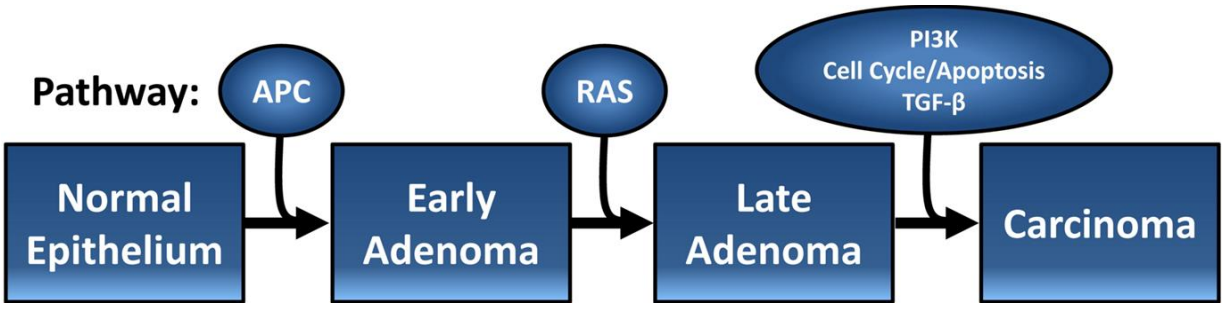

Figure 8. Vogelgram of common genetic events occurring during development of CRC. Ovals show oncogenic changes while rectangles show pathological state. *Reprinted from*

Wikimedia Commons with permission and based upon Fearon ER & Vogelstein B. "A genetic model for colorectal tumorigenesis." Cell. *1990 Jun 1;61(5):759-67.*

The study of circulating tumor cells (CTCs) is becoming increasingly popular, as meta-analyses of large patient cohorts have demonstrated prognostic significance in the ability to detect CTCs in the blood, with counts of >5 CTCs in 7.5 mL of blood yielding a negative prognostic value in both breast and ovarian cancer (62, 63). Though the detection of high CTC counts leads to a statistically significant hazard ratio (HR) of approximately 2 for overall survival, this still implies that 33% of patients dying from disease will actually have low CTCs, and that not all of those with high CTC counts are at risk. Thinking logically about the inefficiency of the metastatic process, it is unsurprising that quantification of CTCs, which enter the circulation relatively early in the metastatic cascade, would not be a perfect indication of mortality due to metastasis. Following invasive cancer cells' acquisition of the ability to degrade the basement membrane and invade the vasculature, they are still unlikely to be able to survive in the circulation, much less form metastases. A previous study demonstrated that <0.1% of cancer cells injected directly into the bloodstream of mice remain viable 24 hours post-injection (42). Even granting direct vascular access to tumor cells in humans by the use of peritoneal shunts to alleviate the pain of malignant ascites of ovarian cancer did not result in death due to metastasis (64). One of the key barriers to survival in the bloodstream is the requirement for anoikis resistance. Anoikis is a form of programmed cell death resulting from loss of cell-to-extracellular matrix (ECM) contact. Usually, cell-ECM contact provides cells with integrin-mediated survival and growth signaling (65). Once this connection is lost, they will soon undergo apoptosis. Successful metastatic tumor cells must overcome this invasion-control mechanism in order to survive in the bloodstream, and one way to do so is by forming multicellular aggregates. The cells of these tumor emboli can provide each other with the pro-survival signals required to live in the absence of ECM contact (66). Additionally, cancer cell aggregation with either other tumor cells or hematopoietic cells can protect tumor cells from shear stress in the

blood (67, 68). Multiple experimental systems have shown the increased efficiency of multicellular aggregates at seeding metastasis compared to the same number of single cells (69, 70) and aggregates are detectable in patients (71-73). Recently, single-cell sequencing has shown that the tumor cell aggregation occurs oligoclonally, suggesting that aggregates are formed prior to tumor cell entry into the bloodstream (73).

The aggregation of tumor cells in the blood can also help the potentially metastatic tumor cells negotiate the next challenge in the cascade, arresting within the vasculature of secondary organs. The journey of tumor cells through the circulation ends one of two ways and both involve getting stuck. One method is vascular occlusion, which occurs when a cancer cell or cell cluster physically blocks the vessel in which it is traveling because its diameter exceeds that of the vessel (74, 75). The second means of arrest within blood vessels is the adhesion to vessel walls, a process similar to that employed by immune cell adhesion and displayed in Figure 9 (76). Briefly, according to fluid dynamics, shear stress is higher near a boundary, in this case the blood vessel wall. At that same point, the blood flow rate will be lower (77). So while blood flowing through large vessels is traveling at a seemingly impossibly fast rate for receptor-ligand binding to occur, cells that bounce close to the walls of the blood vessel actually slow and are pushed toward the wall by shear forces. If the immune or tumor cells express cell surface carbohydrates (frequently in the form of selectin ligands) compatible with those of the endothelial cells (selectins), they begin to roll more slowly along the vessel wall. When tight receptor-ligand binding occurs, such as that mediated by integrins, they firmly adhere to the vessel wall (78). Interestingly, a study of brain metastasis revealed the top gene changed between cancer cells metastatic to the brain versus other organ sites was *ST6GALNAC5*, which encodes a molecule that mediates adhesion specifically to the brain vasculature (79). Additionally, while tumor cells may adhere to the vascular walls through their own actions, this binding may also be mediated by platelets, which express selectins and selectin ligands (74).

Indeed, platelets have long been known to play pro-metastatic roles (80-82); their status as adhesion mediators is key to successful metastasis.

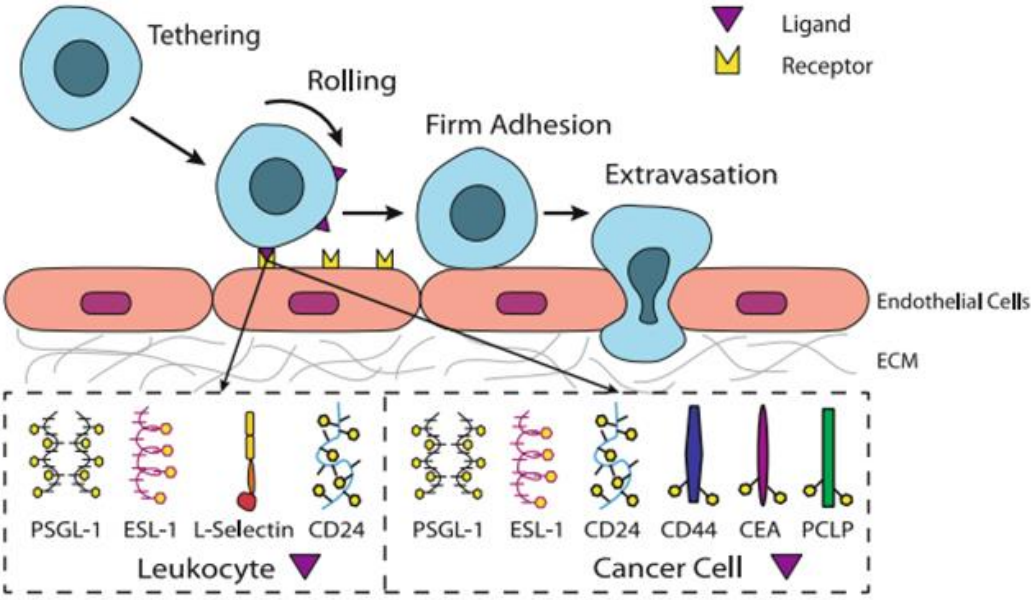

Figure 9. The process employed by tumor cells in adhering to walls of the vasculature is similar to that used by immune cells. In this process, cells traveling through the vasculature at high rates of speed occasionally bump into the vessel walls. If cell surface ligands (boxed with dashed line) meet their counter-receptors on endothelial cells, the cells will slow and begin a rolling motion along the vessel wall. When the leukocyte or cancer cell binding avidity exceeds the shear force of the blood flow, firm adhesion is achieved and the cells may be able to extravasate. *Reprinted with permission from Geng Y, Marshall, JR, & King MR. "Glycomechanics of the metastatic cascade: tumor cell-endothelial cell interactions in the circulation."* Annals of Biomedical Engineering. *2012 Apr;40(4):790-805.*

Once cancer cells have disseminated into the vasculature of secondary organs, they still need to be able extravasate into the organ parenchyma if they are to form true metastases. This act of extravasation occurs in two steps: breach of the blood vessel wall, followed by the physical migration out of the vessel. The migration out of the vessel is a simple matter of

following chemokine gradients into the tissue (83); the chemokines present are tissue-specific and thus demand different phenotypes from the tumor according to the organ involved, a situation analogous to the extravasation of immune cells into target tissues (84). Using a chick embryo chorioallantoic membrane model of metastasis, it was shown that human cancer cells send small cytoplasmic actin-containing protrusions, termed invadopodia (85), through the junctions of endothelial cells in order to breach the blood vessel wall enter into the surrounding organs (86). This vascular breach can be enhanced through cancer cell secretion of VEGF or tumor necrosis factor-α (TNF-α), which can weaken the endothelial cell tight junctions and/or increase the subsequent tumor cell motility (87, 88).

Finally, followed extravasation, tumor cells have technically made it into the organ parenchyma of a secondary organ site. If they are compatible with their new environment, they may grow, develop their own blood supply, and even invade and spread further throughout the body--metastasis of metastasis. However, this step in the metastatic cascade is actually the most demanding of would-be secondary tumor. Upon dissemination and entry into the secondary site, cancer cells still have to adapt to their new environment, which is highly unlikely to be reminiscent of the setting of the primary tumor, and may include dramatically altered nutrient resources and populations of resident cells that inhibit invasive cancer cells both directly and indirectly. Additionally, as was true of growth at the primary site, if metastases are to grow greater than a few millimeters in diameter, they will require their own blood supply. Evidence of the exceptionally inefficient nature and the challenges posed at this step come from multiple clinical and experimental observations. First, in an experimental model, less than 0.04% of cancer cells introduced into the circulation were able to form lung metastases, and it was estimated that only around 20% of cells that were able to survive in the secondary organ site went on to successfully form lung nodules (42). Xenograft studies in mice showed that disseminated cancer cells that survived at secondary organ sites without forming detectable metastases, when isolated from these non-metastatic organ sites and injected into recipient

animals, were able to form spontaneous overt metastases (89). This so-called ‘dormancy’ is one mechanism cancer cells may use to survive for long periods of time if the conditions in a secondary organ are not optimal for growth, either in terms of availability of oxygen, nutrients, or growth factors or due to active inhibition by host cells (e.g. immunosurveillance) (90). Dormancy may also take two distinct forms: mass dormancy refers to those disseminated micrometastases that either cannot obtain the blood supply or nutrition to grow beyond a few millimeters, or are being held in check by immunosurveillance; cellular dormancy refers to quiescent cells that have exited the cell cycle but remain viable (90).The concept of dormancy, although difficult to model and study experimentally, also would account for clinical observations on the timing of metastatic recurrence (91, 92). In breast cancer, it has been shown in multiple large studies that there is a bimodal peak of metastatic recurrences, with highest incidences at 18 months and 5 years following initial therapy (93). However, there remains a non-zero risk of metastatic outgrowth more than 10 years following initial diagnosis, and multiple studies have reported the appearance of overt metastases more than 20 years following initial cancer diagnoses (92, 94-97). The role of immunosurveillance in suppressing metastasis at the secondary site has been shown in humans following organ transplantation, as organ recipients with no prior history of malignancy develop metastatic tumors in their grafted organs (98-100). In each case, it has been shown that the organ donor had a primary cancer. When the organ recipients were put on immunosuppressive drugs in order to prevent organ rejection, the immunological suppression of these dormant cancer cells was abrogated and the cells outgrew in the recipient, in several cases actually killing the organ recipient. In summary, when cancer cells at secondary sites overcome whatever barriers are preventing their outgrowth, through adaptation to the secondary site or changes to the site itself brought on by such processes as aging, inflammation, or immunosuppression, they have achieved the completion of the metastatic decathlon and can grow into overt metastases (101).

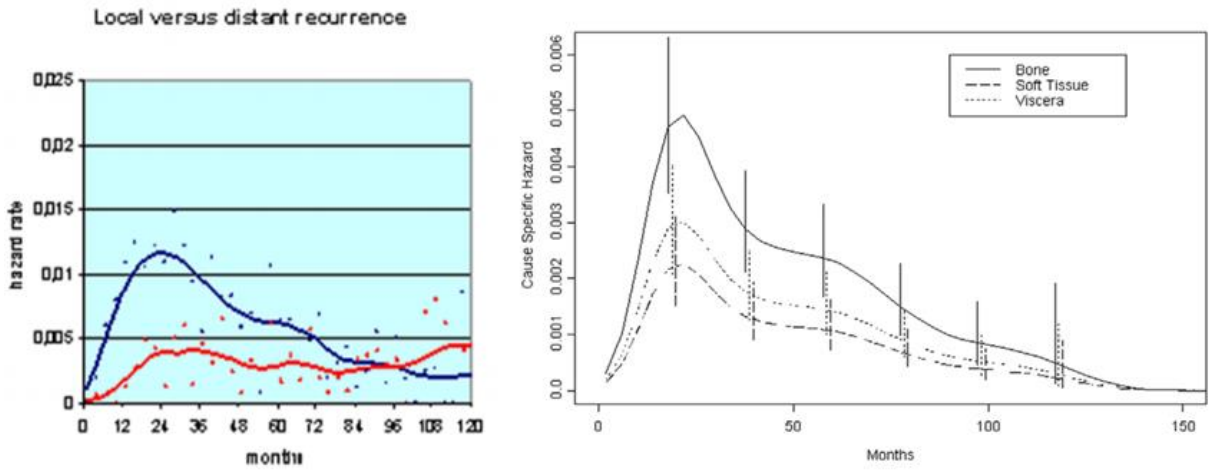

Figure 10. Timing of metastatic recurrence in breast cancer. Left panel shows the hazard ratio of metastatic recurrence (blue) plotted with local recurrence (red). Right panel shows that the timing of metastatic recurrence is similar for bone (top, solid line), visceral organs (middle, dotted line), and soft tissue (bottom, dashed line). X-axis shows months post-initial diagnosis, Y-axis is hazard ratio. *Reprinted with permission from Demicheli R, Biganzoli E, Boracchi P, Greco M, & Retsky MW. "Recurrence dynamics does not depend on the recurrence site."* Breast Cancer Research: BCR*. 2008;10(5):R83.*

It is evident from the rigorous functional demands of the metastatic cascade that the evolutionary champions of such a process are unlikely to represent the same population of cells from which they are derived, and the data have served to support this principle. It was demonstrated that different clonal populations within a primary tumor have different abilities to form metastasis (41), and that only a single metastatic clone (102, 103) or oligoclonal cluster (73) is required to serve as the founder of a metastatic tumor. The disconcerting implication of this fact is that even the best technologies interrogating genomic, transcriptomic, and proteomic analyses of primary tumors are unlikely to yield predictive data on whether and where a primary tumor could be expected to metastasize. Profiling of metastases, however, has shown that their gene expression patterns differ from their associated primary tumors (104, 105) and even led to some elucidation of the mediators of permissive seed and soil interactions hypothesized by

Paget (79, 106). Coupled with the fact that metastases frequently arise as cancer recurrences, following the development of therapeutic resistance, the disparate gene expression by metastases and their associated primary tumors can also help explain the dismal prognosis of metastasis: metastases can possess both de novo (107) and acquired resistance (108) to therapies to which primary tumors and even other metastases respond (109-111). Interestingly, in a case of the seed and soil theory at work, cells of the metastatic microenvironment can even protect these secondary tumors from therapy, as is the case with astrocytes serving chemoprotective roles during brain metastasis (112). Indeed, one of the only examples of successful (albeit not curative) therapeutic targeting for metastasis involves not direct targeting of tumor cells, but the more stable metastatic microenvironment in bone. Bone metastatic cancer cells hijack the physiological bone remodeling process in order to obtain growth factors from the bone matrix (113); remodeling involves the degradation of bone by osteoclasts and the deposition of new bone by osteoblasts (114). In bone metastasis, cancer cells stimulate the osteoclasts into excessive activity (113); the weakening of bones and associated risk of fracture was noted by Paget as evidence for his seed and soil theory (40). Using therapeutic agents, including bisphosphonates, denosumab, and dasatinib, that target the osteoclasts themselves instead of the cancer cells has delayed skeletal-related events, such as fracture, associated with bone metastasis and improved the quality of life of patients (27, 115). It must be noted, however, that any differences observed in overall survival were marginal at best, suggesting that bone metastatic tumor cells can find alternative means of survival even without the aid of osteoclasts (116).

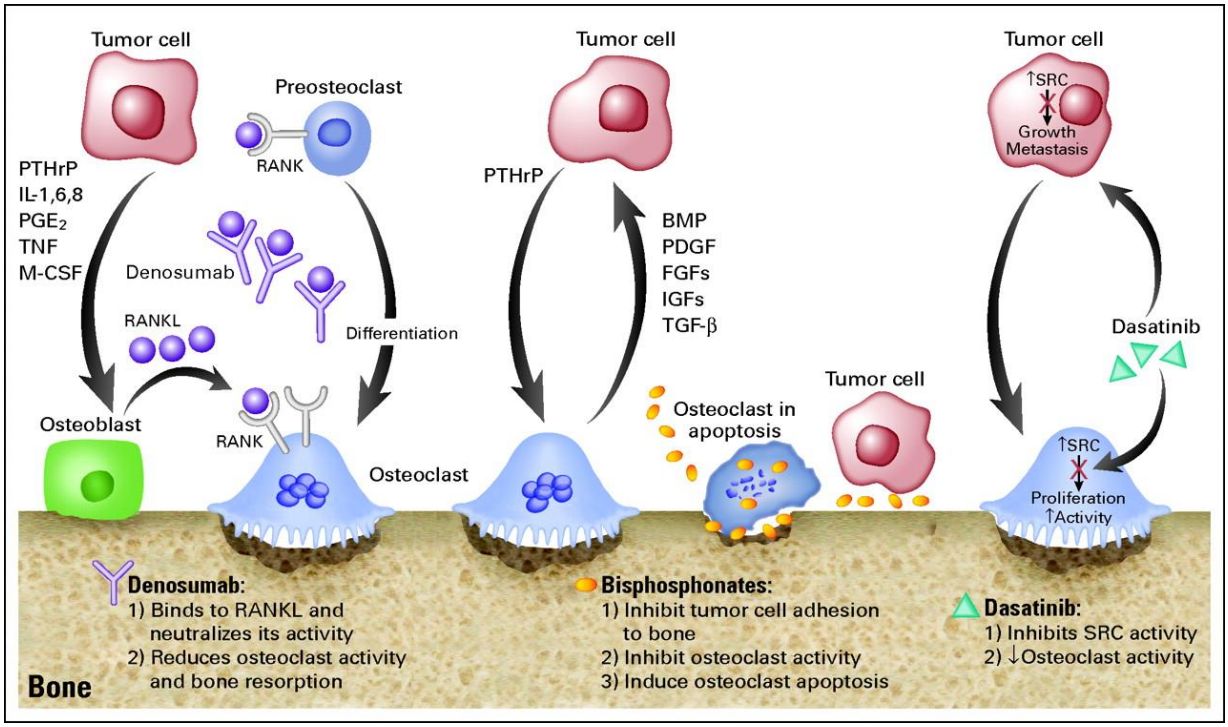

Figure 11. Therapies against bone metastasis target the cells of the bone microenvironment, not the cancer cells. Illustrated here is the vicious cycle of bone metastasis and the steps of the process targeted by bone metastasis-targeted therapy. Left: RANKL secreted by osteoblasts in response to stimulation by chemokines released from cancer cells causes the maturation of osteoclasts, which degrade the bone matrix. Denosumab acts as an antibody against RANKL, thereby decreasing osteoclast activity. Center: bisphosphonates act by inhibiting tumor cell adhesion to bone as well as directly enhancing osteoclast apoptosis. Right: dasatinib is a small molecule inhibitor of SRC, which is key to osteoclast proliferation and activity. Dasatinib may act through direct inhibition of cancer cells or osteoclasts. *Reprinted with permission from Fornier MN. "Denosumab: second chapter in controlling bone metastases or a new book?"* Journal of Clinical Oncology. *2010 Dec 10;28(35):5127-31.*

Recent breakthroughs in the technical ability to perform single-cell sequencing have shed more light on the nature of metastasis by enabling modeling of the evolutionary nature of metastasis. While population-level tumor genomic and transcriptomic profiling allowed researchers to see that indeed primary tumors and metastatic tumors are different in terms of overall gene expression (104, 105), they were unable to definitively provide answers to questions on the nature of metastasis that have been debated for many years (117). Namely, the questions of whether metastasis is a late-arising event in the natural history of a primary tumor (following the linear progression/Vogelgram model of step-by-step acquisition of required phenotypic traits) or dissemination occurs early in the evolutionary course of tumor development followed by a period of dormancy or microenvironmental adaptation (parallel progression). In experimental systems the answer has appeared to be more of the linear progression model, as metastatic subclones increase within cancer cell lines (41) and can be phenotypically selected *in vivo* for increased metastasis-forming capability (118, 119); however, the possibility exists that this observation may be somewhat affected by the experimental systems used (120). Single-cell sequencing has added the ability to interrogate the accumulations of mutations over time and in space, as comparing individual cells within a metastasis as well as between cells of different metastases and cells from metastases to cells from primary tumors are all possible. These analyses have allowed direct observation of the phenomenon reported by Fidler (41) that metastasis can result from the selection of pre-existing subclones within a primary tumor and have served to strengthen the linear progression model of metastasis (121-123). Nonetheless, tumor growth rate kinetic models lend support to the idea of parallel progression (91, 124), as do clinical observations. Even in women diagnosed with breast tumors less than 1 cm in diameter, node-negative, and metastasis-negative (T1a,bN0M0) who undergo a mastectomy, dissemination may have already occurred by the time of diagnosis, as there exists a 2% chance of breast cancer-specific mortality at 5 years and a 5% chance at 10 years (125). Another study showed the probability of distant recurrence

in 171 patients diagnosed with T1a,bN0M0 breast cancer and treated with mastectomy to be 4% (126). Further support for the parallel progression model comes from pancreatic cancer, where clinical data has revealed early dissemination events (127) and experimental data has shown that dissemination can shockingly precede overt primary cancer detection (128). Finally, the existence of the clinical phenomenon of 'cancer of unknown primary' (CUP) serves to bolster the parallel progression model, as in 3-5% of metastatic adenocarcinomas, a primary tumor is unable to be identified, even at autopsy (129). In light of the available data, it would seem most likely that the process of metastasis follows a hybrid of the linear/parallel progression models (130), with metastasis initiated by dissemination of rare clones from within the primary tumor, but with the acquisition of additional phenotypic traits upon reaching the secondary site. The influence of the microenvironment on disseminated cancer cells should not be understated, as the metastatic potential of cancer cells can be reversibly altered by epigenetic modification (59, 131); this reversible modification can occur upon arrival at a secondary site and before metastatic outgrowth (132).

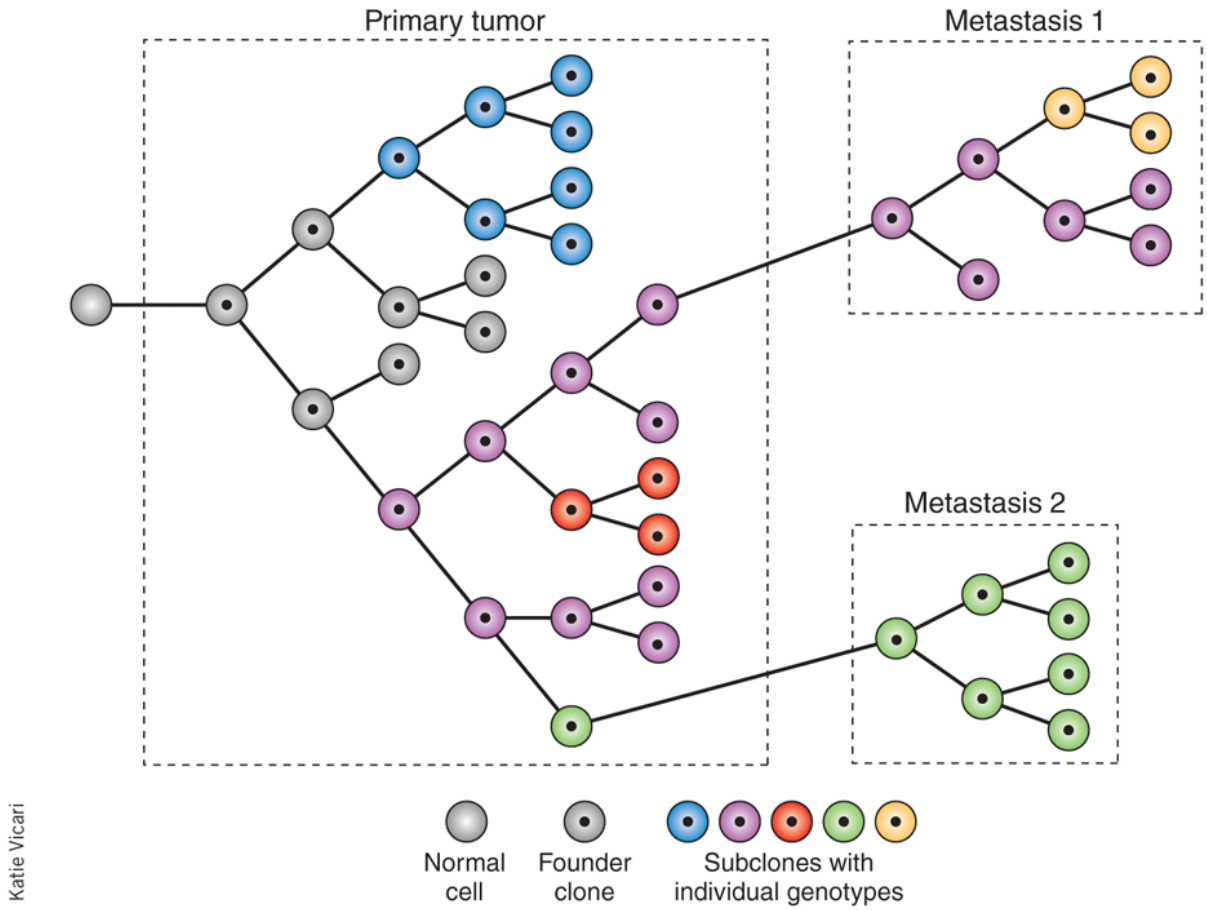

Figure 12. Metastasis arises from clonal populations of cells within the primary tumor. These clonal populations can represent either major (Metastasis 1) or minor (Metastasis 2) populations of cells within the primary tumor, and further evolution occurs following the dissemination of cancer cells, resulting in metastasis that are distinct from their associated primary tumors. *Reprinted with permission from Caldas C. "Cancer sequencing unravels clonal evolution."* Nature Biotechnology. *2012 May;30(5):408-10.*

In light of the highly selective nature of the metastatic cascade, with each step representing a potential barrier to success, it may serve as a useful reminder to consider those conditions necessary for evolution by natural selection to occur. First, within a population there must be some degree of phenotypic diversity. Second, members of a population must be able to reproduce and pass down these heritable differences. Last, there must exist some limit to

the ecosystem such that there is competition for finite resources (133). In the process of metastasis all of these conditions are fulfilled, as cancer's tremendous genomic instability and biological heterogeneity lead to variation within a tumor (134), cell proliferation allows the creation of daughter cells resembling their parent cell, and there is a finite limitation of resources, both nutritional and volumetric, as both are limited within a tumor and within secondary organ sites. Therefore, cancer metastasis is clearly an example of evolution; might co-option of some evolutionary principles serve to enable both a better understanding of metastasis and a better chance for successful intervention in the process (134)? One aspect ripe for such examination is the stepwise nature of the metastatic cascade, which creates an evolutionary scenario replete with population bottlenecks. Indeed, through single-cell genomic analysis, it is possible to observe the results of such bottlenecks, as tumor cells with given genomic patterns within the primary tumor drop out of populations observed in metastases (see Figure 12 above) (121-123). These genomic observations represent strong evidence for the selective nature of metastasis; but since natural selection works on the phenotypic level, additional buttressing would come from evidence of enhanced abilities to perform functions required for metastasis. Unfortunately, most modeling of the steps of metastasis is performed *in vitro* (135, 136), leading to questions about the relevance or requirements of certain findings. However, with the falling costs of sequencing (137), it is now possible to interrogate specific aspects of the metastatic cascade *in vivo* at the single-cell level (138). For now, the best examples of matching of genotype to phenotype in cancer progression come from the population bottlenecks generated by drug treatment. Due to the genomic instability of cancer cells, development of resistance to chemo- or targeted therapies is inevitable, as minor subpopulations of cells exist pre-treatment with mutations that confer drug resistance. Following development of resistance in the clinic (e.g., tumor progression while the patient is still receiving therapy), it is possible to observe an increase in the allelic frequency of certain mutations; these mutations may be in the genes coding the drug targets themselves or in other pathways

involving drug efflux or apoptosis resistance (139-142). Recalling the principles of evolution, organisms (or cells) with differential fitness in a given environment will be more evolutionarily successful, i.e., become a more dominant population in successive generations. However, in a closed system, the expression of new phenotypes is never free; acquisition of new traits requires evolutionary tradeoffs. In this case of drug resistance this can come in the form of adenosine triphosphate (ATP) costs to maintain drug efflux pumps; with up to 33% of cellular ATP being spent on drug efflux, therapy-resistant cells will proliferate more slowly (143). The concept of exploiting evolutionary tradeoffs has been proposed for application to treatment of metastasis (144, 145); by identifying the Achilles' heel exposed by high evolutionary costs at steps during metastasis, it may be possible to use combination therapy to produce an evolutionary double bind, a situation in which a metastasis is forced to fight a war on two fronts. A depiction of such a therapy is shown below in Fig 13 (146). In this hypothetical situation, Treatment 1 is targeted against one phenotype is to control a cancer population; the development of resistance to that therapy incurs an evolutionary cost that can be exploited by Treatment 2. However, as metastases are resistant to conventional therapies (111), intensive and careful study is required in order to expose these potential targetable tradeoffs. Even though metastasis represents evolutionary champions that are living in a state of cellular anarchy, identification of the molecular details of non-negotiable convergent evolutionary phenotypes that allow them to complete the metastatic cascade may enable identification of double bind scenarios.

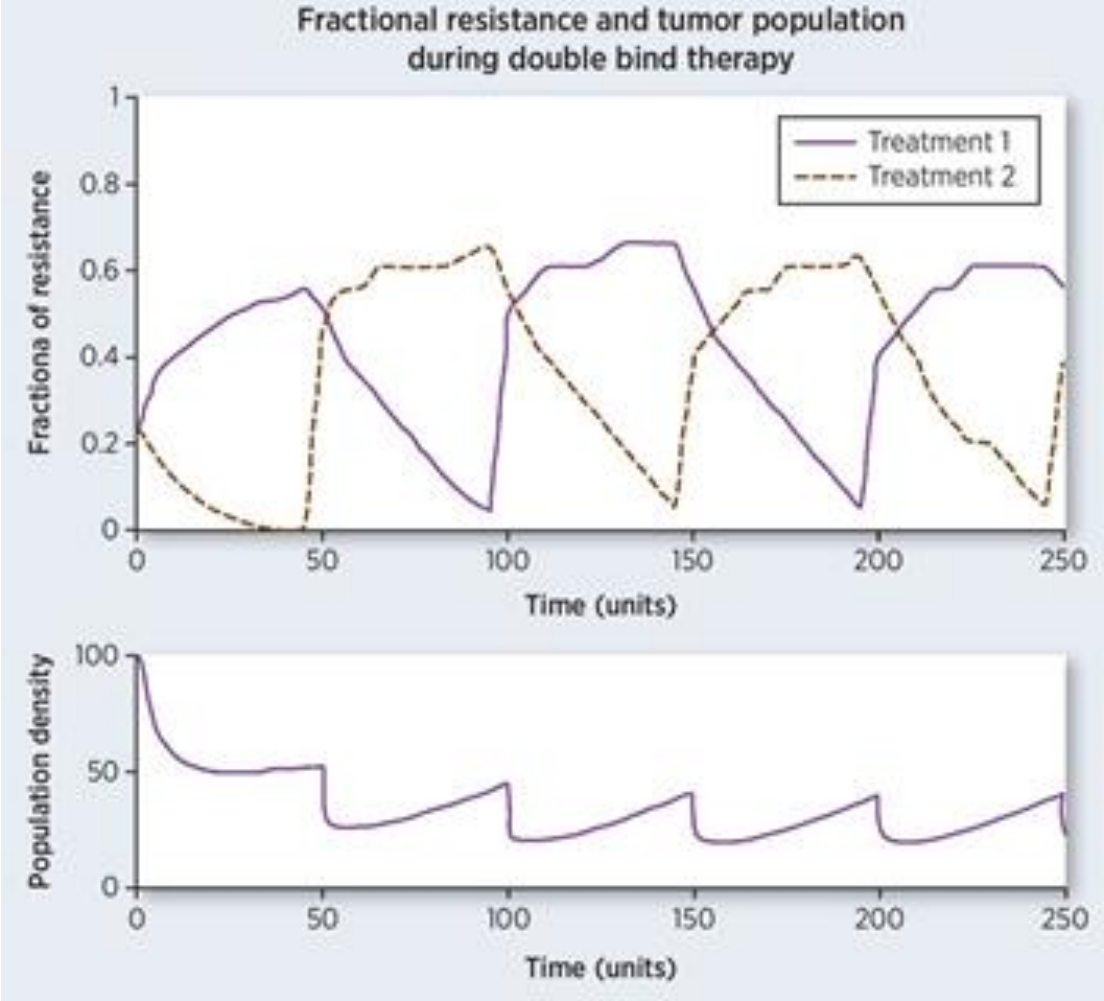

Figure 13. Targeting evolutionary double binds for therapy against metastasis. Top graph shows alternating appearance of populations resistant to Treatment 1 and sensitive to Treatment 2, and vice versa. As resistance phenotype develops to one drug, remaining cells incur evolutionary cost that is exploited by second treatment. Alternation of therapy can continue over time. Bottom graph shows overall population density during alternating treatments, as tumor re-growth would indicate necessity of switching back to the alternate therapy. *Modified and reprinted with permission from Enriquez-Navas PM, Wojtkowiak JW, & Gatenby RA. "Application of Evolutionary Principles to Cancer Therapy."* Cancer Research. *2015 Nov 15;75(22):4675-80.*

1.3 Brain metastasis

1.3.1 Clinical overview of brain metastasis

In the United States, it is estimated that between 6% (147) and 14% (148) of all newly diagnosed cancers will ultimately metastasize to the brain; based on the 1.7 million new diagnoses of cancer expected in 2016 (1), between 100,000 and 240,000 cases can be expected to eventually metastasize to the brain. These numbers represent a conservative projection, for 3 major reasons: 1) autopsies of patients dying due to metastatic cancer are rare, making comprehensive studies difficult and meaning that the apparent numbers seen thus far may be a result of undersampling (149), 2) as improved systemic therapies have lengthened the survival of patients with metastases to other organs, they may go on to develop brain metastasis later (149), and 3) increased detection capability of clinical imaging modalities may allow for the identification of brain metastases that in prior years would have gone unnoticed (150). The primary cancers that most frequently metastasize to the brain are lung, breast, melanoma, and colorectal, accounting for ~45%, ~15%, ~10%, and ~5% of brain metastases, respectively. (149, 151)

Once brain metastasis has occurred, the survival outcomes are dismal. Left untreated, the average survival is less than 2 months (152); palliative therapies including corticosteroids, chemotherapy, and radiotherapy can extend survival, in the best case, to an average of less than one year (153). When only a single brain metastatic tumor is detected, surgery or radiosurgery can be performed; however, the effect of these therapies on survival is still marginal, with life extended only a few months (151). Moreover, at the time of detection, multiple brain metastases are formed in more than 80% of patients, disallowing surgery as a therapeutic option (154, 155). As brain metastasis is almost universally chemoresistant, chemotherapy is usually only used for treating systemic (non-brain) metastasis growing synchronously with the brain metastasis or as salvage therapy (156, 157). Some primary tumors or tumor subtypes are more responsive to therapy targeting specific molecular or functional pathways; while patients

with known brain metastasis are typically excluded from trials for new agents, the enrollment of some patients admitted to trials before diagnosis of brain metastasis has allowed on a small window into the potential of targeted agents in brain metastasis, and it is generally not promising (158). While some targeted therapies do indeed show brain activity and successfully make it into the tumors, they are generally at lower concentrations than outside the brain (159), raising the question of whether efficacious concentrations of the drugs are reached or maintained. Further, these targeted therapies are designed against driver mutations in the primary tumors; it is unclear how necessary they are for the biology of brain metastasis. What is unique about the biology of the brain that makes for such a dismal prognosis in the setting of brain metastasis?

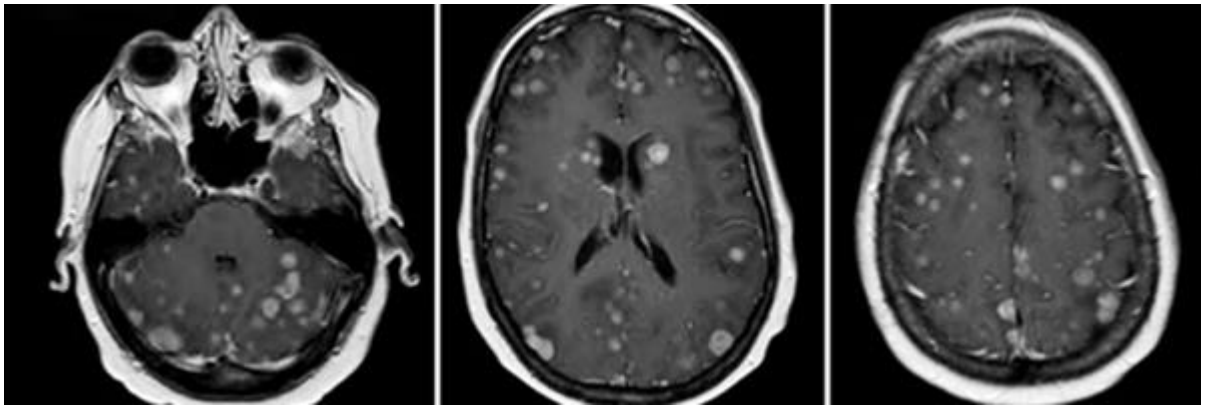

Figure 14. Brain metastasis usually presents as multiple metastases. Magnetic resonance imaging (MRI) showing numerous metastatic lesions throughout the cerebrum and cerebellum of a woman with HER2-positive primary breast cancer. *Reprinted with permission from Ammannagari N, Ahmed S, Patel A, & Bravin EN. "Radiological response of brain metastases to novel tyrosine kinase inhibitor lapatinib."* QJM. *2013 Sep;106(9):869-70.*

1.3.2 Brain as a unique microenvironment for metastasis

The specialization of the brain to suit its functions as the processing and control center for the body has led to the evolution of a number of features and safeguards not seen elsewhere

in the body. As the primary role of the brain is to house and support the neurons that allow for signals to be transmitted to and received from throughout the body, many of these features are specifically designed to support and maintain neuronal function and integrity. The unique nature of the brain microenvironment extends to its resident cell populations, structural composition, blood flow, and nutrient availability. Each of these special characteristics represents a potential challenge to would-be metastatic tumor cells; at the same time, cancer cells with the right features to survive in such an environment can take advantage of the neuroprotective environment in order to gain a foothold that has proven difficult to broach by current therapies.

When speaking of cancer, the most frequently cited brain-specific feature is the presence of a blood-brain barrier (BBB) that separates the brain from the general circulation (160). This 'barrier' is in reference to both form and function, as cells and molecules are excluded from entry by physical obstruction, with the endothelial cells of the brain joined by tight junctions, as well as by active efflux through transporters. The main purpose of this barrier is the maintenance of homeostatic environment for neuronal function (161). Tight junctions, which are composed of proteins including claudins, occludins, and zona occludens (ZO) proteins (162), possess high electrical resistance (163), are surrounded by a thick basement membrane, and supported on the brain-facing side of the BBB by pericytes. The high electrical resistance prevents free diffusion of charged molecules through the BBB, while pericytes physically support endothelial cells and promote their survival and maturation (164). Finally, astrocytic endfeet form the final layer of the BBB. They express glucose transporters for allowing glucose into the brain and P-glycoprotein for pumping drugs/neuroactive compounds out of the brain, and can alter the tightness of the BBB in response to stresses such as hypoxia (165). Oxygen and other lipophilic molecules can directly diffuse into the brain through the endothelial cell membrane, and the brain's high demand for oxygen means that at steady-state levels, the partial pressure of oxygen (pO_2) in the brain is only 35 mmHg (equates to 4.6% oxygen), which maintains a continuous gradient of oxygen into the brain (166). Other required components of

brain function, such as amino acids, are selectively admitted to the brain by specialized transporters (167).

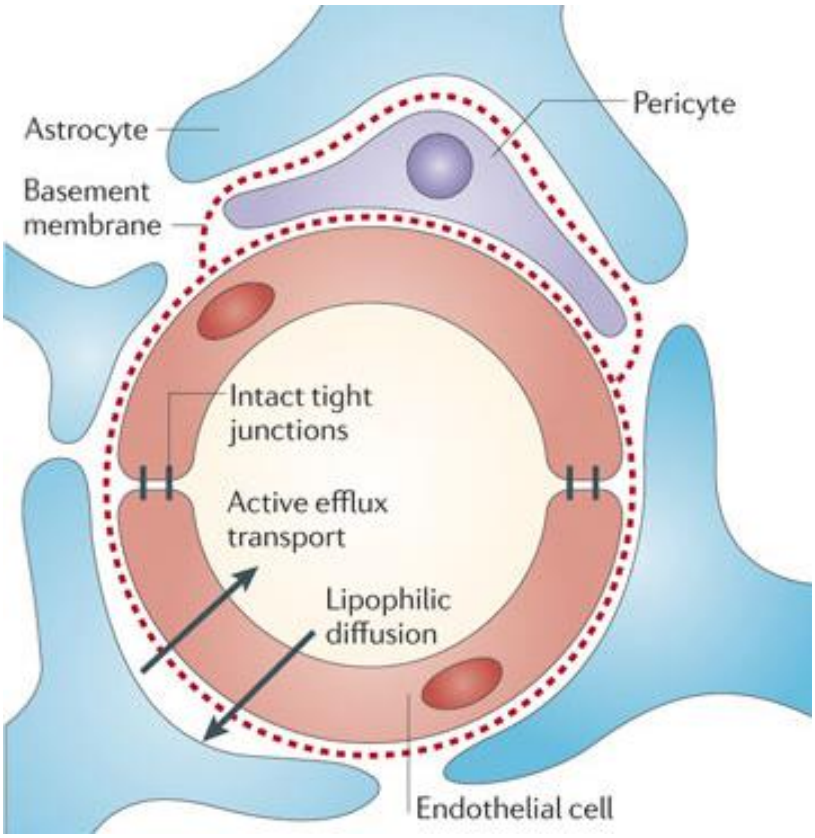

Figure 15. The BBB is formed by specialized cell types in the brain acting in concert. Depicted here is a model of the BBB show its composition by different cell types. The inner lumen (white) is formed by the endothelial cells (red), which are connected by tight junctions. Pericytes (purple) partially cover the abluminal surface of the endothelial cells, which are surrounded by a thick basement membrane (red dotted line). The entire unit is encircled by astrocytes (blue); their endfeet express high levels of P-glycoprotein (as do endothelial cells themselves) and actively exclude most drugs crossing into the brain. Most compounds making it through the BBB are highly lipophilic, allowing them to diffuse across the endothelial cell membrane into the brain. *Modified and reprinted with permission from Steeg PS, Camphausen KA, Smith QR. "Brain metastases as preventive and therapeutic targets."* Nature Reviews Cancer. *2011 May;11(5):352-63.*

As cancer cells arrive and arrest in the vasculature of the brain, the first brain-specific challenge that they encounter is the BBB. An intact physiological BBB prevents the entry of cells into the brain; cells extravasating into the brain would therefore need to pass through the endothelial cell layer either paracellularly (between the cells, through the tight junctions) or transcellularly (through the endothelial cells themselves). While transcellular migration has been observed in immune cell extravasation, only paracellular migration has been detected in metastasis (168). Because tight junctions are composed of a variety of proteins, cancer cells would need to be able to express several proteases in order to penetrate intact tight junctions (169). Alternatively, these junctions can be destabilized by a variety of cytokines, chemokines, and inflammatory mediators frequently expressed by cancer, including VEGF, basic fibroblast growth factor (bFGF), transforming growth factor–β (TGF-β), interleukin-1β (IL-1β),TNF-α, interferon-γ (IFN-γ), CCL2, CXCL8, prostaglandin-endoperoxide synthase 2 (COX2), (79, 87, 88, 170); cancer cells can then secrete MMPs and other proteases in order to disrupt the BM, as in metastasis to other sites. (87, 171).

After bypassing the BBB, cancer cells still have to cope with the unique nutrient composition of the brain. Part of this challenge involves obtaining sufficient oxygen in a tissue with a low pO_2, where there is a high degree of competition from neurons. Neurons solve the problem of maintaining enough oxygen for mitochondrial respiration by never being farther than 40μm away from the nearest capillary (172); cancer cells in the brain converge upon this phenotype as well, as imaging studies on experimental brain metastasis showed that cancer cells stay in contact with blood vessels even following extravasation, until either VEGF-A-mediated neoangiogenesis occurs or, more frequently in brain metastasis, the vasculature is remodeled and co-opted by the cancer cells (75). One of the controversies in the field of brain metastasis is the degree to which the BBB is disrupted following brain metastasis outgrowth. While some studies have detected a heterogeneous permeability to chemotherapeutic agents by brain metastases (173), others have shown that effects of brain metastasis on the leakiness

of the BBB are cell line-dependent, with examples of both intact (174) or disrupted (175) BBB in different contexts. In either case, this distinction is more than academic; if the BBB is not functioning effectively around brain metastases, it might allow for delivery of efficacious doses of therapeutics to brain tumors. Frustratingly, even in advanced brain metastases in which a loss of functional integrity of the BBB would be expected, especially when metastases perform vascular remodeling or neoangiogenesis (75, 176), the accumulation of a wide variety of chemotherapeutic and small molecule targeted therapies still occurs at sub-optimal levels (177).

A better explanation for therapeutic resistance of brain metastasis may lie not in the hijacking of the brain's vasculature by brain metastases, but in the co-option of astrocytes, the brain's essential support cells. Astrocytes in the physiological brain serve homeostatic functions in support of the BBB (178, 179) as well as signaling and delivering nutrients directly to neurons (180). Astrocytes' homeostatic functions include prevention of cellular invasion of the brain parenchyma; cancer cells breaching the BBB are soon met by astrocytes that release Fas ligand (FasL) to trigger cancer cell apoptosis (181). Successful brain metastases win this molecular arms race by expressing serpins, which prevent astrocytic release of FasL. After evading elimination by astrocytes, cancer cells can take advantage of the protective benefits that astrocytes usually afford neurons by a variety of mechanisms. Through gap junction communication, astrocytes upregulate survival genes in brain metastatic cells, promoting chemoresistance (182). This effect involves the engagement and upregulation of the endothelin axis (112); antagonism of the endothelin axis chemosensitized tumor cells and significantly extended survival in models experimental brain metastasis of lung and breast cancer (183). In addition to gap junction communication, brain metastases can activate the pro-growth/survival effects of astrocytes by secretion of IL-1β (184) or CCL2 (132), and have even been shown to enhance the differentiation of neural progenitor cells into astrocytes (185).

On top of oxygen availability, the limited availability of nutrients in the brain makes for a significant evolutionary bottleneck in the pathogenesis of brain metastasis. As the BBB excludes most molecules from simply diffusing into the brain, specialized transporters are necessary for their entry. These transporters exist for the import of glucose and some amino acids; the high capacity of the endothelial cells glucose transporter GLUT-1 of 1420 nmol/min x g tissue ensures the continuous import of glucose into the brain (186). The availability of glucose, inability of other metabolic substrates, and high energy demands of the brain together results in the brain's utilization of 20% of the body's glucose (187), which is evident by the intense background signal of the brain in ^{18}F-deoxyglucose (18-FDG) positron emission tomography (27) (27) imaging (188). Astrocytes and neurons can both utilize glucose that makes it into the brain, astrocytes through GLUT-1 and neurons through GLUT-3, which has a higher glucose affinity (189). Once inside the cell, glucose can be used for either ATP synthesis or the generation of other biomolecules. In either event, the first step of glucose metabolism is the phosphorylation of glucose by hexokinase, generating glucose-6-phosphate (190). At this point, the glucose-6-phosphate can either continue down the glycolysis pathway and be used for ATP generation, or be shunted into the pentose phosphate pathway in order to generate NADPH be used for the production of other biomolecules (190). Brain metastasis has been observed to utilize both glycolysis and the pentose phosphate pathway. A study of human breast cancer brain metastases, which at least in their early stages of colonization are still restricted by a functional BBB, showed that the gene most highly upregulated relative to unmatched primary tumors was hexokinase 2 (HK2), showing the importance of glycolysis for intracerebral tumor growth and survival (191). A second study using experimental brain metastasis models showed enhanced utilization of glucose in both glycolytic and pentose phosphate pathways (192). That the same pathway was repeated by independent studies serves to demonstrate that the physiological constraints imposed by the brain must be overcome in order for successful metastasis.

While it has been widely reported that due to the BBB, amino acids exist at lower levels in the brain than the plasma, literature reports quantifying this phenomenon are scarce. Further, the presence of the large neutral amino acid transporter 1 (LAT1) system enables the facilitated diffusion of some amino acids (193), so quantification of the true concentration of amino acids available to cells in the brain would be ideal. While these data are not available, an Alzheimer's disease study from 1990 did examine the cerebrospinal fluid (CSF) content of amino acids. Comparison of the amino acid content in plasma and CSF of the healthy volunteers of that study (n=11) was performed in Table 3, and revealed that the only amino acid found at comparable levels in the general circulation and the CSF is glutamine, an important precursor of the neurotransmitters glutamate and γ-aminobutyric acid (GABA) (194). This is suggestive that utilization of glutamine may be an important functional constraint on successful brain metastasis growth.

Table 3. Amino acid content of human cerebrospinal fluid (CSF) and plasma.

Amino acid	CSF concentration (μM)	Plasma concentration (μM)	CSF/plasma ratio
Glutamic acid	42	62	0.68
Glutamine	505	500	1.01
Taurine	9	77	0.12
Alanine	34	319	0.11
Glycine	21	225	0.09
Isoleucine	5	58	0.09
Leucine	14	119	0.12
Methionine	5	22	0.23
Phenylalanine	9	54	0.17
Serine	30	109	0.28
Threonine	32	110	0.29
Tryptophan	0	41	0
Tyrosine	14	64	0.22
Valine	20	233	0.09
Arginine	23	87	0.26
Histidine	20	88	0.23
Lysine	25	181	0.14
Ornithine	7	69	0.1

The concentrations of amino acids in the CSF or plasma of healthy human volunteers are shown. Most amino acids are relatively scarce in the brain, with the lone exception being glutamine, which is found at levels equal to its plasma concentration. *Table modified and reprinted with permission from Basun H, Forssell LG, Almkvist O, Cowburn RF, Eklöf R, Winblad B, & Wetterberg L. "Amino acid concentrations in cerebrospinal fluid and plasma in Alzheimer's disease and healthy control subjects."* J Neural Transm Park Dis Dement Sect. *1990;2(4):295-304.*

In general, glutamine metabolism in the brain occurs in the form of a cycle rather than as a unidirectional catabolic process. This series of reactions is known as the glutamine-glutamate cycle, and it is responsible for maintaining the supply of the neurotransmitter glutamate while also preventing constitutive neuronal hyperpolarization. Since glutamate can be converted into glutamine, which is non-neuroactive, glutamine is the preferred form of the compound when in the brain. The glutamine-glutamate cycle occurs when glutamate is released into a glutamatergic synapse by the pre-synaptic neuron. Some glutamate binds to its receptors on the post-synaptic neuron, but there is excess synaptic glutamate. This glutamate is taken up by the surrounding astrocytes, which express high levels of excitatory amino acid transporters (EAATs). Inside the astrocytes, the glutamate is metabolized by glutamine synthetase, and processed into glutamine by the addition of an amino group. This glutamine is then released by the astrocytes and taken up by pre-synaptic neurons. It is within pre-synaptic neurons that glutaminolysis occurs, with glutaminase breaking down glutamine into its constituents glutamate and ammonia. The newly synthesized glutamate is then packaged into vesicles and released into the synapse, and the cycle proceeds again. Notably, cancers and cancer cell lines have exhibited the potential to participate in the glutamine-glutamate cycle, demonstrating a similar phenotype as neurons, with uptake of glutamine and release of glutamate (195-198).

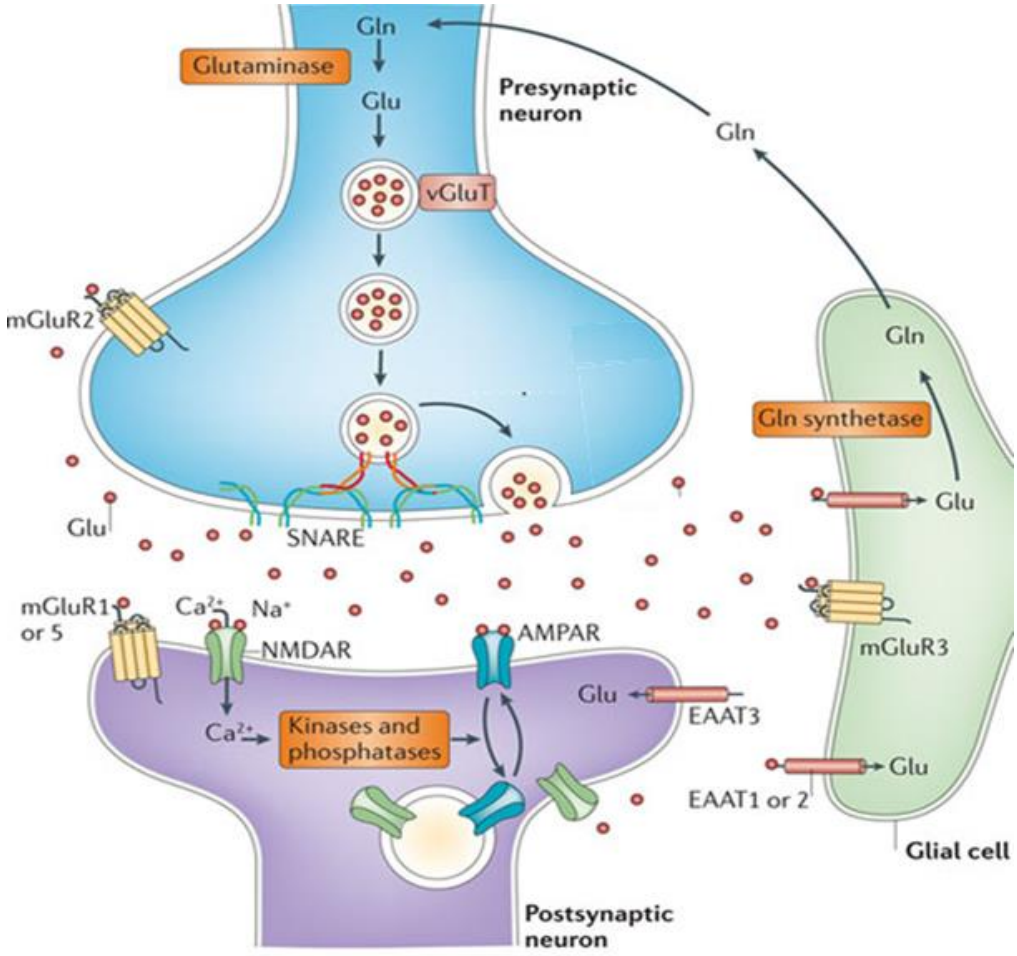

Figure 16. The glutamine-glutamate cycle. Glutamine and glutamate are both present and continuously being exchanged in normal brain physiology. Glutamate-containing vesicles within the presynaptic neuron (blue) fuse to the neuronal cell membrane and are released into the synapse. Some of this glutamate binds to glutamate receptors (mGluR, NMDAR, or AMPAR) on the post-synaptic neuron (purple); the remainder is taken up by neighboring astrocytes via their excitatory amino acid transporters (EAATs) in order to prevent neuronal hyperpolarization. Within the astrocyte, glutamine synthetase converts ammonia and glutamate into glutamine, which is then transported to the pre-synaptic neuron. Within the neuron, then glutamine is converted to glutamate and the process is repeated. *Modified and reprinted with permission from Popoli M, Yan Z, McEwen BS, & Sanacora G. "The stressed synapse: the impact of stress and glucocorticoids on glutamate transmission."* Nature Reviews Neuroscience. *2012 Jan;13(1):22-37*

Moreover, both brain metastasis and primary tumors have previously been reported to exhibit altered glutamine metabolism (199). Specifically, they have both been shown to possess an enhanced ability to utilize glutamine as both an energy source and as a precursor to cellular building blocks, including purines, pyrimidines, and non-essential amino acids (200-202). However, it remains unknown whether brain metastatic cells possess an intrinsic ability to better utilize glutamine, or if this phenotype arises out of selection by the brain environment. Finally, a mechanistic understanding of the regulation and cause of this enhanced glutamine utilization is lacking, meaning that although the phenotype is biologically important and serves as an evolutionary bottleneck for metastatic growth in the brain, it cannot currently serve as a therapeutic target.

1.4 Hypothesis and specific aims

Brain metastasis represents an incredibly selective process that few cancer cells have the capability of performing. While prior studies have focused on those genes that are most differentially expressed between brain and non-brain metastases or between brain metastases and primary tumors, here I propose that kinases may enhance key phenotypes that promote brain metastasis growth. Identification of such kinases could elucidate the functional restraints placed on metastatic cells arriving in the brain and potentially identify new avenues of intervention.

To test this hypothesis, I propose the following two specific aims:

Aim 1: perform an *in vivo* functional genomics screen to identify kinases potentially promoting the growth and formation of breast cancer brain metastasis.

Aim 2: Validate the top potential hit from this screen as functionally important in the process of brain metastasis.

Chapter 2: Materials and Methods

Kinase library preparation

The kinase open reading frame (ORF) library used to perform the *in vivo* kinome screen was an expanded version of the library used in (203), containing 353 ORFs compared to 258 ORFS in the original library. The ORFs were contained in the retroviral vector pWZL-Neo-Myr-Flag DEST, allowing expression of ORF sequences under control of the CMV promoter and stable selection in target cells by G418.

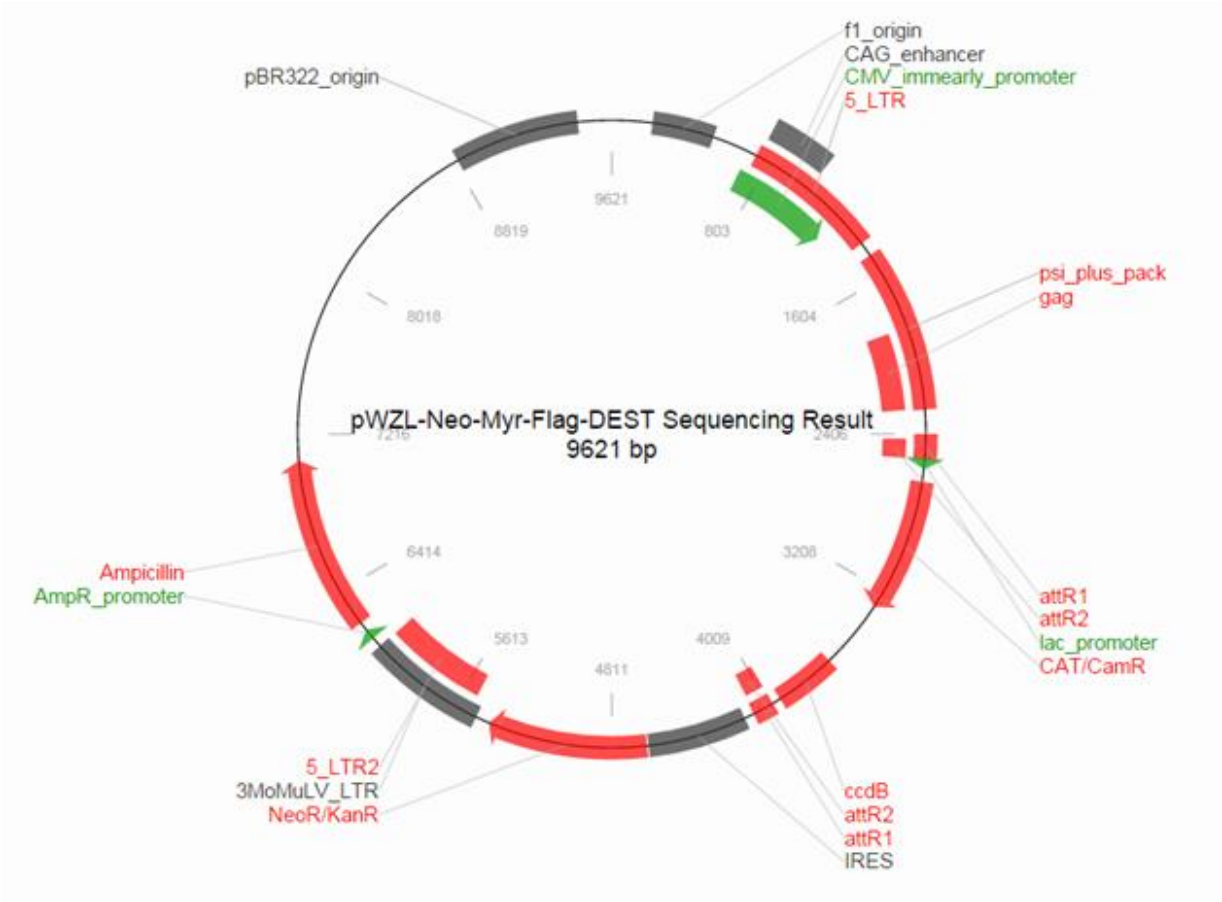

Figure 17. Kinase ORF library is expressed in the pWZL-Neo-Myr-Flag-DEST retroviral vector. Expression clones were generated by Gateway LR reactions, which inserted single kinase sequences between the attR1 sites. *Reprinted from Addgene.*

In order to express the ORFs in a pooled format, five 96-well plates containing glycerol stocks of the ORFs were divided into quadrants of 24 wells. Five microliters of each glycerol

stock was inoculated into 3 mL of LB broth containing 100 µg/mL carbenicillin and grown at 37°C in a Forma Orbital Shaker (Thermo Fisher) at 250 rpm overnight. The following day, pools of ORF clones were generated by combining groups of 24 clones, with each pool representing one quadrant of each kinase library plate. Inoculum from each ORF clone (1 mL per clone; 24 mL per pool) was added to fresh LB media containing 100 µg/mL carbenicillin for a total volume of 100 mL and grown for an additional 4 hours. Following this 4 hour growth period, the inoculated LB broth for each pool was centrifuged at 4000 x g for 10 minutes at 4°C. Plasmid DNA was isolated using a Qiagen Maxiprep kit according to the manufacturer's protocol and quantified using a NanoDrop ND-1000 spectrophotometer.

Cell lines and cell culture

Cell lines were cultured and maintained in Dulbecco's Modified Eagle Medium-Ham's Nutrient Mixture F-12 (DMEM/F12), which contains 17.5 mM glucose and 2 mM glutamine, supplemented with 10% fetal bovine serum (FBS) and 100U/mL penicillin/streptomycin (Gibco). Cells were regularly tested for mycoplasma contamination using the MycoAlert Mycoplasma Detection Kit (Lonza). For later experiments involving Basal Medium Eagle (BME), cells were cultured in BME, which contains 5.56 mM glucose, supplemented with 5% dialyzed FBS. The amount of glutamine added varied by experiment. Cell lines used were obtained from American Type Culture Collection (ATCC), and included Phoenix-AMPHO, MDA-MB-231, HCC1954, and HEK293T. MDA-MB-231.TdTomato (231.TdTomato) and MDA-MB-231.luciferase.GFP (231.luc.GFP) were generated by Gateway cloning and lentiviral transduction, followed by fluorescence-associated cell sorting (FACS) for selection of fluorescent-positive cells.

Fluorescence-associated cell sorting (FACS)

FACS was performed in the Flow Cytometry and Cellular Imaging Core (UTMDACC) on a Becton Dickinson FACS Aria II. Following trypsinization, cells were filtered through 35 µm cell strainers into a 5 mL Falcon tube (Corning) to ensure a single cell suspension. Cells were

analyzed on the FACS Aria II using the FITC and PE channels for 231.luc.GFP and 231.TdTomato cells, respectively; non-fluorescently labeled cells served as a negative control. The top 10% of fluorescent cells were collected and cultured in 200U/mL penicillin/streptomycin to eliminate any potential contamination acquired during FACS. Stably transfected target cells were frozen in aliquots at low passage number.

Retroviral transfection

For retroviral production, the amphotropic Phoenix cell line (ATCC) was used. Phoenix cells are derived from the HEK293T cell line and allow for packaging plasmid-free retroviral production, due to gag-pol and viral envelope protein expression (204). Briefly, wells of a 6-well plate were pre-coated with poly-L-lysine, following by the addition of 2.5 x 10^5 Phoenix cells to each well for a confluency of approximately 70% the following day. Prior to transfection, media was replaced with 1 mL of DMEM/F12 containing FBS. Separate dilutions of 1 µg plasmid DNA and µL LipoD293 reagent (Signagen) were made in serum-free DMEM/F12 and mixed via pipetting, according to the manufacturer's protocol. LipoD293 reagent was then added to the plasmid DNA and vortex-mixed. The liposomal-plasmid DNA mixture was allowed to incubate at RT for 15 minutes, and then added drop-wise to the Phoenix cells. After 18 hours, 1.5 mL of DMEM/F12 media with 10% FBS was added to each well. Two days post-transfection, the retrovirus-containing media was aspirated into a 10 cc syringe fitted with an 18-gauge needle and filtered through a 0.45 µm filter to remove Phoenix cell debris. Target cells were plated at 10% confluency in 6-well plates the day before virus collection, so that at the time of retroviral infection they were 20% confluent. The virus-containing media, which totaled 2 mL due to evaporation and dead volume in the syringe and filter, was added to target cells along with 8 mL of fresh DMEM/F12 with 10% FBS and 10 µL of 5 µg/mL polybrene. After 48 hours of infection and expansion, G418 was added to the target cells to select for plasmid expression.

Lentiviral transfection

Lentiviral transfection was performed similarly to retroviral transfection, except HEK293T cells (293T) were used to produce lentivirus. Since 293T cells do not contain packaging or envelope plasmids, exogenous packaging plasmid DNA (psPAX2 [Addgene plasmid # 12260], gift from Didier Trono) and envelope plasmid DNA (pMD2.G [Addgene plasmid # 12259], gift from Didier Trono) was included at the time of liposomal-DNA complex formation, in a ratio of 4:3:1 (target DNA:psPAX2:pMD2.G). Additionally, as active cell division is dispensable for lentiviral DNA to integrate into the cellular genome, the target cells were plated at 25% confluence and were approaching 50% confluence on the day of infection.

Intracarotid injection

All animal procedures were approved by the UTMDACC Institutional Animal Care and Usage Committee (IACUC). Accordingly, animals received humane care as per the Animal Welfare Act and the NIH "Guide for the Care and Use of Laboratory Animals." For intracarotid injection, 8-week-old female Swiss nude mice were purchased from the Department of Experimental Radiation Oncology at UTMDACC. Mice were anesthetized with ketamine (90 mg/kg body weight) and xylazine (10 mg/kg body weight) and restrained supine on a glass board. Their heads were secured to the board by placing a rubber band placed around the teeth of the upper jaw. The surgical site was disinfected with Betadine and 70% ethanol, and a 1 cm incision made slightly left of the midline, starting from the first mammary gland up into the neck area. The trachea was then exposed by blunt dissection. Under a dissecting microscope, the thin layer muscle was dissected in the carotid muscular triangle to expose the right common carotid artery. The artery was then separated from the vagal nerve and jugular vein. A 5-0 silk suture was placed under the proximal part of the common carotid artery and tied tightly to prevent blood flow from the heart to the injection site. A second ligature was then placed under the common carotid artery distal to the expected injection site and tied loosely. A 3-4 mm sterile cotton ball was briefly soaked in Hank’s Buffered Saline Solution (HBSS) for lubrication and

then placed under the artery between the two sutures to elevate the common carotid artery in order to control the blood regurgitation from the distal part. Cell suspensions (100 µL of cancer cells in HBSS) were drawn into a 1-cc insulin syringe without the formation or presence of bubbles. Cells were then injected slowly and the needle retracted. The second ligature distal to the injection site was quickly tied to prevent leakage of the injected cells, and the ends of the silk ligatures trimmed. The skin of the surgical site was then stapled together and the animals given subcutaneous buprenorphine to relieve pain. The animals were placed on a reusable chemical heating pad until they regained consciousness. At the endpoint of the experiment, mice were euthanized according to IACUC guidelines by CO_2 asphyxiation followed by cervical dislocation.

Mammary fat pad injections

For mammary fat pad injections, 8-week-old female Swiss nude mice were purchased from the Department of Experimental Radiation Oncology at UTMDACC. Cancer cells were prepared at 2x the intended injection concentration in HBSS, and then diluted 50:50 with Matrigel and placed on ice. Mice were anesthetized with ketamine (90 mg/kg body weight) and xylazine (10 mg/kg body weight). The cells were injected into the #3 mammary fat pads using a 25G needle without incision. Injection efficiency was measured the day after injection using *in vivo* imaging system (IVIS) analysis. At the endpoint of the experiment, mice were euthanized according to IACUC guidelines by CO_2 asphyxiation followed by cervical dislocation.

In vivo *imaging system (IVIS) analysis*

Luciferase-labeled tumor cell growth was monitored *in vivo* by IVIS. Imaging was performed in the Small Animal Imaging Facility of UTMDACC on an IVIS-200 (Xenogen). Prior to imaging, mice were injected intraperitoneally with 100 µL of D-luciferin potassium salt (Biosynth) diluted at 15 mg/mL in phosphate-buffered saline (PBS) and anesthetized by

isoflurane/O_2 5 minutes after D-luciferin injection. Luminescent images of tumor cells were captured using the Living Image 3.2 software.

Recovery of cancer cells from in vivo *tumors*

For recovery of cells from *in vivo* brain metastases, tumor cells had to be harvested from the brains of metastasis-bearing animals. Briefly, following euthanasia of a brain metastasis-bearing mouse, the brain was placed in a petri dish on ice. A 10 cm cell culture dish was pre-coated by briefly rinsing with poly-L-lysine to support cell attachment, and a 100 µm cell strainer placed in the dish with 5 mL complete media with 200U/mL penicillin/streptomycin. Forceps were used to place the brain in the cell strainer, and the brain was homogenized using the plunger of a 5 mL syringe, rinsing the strainer periodically with 1 mL of complete media with 200U/mL penicillin/streptomycin (up to 10 mL total) until the strainer was mostly cleared. The brain homogenate was then cultured overnight at 37°C. The following day, the supernatant was removed and added to a second poly-L-lysine coated dish, and fresh media with antibiotics was added to the original dish. After 1-3 days, tumor cell colonies were visible through the floating brain debris. Once colonies were numerous but still relatively low confluency, both primary and secondary plates were trypsinized and combined into single 15 cm dish with normal cell culture media. As cells approached 90% confluency, they were aliquoted and either frozen as a newly established Br subline (HCC1954Br) or used for genomic DNA extraction in the kinase library screen.

RNA isolation

Total RNA was isolated from cells or tissues using RNAzol RT (Molecular Research Center, Inc.) according to manufacturer's instructions. For direct RNA isolation from tissues, brain were minced by with scalpels at time of animal sacrifice and stored at -80°C in RNA stabilizing agent RNAlater (Sigma-Aldrich) until time of RNA isolation. RNA was quantified using an ND-1000 spectrophotometer (NanoDrop).

Complementary DNA (cDNA) synthesis

cDNA was reverse transcribed using the iScript cDNA synthesis kit (Bio-rad), according to manufacturer's instructions. A mixture of random hexamers and oligo(dT) primers were used.

Genomic DNA (gDNA) extraction

gDNA was isolated using the DNEasy Blood & Tissue kit (Qiagen), according to manufacturer's instructions. DNEasy provides column and centrifugation-based DNA isolation. DNA was quantified using an ND-1000 spectrophotometer (NanoDrop).

Polymerase chain reaction (PCR), Reverse transcriptase-PCR (RT-PCR), quantitative PCR (qPCR), and qRT-PCR

PCR to analyze DNA or gene expression of gDNA or cDNA was performed one of the following three ways:

1. presence/absence analysis: PCR of gDNA or RT-PCR of cDNA was performed on a C1000 Touch thermal cycler (Bio-rad) using a Taq-based protocol. For kinase ORF PCR analysis, the optimal annealing temperature was determined to be 52° C and the extension time 4 minutes to accommodate the widest range of target sizes while maintaining the specificity. Custom primer pairs for analyzing the kinase ORFs were designed using VectorNTI software (Invitrogen) and ordered from Sigma and included NeoF (5'-GGATTGCACGCAGGTTCT-3') and NeoR (5'-GCTTCAGTGACAACGTCGAG-3') and KSPF (5'-CAAAGACGATGACGACAAGCA-3') and KSPR (5'-CTTCCTTCACGACATTCAACAGA-3'). PCR products were analyzed on a standard 1% agarose DNA gel using ethidium bromide for ultraviolet (UV) visualization.

2. TaqMan: validated, human-specific, FAM-labeled TaqMan gene expression arrays were purchased from Thermo Fisher. Probes used were CDK16 (Hs00178837_m1), GLS (Hs00248163_m1), GLS2 (Hs00998733_m1), GFPT1 (Hs00899865_m1), and 18S-VIC (4310893E). Due to its labeling with the fluorophore VIC instead of FAM, the primer assay against 18S ribosomal RNA (18S-VIC) could be included in each well as an internal control. qRT-PCR was performed on a StepOne Plus instrument (Applied Biosystems) using KAPA PROBE FAST reagents (KAPA). Results were analyzed using StepOne software and data were normalized to 18S signal.
3. SYBR Green: the same primer pairs as in "presence/absence analysis" above were used. KAPA SYBR FAST reagents were used to perform qPCR on a StepOne Plus instrument. Cycle threshold (Ct) values were calculated for kinase ORF amplification and used to establish sample-specific PCR conditions required to obtain satisfactory quantities of DNA for sequencing.

TOPO cloning

TOPO cloning was performed using a TOPO TA Cloning kit (Thermo Fisher), according to manufacturer's instructions. PCR products with A-overhangs, resulting from Taq-based amplification, were subcloned into pCR-4-TOPO vectors and transformed into competent E. coli. Transformed E. coli were inoculated into LB media and minipreps (Qiagen) were performed. The resulting DNA was Sanger sequenced by the DNA Analysis Core (UTMDACC) from pCR-4-TOPO-specific primers M13F (5'-GTAAAACGACGGCCAG-3') and M13R (5'-TCACACAGGAAACAGCTATGAC-3'). The sequences were then analyzed by the National Library of Medicine's Basic Local Alignment Search Tool (BLAST).

shRNA

shRNA-encoding plasmids expressed in the lentiviral pGIPZ vector were obtained from the shRNA and ORFeome Core at UTMDACC, which distributes shRNA from GE-Dharmacon.

The shRNAs used to target PCTK1 were clones V2LHS_202028, V2LHS_59072, V3LHS_310893, V3LHS_310895, and V3LHS_310898, which are referred to ordinally as shPCTK1-1, shPCTK1-2, shPCTK1-3, shPCTK1-4, and shPCTK1-5 for the remainder of this dissertation. Stable vector-expressing cancer cells were selected both by puromycin resistance and FACS sorting for GFP positivity, as both selective markers are encoded by the vector. Knockdown efficiency was assayed at the RNA and protein levels by qRT-PCR and western blotting, respectively.

Next-generation sequencing (NGS) of kinome screen samples

gDNA from tumor cells recovered from *in vivo* brain metastases was amplified by PCR using kinase vector-specific primers KSPF (5'-CAAAGACGATGACGACAAGCA-3') and KSPR (5'-CTTCCTTCACGACATTCAACAGA-3'). The number of PCR cycles required to amplify the minimum amount of DNA required for NGS barcoding was empirically determined by SYBR Green-based qPCR. Following kinase vector-specific amplification, column-based purification of PCR products was performed using MinElute columns (Qiagen). DNA barcoding, adapter ligation, and library preparation were performed using the NEXTflex DNA Sequencing Kit (Bioo Scientific) according to the manufacturer's instructions, with unique barcodes added to each *in vivo* sample. The resulting barcoded DNA libraries were analyzed by a MiSeq instrument (Illumina) using 150-base pair (bp), paired-end (PE) sequencing. Reads were normalized to the total total reads for each barcode, such that each *in vivo* sample had equal representation using MiSeq Reporter. Fastq files from Illumina paired-end sequencing were mapped to human transcriptome version hg19 using tophat2 (https://ccb.jhu.edu/software/tophat/index.shtml). Mapped reads were converted to bedGraph files using HOMER (http://homer.salk.edu/homer/). For each kinase in each pool of the screen, the expression was estimated by collecting all bedGraph reads falling inside the gene boundaries (based on refseq gene definitions, available at http://hgdownload.soe.ucsc.edu/downloads.html).

RNA sequencing (RNA-seq) of human brain metastases

The RNA-seq data presented about gene expression within human brain metastases was obtained via a collaboration with Drs. Jodi Saunus and Sunil Lakhani at the University of Queensland, and the methods used for RNA-seq are published (205). Briefly, RNA-seq was performed on 32 human brain metastases. RNA was extracted from fresh-frozen brain metastasis surgical samples using the Qiagen AllPrep Kit, according to the manufacturer's instructions, and quantified using a Bioanalyser (Agilent). From their publication:

> The protocol for Ribosomal depletion and RNA library construction was performed on 1 µg total RNA from each sample, using TruSeq Stranded Total RNA kit with Ribo-Zero Human/Mouse/Rat Set A (Illumina, cat. no. RS-122-2201). Libraries were prepared according to the manufacturer's protocol (TruSeq Stranded Total RNA Sample Prep Guide), with minor modifications to the fragmentation time (0 min fragmentation was used to increase the insert length). The libraries were quality checked and quantified using the Bioanalyser High Sensitivity DNA kit (Agilent).
>
> All the RNA libraries were indexed, allowing multiplexed sequencing. Prior to on-board cluster generation and sequencing run, the pooled library was denatured by using 0.1 N NaOH and diluted to the required concentration (7 pM). Libraries were sequenced as 100 bp paired-end reads on the Illumina HiSeq 2000. RNA data were analysed using RSEM [7] and a normal expected count was used for expression values (using TMM normalization in the edgeR package), which was then transformed to normalized counts/million.

From Saunus et al (2015), Integrated genomic and transcriptomic analysis of human brain metastases identifies alterations of potential clinical significance. J. Pathol., 237: 363–378. doi: 10.1002/path.4583. Reprinted with permission

Hard agar assay

In brief, 1 mL of DMEM containing 23% FBS and 0.6% agar (Lonza) was plated into individual wells of 24-well plates (BD Biosciences). Cancer cells were trypsinized and resuspended in DMEM containing 10% FBS. The resulting cell mixture was then passaged through a 40-µm cell strainer (BD Biosciences) to generate a single-cell suspension. Cells were resuspended at a density of 4000 cells/well in 1 mL of DMEM containing 23% FBS and 0.9% agar. This cell-containing mixture was then pipetted gently over the bottom layer of agar (0.6%) in the wells. The numbers and diameters of tumor colonies were calculated using a microscope when the tumor colonies became visible, and the experiment was terminated after 60 days.

Western blot analysis

Total cell lysates were obtained by resuspending cell pellets in immunoprecipitation (IP) lysis buffer (20 mM Tris [pH 7.5], 150 mM NaCl, 1 mM EDTA, 1 mM EGTA, 1% Triton X-100, 2.5 mM sodium pyrophosphate, 1 mM beta-glycerolphosphate, 1 mM sodium orthovanadate, 1 mM PMSF, and protease inhibitor cocktail). Following addition of lysis buffer, lysates were sonicated or passed through syringe with 22G needle 15 times followed by centrifugation. The supernatant was transferred to a new tube, and protein concentration was determined by BCA protein Assay Kit (Pierce), using known amounts of bovine serum albumin (BSA) to standardize protein concentration. Cell lysates containing equal amounts (20-40µg, depending on experiment) of protein were subjected to electrophoresis using sodium dodecosulfate-polyacrylamide gel elecotrophoresis (SDS-PAGE) and transferred to polyvinyldifluoride (PVDF) membranes (Bio-Rad). PBS-Tween (PBST) was prepared as 0.1% (v/v) of Tween 20 in PBS. Membranes were blocked with 5% milk PBST for 30-60 minutes at room temperature, followed by primary antibody incubation overnight at 4°C. After three washes with PBST (5 minutes each), membranes were incubated with HRP-conjugated secondary antibody (in 5% milk in PBST) for 60 minutes at room temperature followed by three 5-minute washes with PBST, and signal was detected by enhanced chemiluminescence (ECL) (Amersham) per the manufacturer's instructions. Antibodies used were PCTK1: rabbit anti-human CDK16, clone HPA001366 (Sigma) and mouse anti-β-actin, clone AC-74 (Sigma)

Invasion

Transwell invasion assay was performed as previously described, with some modifications (206). 15 µL of Matrigel (Corning) diluted 1:4 in PBS was added to the top chamber of a 24-well transwell plate (Millipore). After Matrigel polymerization, the bottom chambers were filled with 600 µL DMEM/F12 medium containing 10% FBS. The top chambers were seeded with 5×104 cancer cells per well in 200 µL serum-free medium. After 24 hours,

the experiment was terminated by scraping remaining cells off of the top chamber with a cotton swab. Invaded cells were fixed in 4% paraformaldehyde and stained with 0.05% Crystal Violet. Images were taken using an Olympus digital microscope and invading cells were counted manually. The assays were performed in technical and biological triplicate.

Migration

Transwell migration assay was performed as previously described, with some modifications (206). The top chambers of a 24-well transwell plate (Millipore) were seeded with 3×10^4 cancer cells in 200 µL DMEM/F12 serum-free medium per well. Then, 300 µL DMEM/F12 medium containing 10% FBS was added to the bottom chamber. After 18 hours, the experiment was terminated by scraping remaining cells off of the top chamber with a cotton swab. Migrated cells were fixed in 4% paraformaldehyde and stained with 0.05% Crystal Violet. Images were taken using an Olympus digital microscope and invading cells were counted manually. The assays were performed in technical and biological triplicate.

Glutamine uptake and metabolite tracing/mass spectrometry (MS)

For experiments measuring rates of glutamine uptake and glutamate release over time, samples were analyzed on a 2900D Biochemistry Analyzer (YSI). MassLynx software version 4.1 was used for data acquisition and analysis of glutamate and glutamine. Spectra of enriched peaks were compared against reference spectra.

Immunohistochemistry (IHC)

IHC staining of PCTK1 on formalin-fixed, paraffin-embedded samples was performed using rabbit anti-human CDK16, clone HPA001366 (Sigma). Briefly, slides were deparaffinized by heating on a slide warmer for 20 minutes, followed by rehydration via a series of 3-minute wash steps. Slides were submerged in xylene 2x, 100% ethanol 2x, 90%

ethanol 1x, 80% ethanol 1x, and 70% ethanol 1x, and transferred to running water to rinse. Heat-induced antigen retrieval was then performed using sodium citrate buffer, pH 6.0, in a pressure cooker for 10 minutes. Blocking of non-specific epitope binding was achieved with Protein Block (Dako). Primary antibody incubation was performed overnight at 4°C, at an empirically determined dilution of 1:100 in Antibody Diluent (Dako). The next day, slides were incubated for 15 in 0.3% H_2O_2 in Tris-buffered saline (TBS) to quench their endogenous peroxidase activity. Secondary antibody staining was then performed using the Polink-2 HRP Plus Rabbit DAB system (GBI) according to manufacturer's protocol, except TBS and TBS-Tween (TBST) were used in place of PBS and PBST, respectively. Following secondary antibody incubation and chromogen development, slides were counterstained with hematoxylin, dehydrated, and mounted using organic mounting media.

Chapter 3: Kinome Screen

To test whether heretofore unknown kinases may indeed be drivers of brain metastasis, we set out to perform an unbiased *in vivo* screen. MDA-MB-231 cells were selected as the cell background for this screen because they were originally derived from the pleural effusion of a patient with claudin-low TNBC, and TNBC has the highest relative rate of brain metastasis among breast cancer subtypes. First, pools of retroviral constructs were used to infect MDA-MB-231.luciferase.GFP (231.luc.GFP) cells at low multiplicity of infection (MOI) to avoid integration of multiple kinases into a single cell. G418 selection of the kinase-overexpressing cells began at a concentration of 400 µg/mL and increased by 200 µg/mL every 3 days, up to a total concentration of 1 mg/mL. At this point, (14 days post-infection) RNA was isolated from some of the cells and analyzed by RT-PCR targeting a 250-bp sequence within the Neomycin resistance (NeoR) marker, which is contained in in the kinase library vector as a selection marker and conveys G418 resistance to eukaryotic cells. The results, seen in Figure 18, showed a band at the expected size of 250 bp.

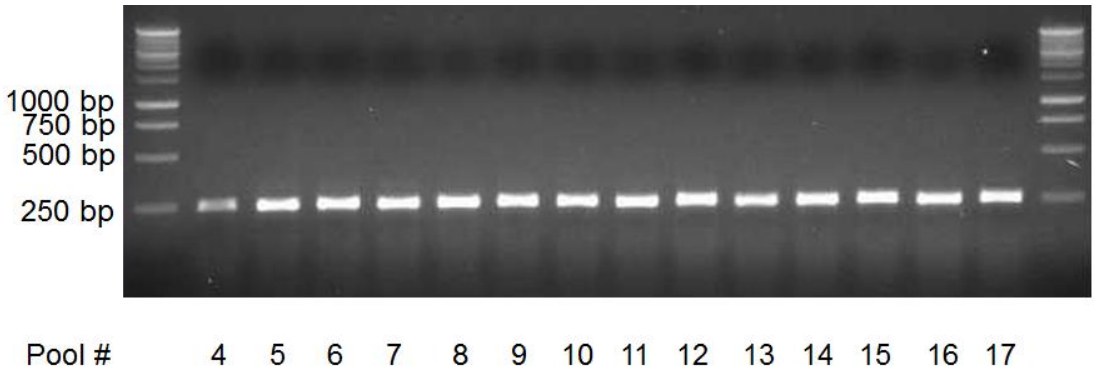

Figure 18. Neomycin resistance marker is present in MDA-MB-231 cells transfected with kinase ORF pools. Following retroviral transduction with kinase pools and G418 selection, RT-PCR was performed using primers specific for a 250-bp portion of the G418 resistance marker.

The kinase pool-overexpressing 231.luc.GFP and corresponding control cells, which expressed tandem dimer Tomato, a bright RFP [tdTomato, (207)], were used for the brain metastasis growth screen. The cells were mixed at a 3:1 ratio (kinase pool:control), as the kinase pool population consisted of numerous (up to 24) subpopulations of cells overexpressing each kinases of the pool individually, and injected into 5 animals per pool via the left common carotid artery, see Figure 19 for details. Luciferase was detected in the mice 24 hours later, thus ensuring successful injections. It was expected that if no kinases in a given pool imbued the 231.luc.GFP cells with a growth advantage, the mice would require euthanasia around day 60 post-injection, based on previous observations on the growth characteristics of the MDA-MB-231 cell line. Additionally, as the internal control cells were labeled with tdTomato instead of GFP, pools containing potential “hits” should lead to a much higher ratio of GFP:tdTomato signal by fluorescence imaging.

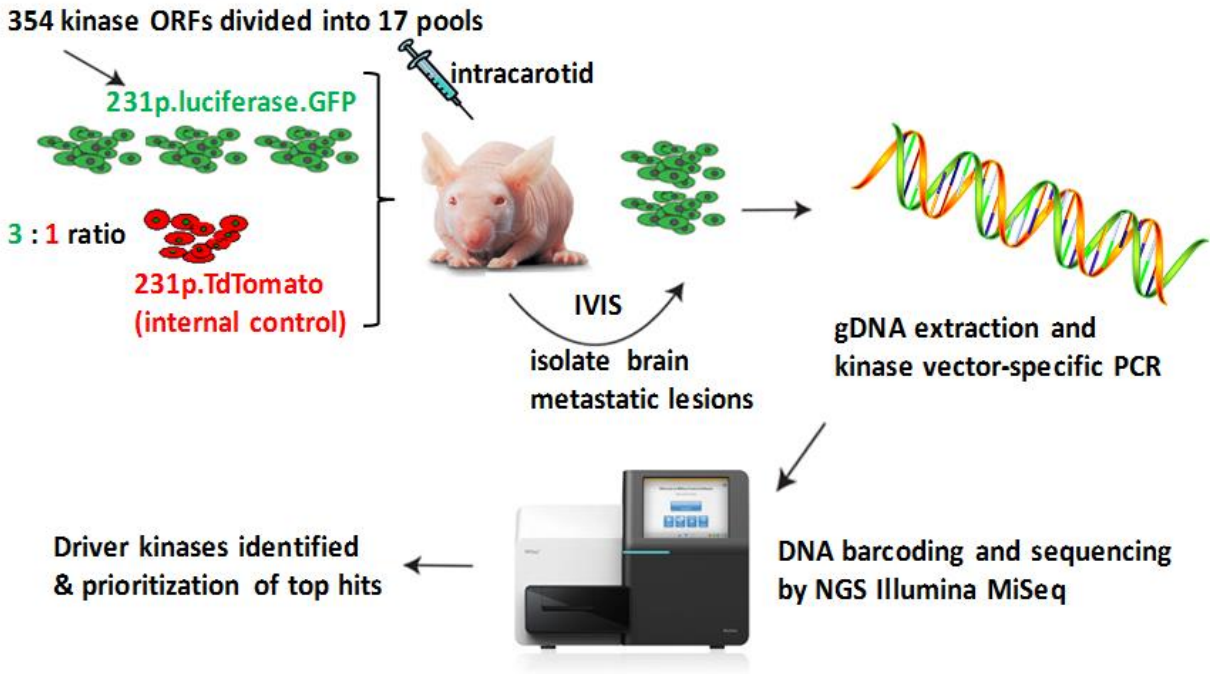

Figure 19. Schematic of *in vivo* kinome screen for drivers of brain metastatic growth. MDA-MB-231 parental cells (231p) stably expressing luciferase, GFP, and pools of up to 24 kinases (231p.luciferase.GFP) were mixed with 231p cells expressing TdTomato and an empty pWZL-Neo-Myr-Flag-DEST vector (231p.TdTomato). Cells were mixed at a 3:1 ratio of kinase pool:vector and 2 x 10^6 cells were injected into nude mice. When animals displayed neurological symptoms and their heads were determine to be extremely luciferase-positive by IVIS, mice were sacrificed and brain lesions isolated using a dissecting microscope based on GFP-positivity. Portions of the lesions were subjected to direct RNA extraction, while the remainder was dissociated and the cells cultured *in vitro* as passage 0. gDNA was extracted from the recovered cells and kinase vector sequences amplified by targeted PCR. This DNA was sequenced by MiSeq, yielding a quantitative readout of *in vivo* selection.

Indeed, most of the kinase pools led to dramatic phenotypes, with mouse survival reduced from 60 days to approximately 40 days, which is more reminiscent of the brain-selected line MDA-MB-231.Br (208) than the parental MDA-MB-231 cell line. Prior to euthanasia, the

mice were imaged by IVIS to determine luciferase signal (Figure 20). When the mouse brains were examined for fluorescence by dissecting microscope, it was evident that the GFP signal was predominant; any tdTomato signal observed in brains of mice sacrificed at early time points was of relatively minor contribution (Figure 21).

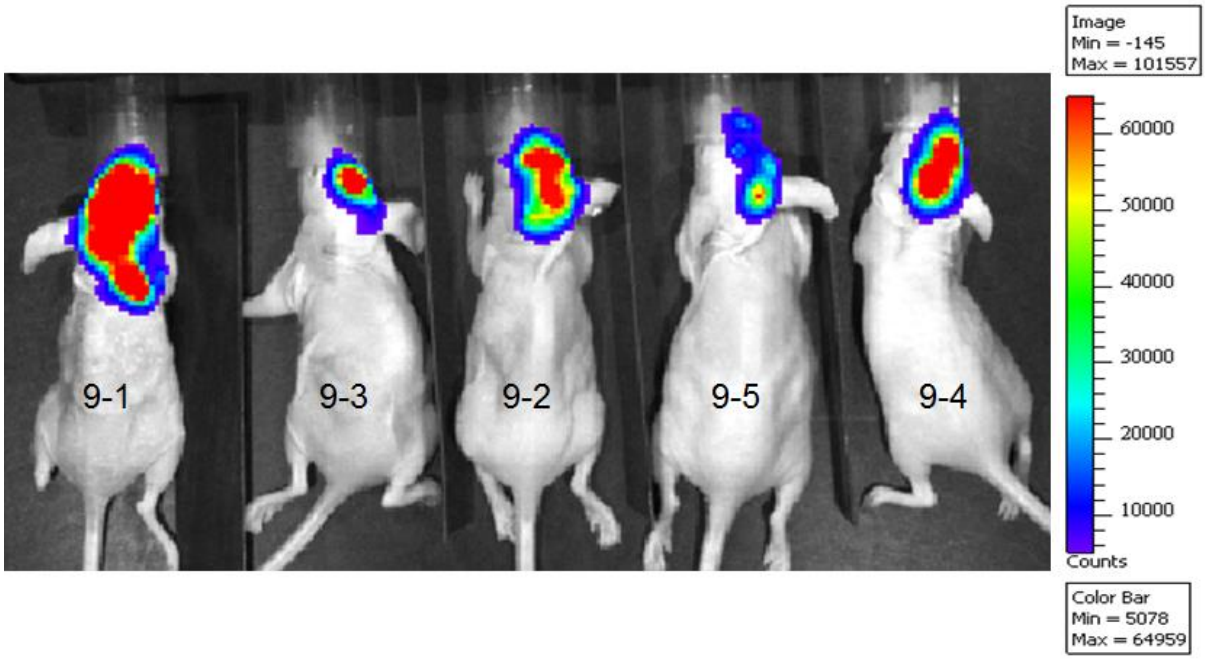

Figure 20. IVIS images of pool 9 mice 45 days post-injection. Mice from pool 9 are shown for representative purposes. Mice are numbered 9-1 to 9-5 to reflect order in which they were euthanized. Mice 9-1, 9-2, and 9-3, which appear emaciated and hunched in this image, were sacrificed immediately following IVIS imaging, with 9-4 and 9-5 following 3 days later.

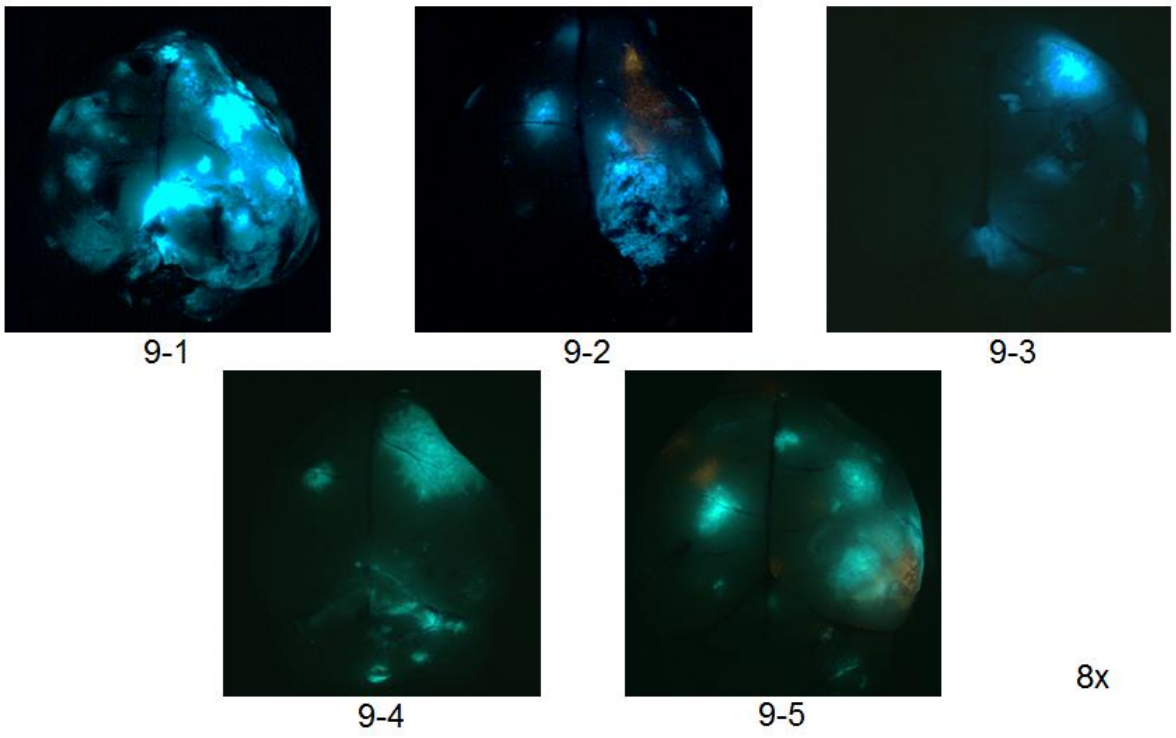

Figure 21. Mouse brains are strongly positive for GFP following injection with pool 9-overexpressing cells. Mouse brains were removed and examined using a SteREO Discovery.V20 dissecting microscope (Zeiss). While some TdTomato signal was visible in the brains of injected mice (9-2 and 9-5), the lesions were predominantly GFP-positive. Fluorescent images shown are at 8x magnification.

After imaging brains for fluorescence, the tissue was finely minced; half was stored in RNAlater until the time of RNA extraction and half was used in an attempt to recover the *in vivo*-selected tumor cells. The *in vivo*-derived cells recovered in this way were aliquoted when they reached 70-80% confluence and stored for later analysis (Figure 22, Table 4).

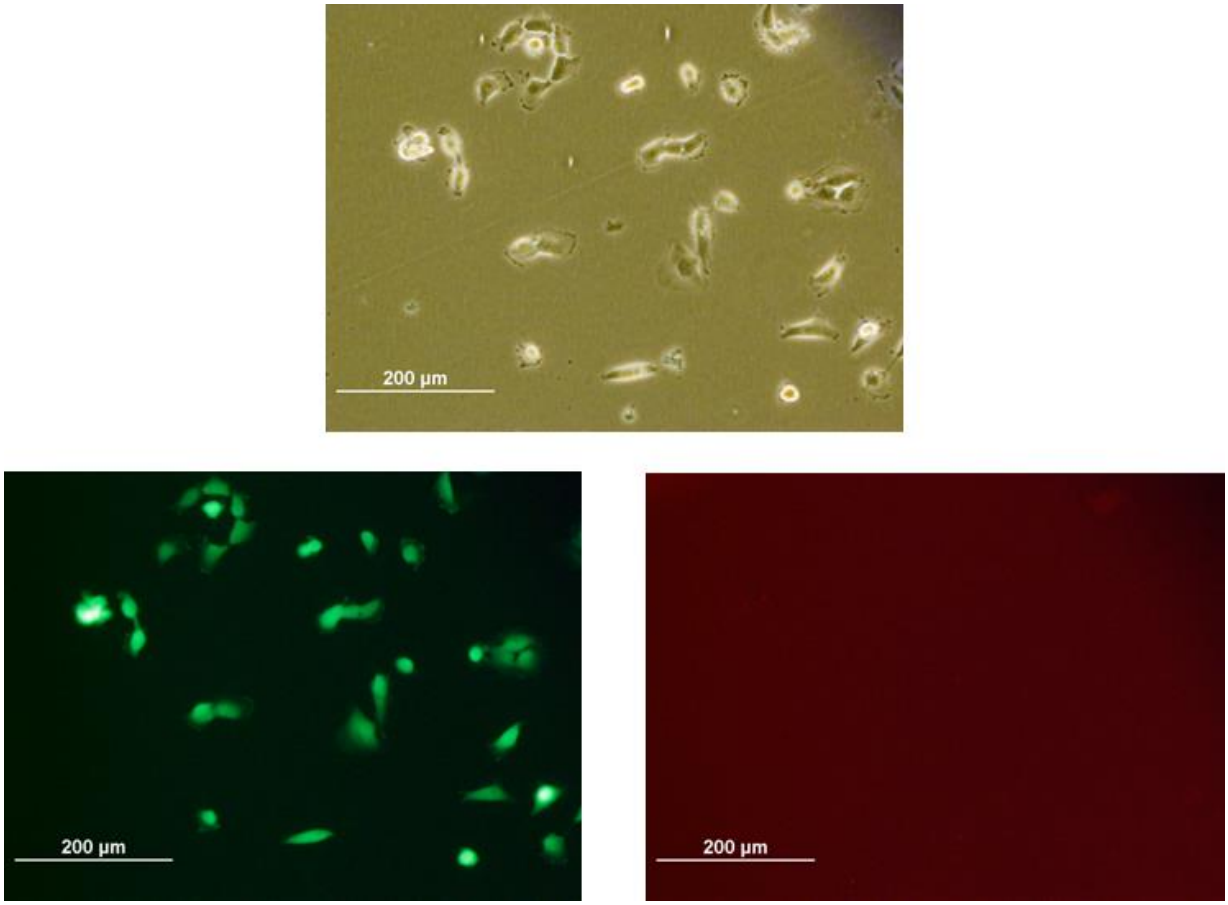

Figure 22. Brain metastasis cells recovered *in vitro* are GFP-positive. Fluorescence signals from tumor cells that were successfully recovered from *in vivo* lesions were assessed by an Olympus IX70 fluorescent microscope. Nearly all of the tumor cells were GFP-positive and TdTomato-negative. Images shown here are from mouse 9-1 (pool 9). Images were acquired using a 10x objective and DPController software (Olympus).

Table 4. Summary of sample information for kinome screen experiments

Pool number	Animals in group	Animals sacrificed before day 60	Animals from which cells successfully recovered
1	4	4	2
2	5	5	4
3	4	4	2
4	5	4	4

5	5	5	4
6	5	5	1
7	5	5	5
8	5	5	4
9	5	5	5
10	5	0	0
11	4	4	3
12	5	0	0
13	5	5	3
14	6	6	6
15	5	5	3
16	5	0	0
17	5	4	2

To determine which kinases were responsible for the growth advantages observed *in vivo*, it was necessary to employ genetic sequencing techniques. Initially, RNA isolated directly from brains or those recovered cell lines successfully established from brain metastases was subjected to kinase vector-specific RT-PCR and analyzed by gel electrophoresis. The results showed that the banding patterns were indeed different in the *in vivo*-selected brain tissue and recovered brain metastatic cells compared to their corresponding pre-injection controls (Figure 23).

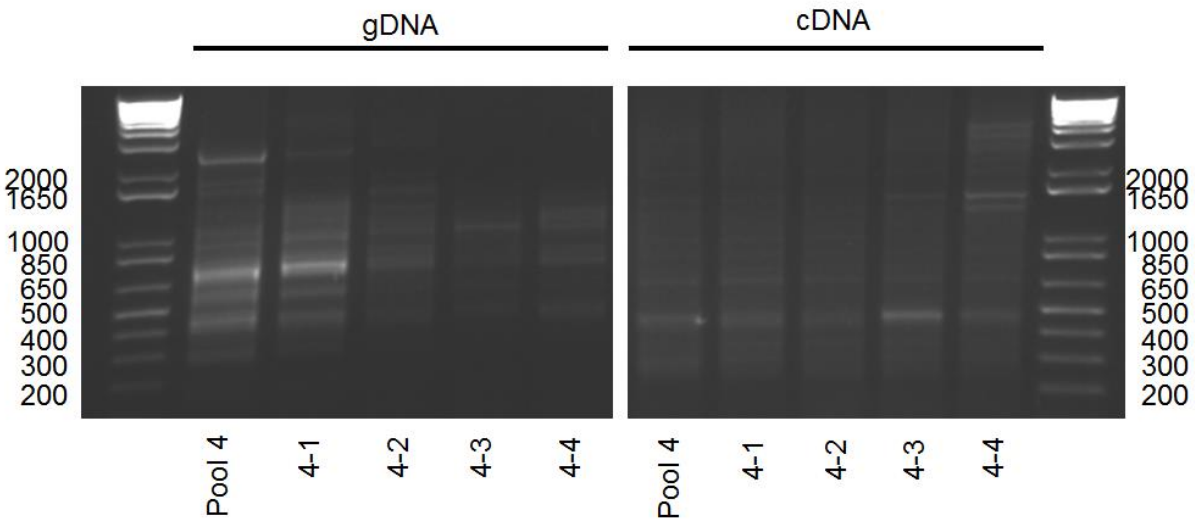

Figure 23. PCR analysis provides evidence of selection occurring *in vivo*. DNA gel showing PCR (left) and RT-PCR (right) with kinase vector-specific primers. Banding pattern strikingly differs between *in vitro*, pre-injection cells (Pool 4) and tumor cells recovered from brain metastasis-bearing animals (4-1 through 4-4). 25ng of gDNA or 50ng of cDNA served as PCR templates.

Following RT-PCR with *Taq* DNA polymerase, TOPO cloning was used to isolate individual kinase sequences. The pooled PCR products representing each *in vivo* sample were TOPO cloned, and 10 bacterial clones per each *in vivo* sample were grown in LB and miniprepped. The resulting DNA was sequenced, and this approach identified 8 kinase sequences isolated from *in vivo* samples from pools 1 to 5, included below in Table 5.

Table 5. Kinase sequences detected by TOPO cloning of cDNA from recovered tumor cells from pools 1 to 5.

NCBI Gene ID	Official Symbol	Gene Description	RefSeq Accession Number
1163	CKS1B	CDC28 protein kinase regulatory subunit 1B	NM_001826
1111	CHEK1	CHK1 checkpoint homolog (S. pombe)	NM_001274

7371	UCK2	uridine-cytidine kinase 2	NM_012474
3932	LCK	lymphocyte-specific protein tyrosine kinase	NM_005356
5127	PCTK1	PCTAIRE protein kinase 1, transcript variant 2	NM_006201
150274	RP3-366L4.2	J-type co-chaperone HSC20	NM_172002
805	CALM2	calmodulin 2 (phosphorylase kinase, delta)	NM_001743
8877	SPHK1	sphingosine kinase 1	NM_021972

Seeking a more quantitative and comprehensive identification of all those kinase sequences enriched *in vivo*, we set out to use NGS to analyze the brain metastatic cells recovered from the mice. Because of the stable retroviral integration of the kinase ORFs into the genome of the MDA-MB-231 prior to tumor cell injection, it was possible to analyze the gDNA of the tumor cells for kinase enrichment. gDNA was extracted from the pre-injection and recovered tumor cells, and quantitative PCR using kinase vector-specific primers performed on the gDNA (Figure 23, left). This DNA was barcoded and sequenced by MiSeq (Illumina). The raw sequence files were mapped to the human genome and the total read count of each barcode normalized by Dr. Jun Yao, a bioinformatician in the Department of Molecular and Cellular Oncology at UTMDACC. The reads of each kinase sequence in every brain metastasis-derived sample were compared relative to their expression in the pre-injection kinase-overexpressing cells (Figure 24), and the kinases were ranked according to average enrichment *in vivo.* Focusing only on those kinases enriched (relative expression >1) in multiple animals resulted in a list of 31 sequences (Table 6).

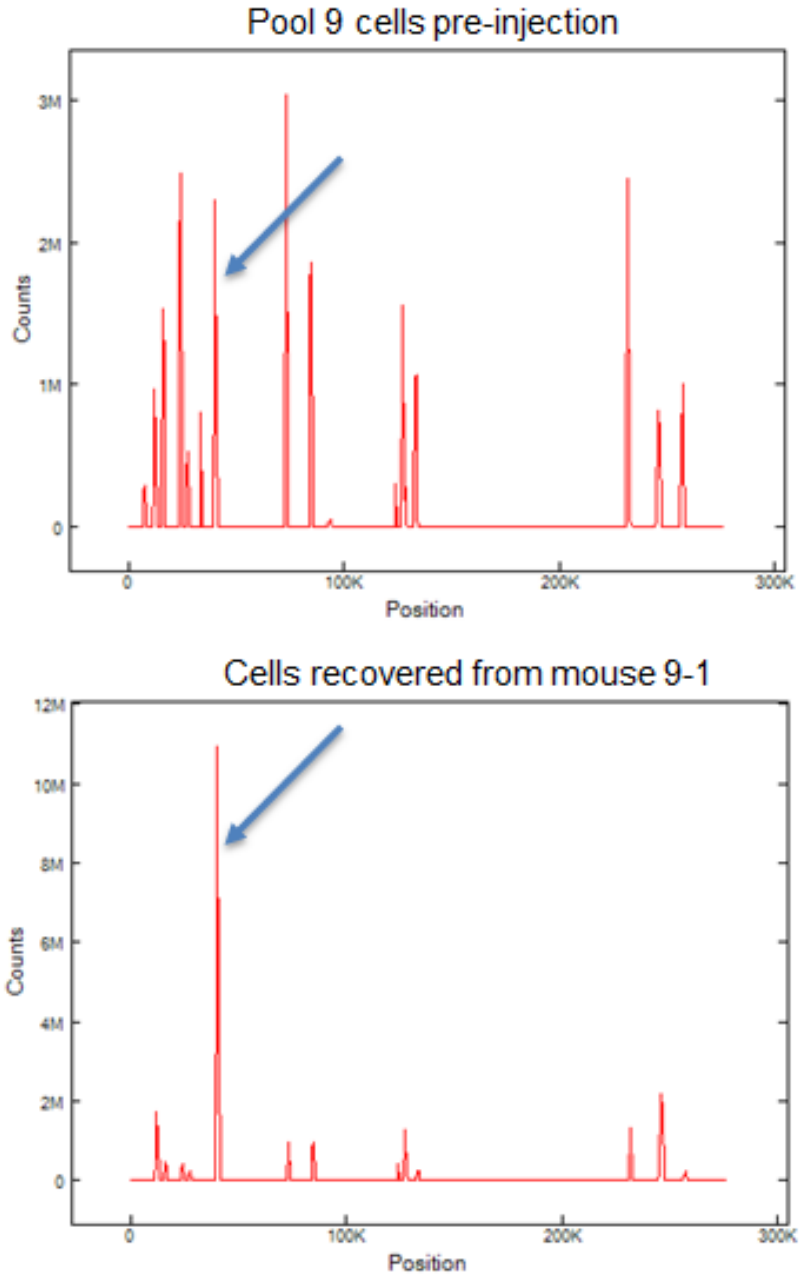

Figure 24. Coverage plots reveal relative sequence enrichment following *in vivo* selection. Comparison of kinase sequence read counts prior to and following *in vivo* selection demonstrates appreciable loss of most sequences *in vivo*. The lone exception, indicated with a blue arrow, is MAPK12, which had its read count rise from just over 2 million to 11 million. Coverage plots were generated with MiSeq Reporter.

Table 6. Kinase sequences enriched *in vivo* as determined by NGS.

NCBI Gene ID	Official Symbol	Gene Description	RefSeq Accession Number
79934	ADCK4	aarF domain containing kinase 4	NM_024876
269	AMHR2	anti-Mullerian hormone receptor, type II	NM_020547
695	BTK	Bruton agammaglobulinemia tyrosine kinase	NM_000061
805	CALM2	calmodulin 2 (phosphorylase kinase, delta)	NM_001743
808	CALM3	calmodulin 3 (phosphorylase kinase, delta)	NM_005184
814	CAMK4	calcium/calmodulin dependent protein kinase IV	NM_001744
1020	CDK5	cyclin-dependent kinase 5	NM_004935
8851	CDK5R1	cyclin-dependent kinase 5, regulatory subunit 1 (p35)	NM_003885
1198	CLK3	CDC-like kinase 3	NM_001292
26007	DAK	dihydroxyacetone kinase 2 homolog	NM_015533
2444	FRK	fyn-related kinase	NM_002031
3099	HK2	hexokinase 2	NM_000189
3985	LIMK2	LIM domain kinase 2	NM_005569
5609	MAP2K7	mitogen-activated protein kinase kinase 7	NM_145185
6300	MAPK12	mitogen-activated protein kinase 12	NM_002969
5598	MAPK7	mitogen-activated protein kinase 7, transcript variant 2	NM_002749
57787	MARK4	MAP/microtubule affinity-regulating kinase 4	NM_031417
10298	PAK4	p21(CDKN1A)-activated kinase 4	NM_001014831
5106	PCK2	phosphoenolpyruvate carboxykinase 2 (mitochondrial)	NM_004563
5127	PCTK1	PCTAIRE protein kinase 1, transcript variant 2	NM_006201
5211	PFKL	phosphofructokinase, liver	NM_001002021
5213	PFKM	phosphofructokinase, muscle	NM_000289

10654	PMVK	phosphomevalonate kinase	NM_006556
5567	PRKACB	protein kinase, cAMP-dependent, catalytic, beta	NM_002731
5568	PRKACG	protein kinase, cAMP-dependent, catalytic, gamma	NM_002732
5580	PRKCD	protein kinase C, delta	NM_006254
5584	PRKCI	protein kinase C, iota	NM_002740
6794	STK11	serine/threonine kinase 11	NM_000455
83983	TSSK6	testis-specific serine kinase 6	NM_032037
7371	UCK2	uridine-cytidine kinase 2	NM_012474
51530	ZC3HC1	zinc finger, C3HC-type containing 1	NM_016478

Generating such an extensive list of potential novel drivers of brain metastatic growth was promising; however, as the kinome screen was performed in a pooled format, the possibility existed that some of the would-be hits were mere artifacts of the screening process, passenger genes being buoyed by their neighbors. Therefore, all the potential hits require functional validation before being truly implicated in brain metastasis. In order to do so, the ORFs representing the potential “hit” kinases were individually used to generate stable MDA-MB-231 transfectants. As it would have been time- and cost-prohibitive to interrogate all 31 ORFs in mice, another filter for hit prioritization proved necessary. Tumor cell growth in hard agar (0.9%) has been previously established to be indicative of brain metastasis-initiating potential (209), a secondary functional screen was performed on single ORF-overexpressing cell lines. The assay indeed demonstrated differences among the potential hits in their ability to form colonies in hard agar, further informing “hit” ranking (Figure 25, Table 7).

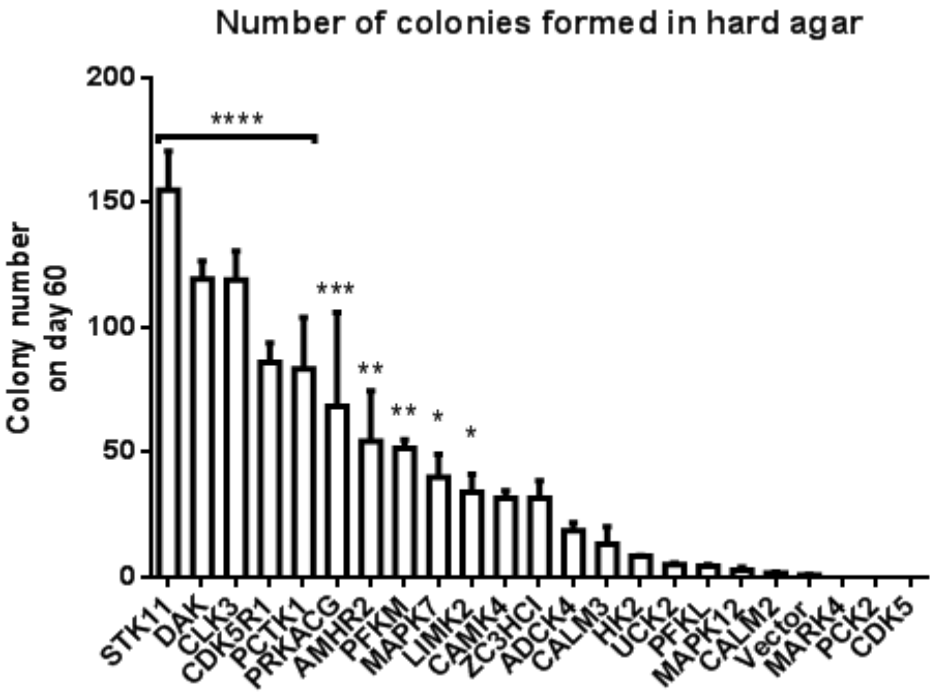

Figure 25. *In vitro* hard agar growth assay of single kinase-overexpressing MDA-MB-231 cells shows that overexpression of most kinases enhances colony formation. Colonies >75 μm following 60 days of culture were counted. One-way ANOVA showed significant difference between groups, $F(22,46)=15.56$, $p<0.0001$. Fisher's LSD multiple comparisons test showed that the top 10 cell lines had a statistically significant colony-forming advantage over the vector group, indicated with * on the graph. Experiments were performed in triplicate. Error bars indicate SEM of colony number per well.

Because the kinome screen was based on the principle of generating artificial heterogeneity prior to testing for *in vivo* selection, it was necessary to demonstrate that the newly identified hits are actually expressed in human brain metastases and did not exist exclusively in the artificial setting of this screen. Through a collaboration with the a group from the University of Queensland (Australia), we examined the expression of all potential hits by RNA-seq of a collection of 32 human brain metastasis specimens, including 8 cases of breast

cancer (205). Analysis showed again showed a wide range of expression, with CALM2 and HK2 expressed in the top 5% of all expressed genes (Figure 26, Table 7).

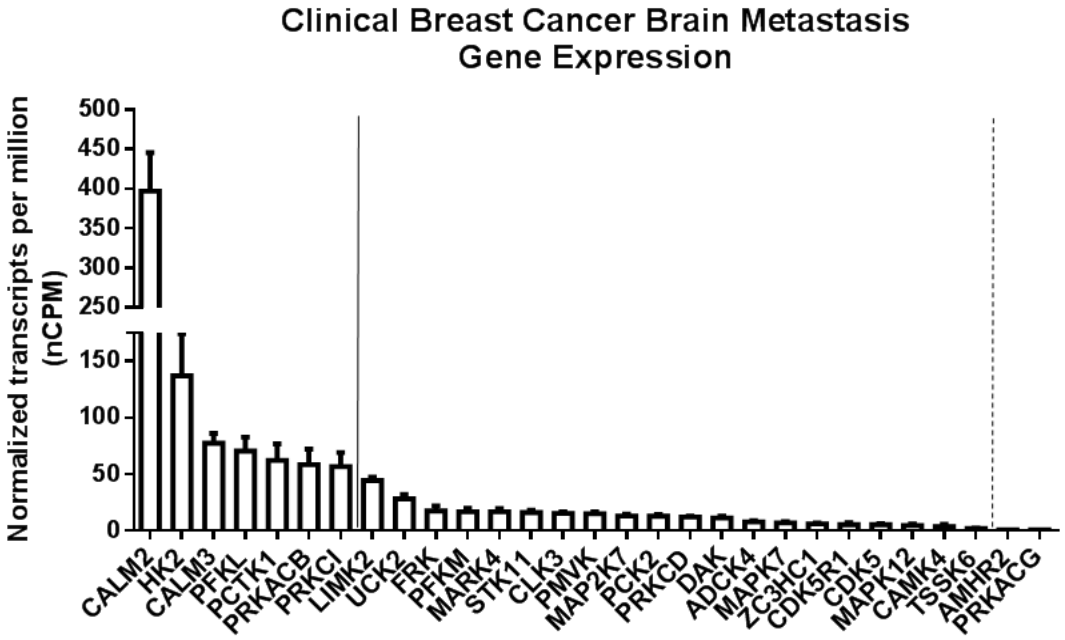

Figure 26. Expression of putative kinase hits in human brain metastasis according to RNA-seq. Genes are ordered according to average expression (normalized to transcripts per million reads, nCPM) in all samples. Solid gray line distinguishes those genes expressed as upper outliers, calculated as [Q3+(1.5 x IQR)]. Dashed gray line indicates those genes considered as "expressed," as their transcript expression level was greater than 1 transcript per million. Error bars indicate SEM of nCPM.

The expression data in brain metastasis was then combined with the hard agar colony-forming ability to rank the potential hit kinases in order of likelihood of their contribution to accelerated brain metastatic growth. The top-ranking potential hit thus identified was PCTK1 (Table 7).

Table 7. PCTK1 is the top candidate kinase based on hard agar colony-forming ability and expression in human breast cancer brain metastases.

Gene	Hard agar colony formation rank	Human brain metastasis expression rank	Rank-sum
PCTK1	5	5	10
STK11	1	13	14
CALM3	14	3	17
CLK3	3	14	17
HK2	15	2	17
PRKACB	11	6	17
LIMK2	10	8	18
PRKCI	11	7	18
PFKM	8	11	19
CALM2	19	1	20
DAK	2	19	21
PFKL	17	4	21
FRK	11	10	21
UCK2	16	9	25
PMVK	11	15	26
CDK5R1	4	23	27
MAP2K7	11	16	27
PRKCD	11	18	29
MAPK7	9	21	30
MARK4	20	12	32
ADCK4	13	20	33
ZC3HCI	12	22	34
AMHR2	7	28	35
PRKACG	6	29	35

CAMK4	11	26	37
PCK2	21	17	38
TSSK6	11	27	38
BTK	11	30	41
PAK4	11	31	42
MAPK12	18	25	43
CDK5	22	24	46

Chapter 4: Investigation and validation of PCTK1 as a driver of brain metastatic growth

PCTK1, also known as cyclin-dependent kinase 16 (CDK16), is a serine/threonine kinase originally named PCTAIRE-1 after its discovery in 1992 (210). It exists in 3 isoforms, with isoform 1 encoding a protein of 55.7 kilodaltons (kDa) and isoforms 2 (63.4 kDa) and 3 (56.4 kDa) possessing extended N-terminal domains. It is classified as an atypical cyclin-dependent kinase (cdc2/CDC28-related protein kinase gene family) family member, as its cyclin-binding domain contains a serine to cysteine substitution (i.e., PCTAIRE instead of PSTAIRE) (210). This non-traditional cyclin-binding domain leads to binding of cyclin Y (CCNY) (211). A PCTK1 knockout mouse model revealed that PCTK1 is indispensable for spermatogenesis; homozygous knockout male mice are infertile, while females produce viable offspring (211). No other phenotypes of the knockout model were noted (211). However, commensurate with its mRNA expression in the brain, PCTK1 has also been shown to regulate neuronal differentiation and outgrowth (212). Intriguingly, this kinase has also been identified as a substrate of CDK5, another kinase identified in the previous *in vivo* kinome screen (213). Phosphorylation of PCTK1 by activated CDK5 is required for its activity in dendrite development (214).

In spite of the gains made in better understanding the physiological roles of PCTK1, a great deal of its characterization remains elusive. First and foremost, as a kinase, PCTK1 is thought to primarily function through phosphorylation of downstream targets. Indeed, it possesses an activation loop and has been shown to phosphorylate N-ethylmaleimide-sensitive fusion protein (NSF) (215), KAP0 (216), and cyclin Y (217). However, elegantly designed studies attempting to characterize a consensus substrate motif for PCTK1 have failed to agree with each other (216, 218), although they did both conclude that the PCTK1 substrate motif does not coincide with that of typical CDK family motifs. In addition to the lack of clarity of PCTK1's targets, its upstream regulators remain a topic of debate, as the role of cyclin Y as the sole activator of PCTK1 has been questioned, with both cyclin Y-like 1 (CCNYL1) (219) and

CDK5 (212) suggested as alternative regulators. Therefore, unlike classic proliferation-related cyclins, it may be that the activity of PCTK1 is totally independent of cyclin binding.

PCTK1 has only recently been implicated in cancer, and its biological roles in this disease setting remain largely unresolved. It has been demonstrated *in vitro* that PCTK1 knockdown sensitizes prostate and breast cancer cells to the TNF-related apoptosis-inducing ligand (TRAIL) extrinsic cell death pathway (220). Additionally, PCTK1 has been shown in prostate cancer cells to phosphorylate the tumor suppressor p27 (also known as Kip1, cyclin-dependent kinase inhibitor 1B), resulting in its degradation and cell cycle progression (221). In an *in vitro* screen, it was shown that siRNA-mediated knockdown of PCTK1 slowed the growth of a *MYC*-amplified medulloblastoma cell line, suggesting PCTK1's involvement in the mammalian target of rapamycin (mTOR) pathway. Lastly, PCTK1 has been shown to be overexpressed at the mRNA and protein levels in serous epithelial ovarian carcinoma (EOC) tissues compared to matched normal tissues, although the authors suggest that this is a negative feedback mechanism to promote the differentiation of tumor cells and inhibit proliferation. Notably, the involvement of PCTK1 in metastasis has thus far been unexplored.

PCTK1 was the top candidate kinase based upon its expression in clinical brain metastasis as well its ability to enhance colony formation in hard agar, but because the kinome screen was performed in a pooled format, it was necessary to functionally validate PCTK1 in a single kinase-overexpression context. Therefore, the PCTK1-overexpressing MDA-MB-231.luc.GFP (231.PCTK1) and its corresponding control line (231.vector) generated for the hard agar screening experiments were validated for PCTK1 overexpression at the mRNA and protein levels (Figure 27) and were injected into the carotid artery of mice (100,000 cells per mouse). The cell number was halved in this experiment compared to the kinome screen in order to provide a larger window of observation. Following intracarotid injection, the mice were monitored weekly by IVIS luciferase imaging and sacrificed when they reached morbidity.

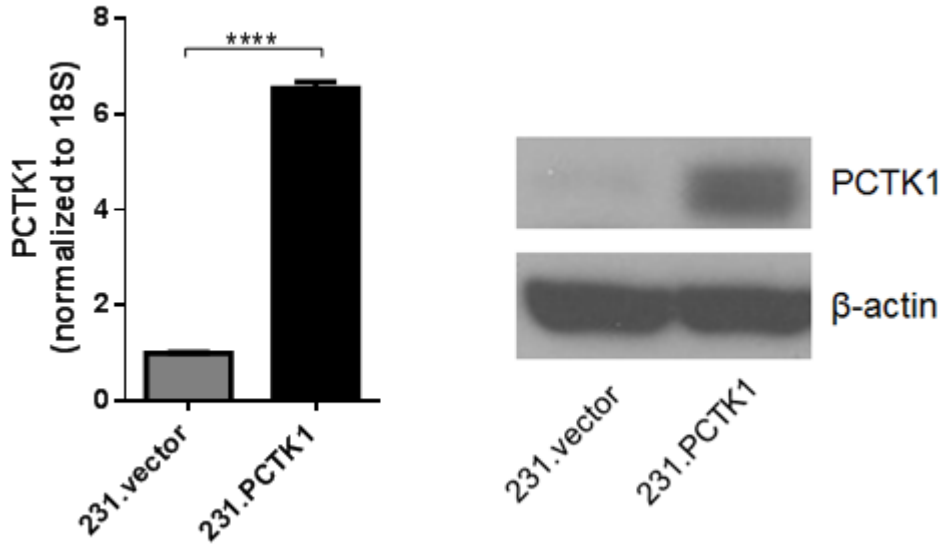

Figure 27. PCTK1 is overexpressed at RNA and protein level in 231.PCTK1 cells. Left: qRT-PCR with TaqMan primers shows that *PCTK1* mRNA expression is enhanced more than sixfold compared to controls. qRT-PCR of 18S mRNA was used for normalization. The p-value was <0.0001 according to unpaired t-test. Right: Western blot for PCTK1 protein expression. β-actin was used as a loading control.

PCTK1 overexpression led to enhanced brain metastatic growth relative to the vector control cells to the extent that luciferase images of the mouse brains began to become saturated by day 32 post-injection (Figure 28). Additionally, PCTK1-overexpressing cells significantly reduced mouse survival relative to the control group, demonstrating that PCTK1 indeed can accelerate brain metastasis growth even outside the pooled format of the kinome screen (Figure 29). The brain metastases formed by 231.PCTK1 were invasive from the leptomeninges into the parenchyma, and formed large ventricular masses, while 231.vector mostly formed smaller tumors in the ventricles (Figure 30).

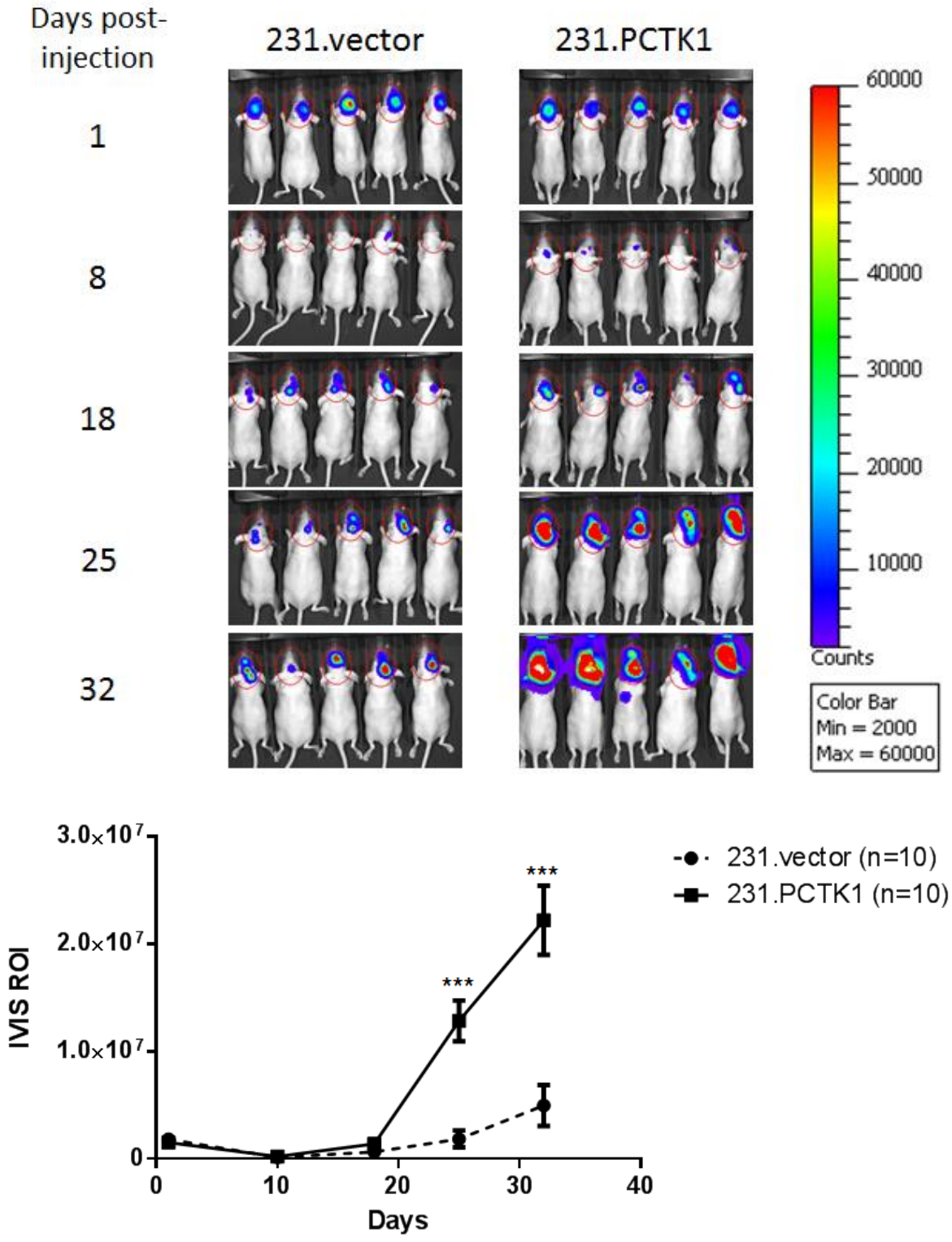

Figure 28. PCTK1 overexpression enhances brain metastasis growth *in vivo*. IVIS imaging was performed using an IVIS-200 (Xenogen) to assess the growth of brain metastases *in vivo*.

MDA-MB-231.luciferase cells expressing vector (231.vector) or PCTK1 (231.PCTK1) were injected into the carotid artery of nude mice to form experimental brain metastasis (each group: n = 10). Metastatic growth in the brain was measured beginning 1 day post-injection by luciferase activity. Top: IVIS images from 5 representative mice per group are shown. The scale bar to the right of the images indicates signal intensity, a surrogate marker of brain metastasis burden. The signal from mice injected with 231.PCTK1 started to become saturated by day 32 post-injection. Bottom: quantification of IVIS luciferase signal. The y-axis shows the amount of luminescence captured from a defined region of interest (ROI), which was an oval-shaped region of standardized size around each animal's head. T-tests were performed at each time point and the Holm-Sidak method was used to correct for multiple comparisons.

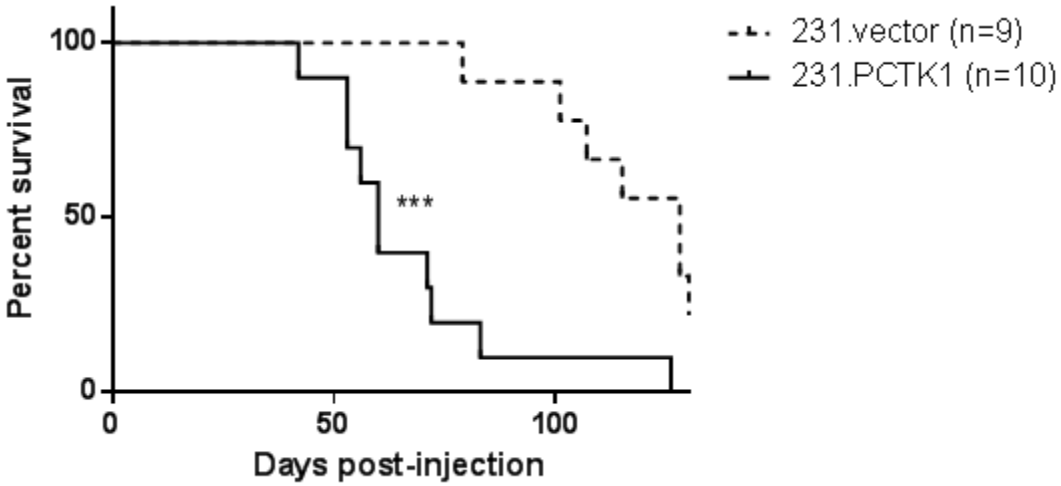

Figure 29. PCTK1 overexpression in MDA-MB-231 significantly shortens survival in experimental brain metastasis model. Mice injected intracarotidly with 231.PCTK1 or corresponding vector cells were compared for their brain metastasis-specific survival. PCTK1 overexpression shortened survival from a median time of 128 days to 60 days. Survival curves were significantly different (p=0.0004) according to Mantel-Cox log-rank test.

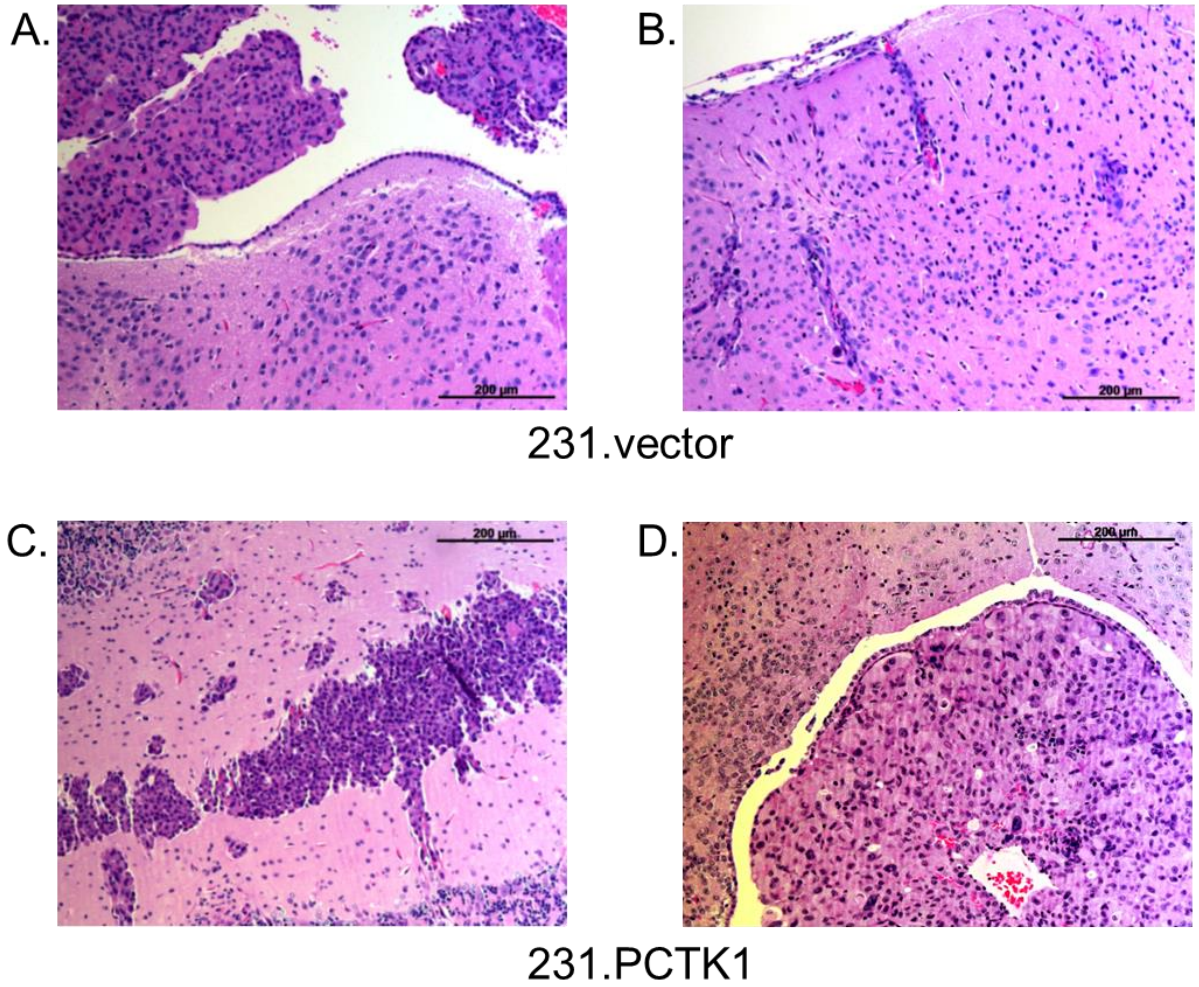

Figure 30. PCTK1 overexpression enhances brain metastasis growth in ventricles and invasion into the parenchyma. (A) and (B): Hematoxylin and eosin (H&E) staining of 231.vector brain metastases. 231.vector cells formed lesions in the ventricles (A) and small lesions in the parenchyma (B). (C) and (D) H&E staining of 231.PCTK1 brain metastases. (C) shows tumor cells growing throughout the parenchyma, while (D) shows 231.PCTK1 cells filling the ventricle. All images acquired at 10x magnification; scale bars represent 200 µm.

After the observation of PCTK1's enhancement of brain metastasis, and given the limited functional knowledge about PCTK1, a natural question was whether the PCTK1-driven tumor growth was metastasis-specific or a shared feature of primary tumors and metastases. Therefore, luciferase-labeled 231.vector or 231.PCTK1 were injected into the mammary glands of nude mice to form mammary fat pad tumors (each group: n = 12 [6 mice with bilateral tumors]). PCTK1 overexpression did not lead to enhanced primary tumor growth in this model, suggesting that its pro-tumoral functions are metastasis-specific (Figure 31).

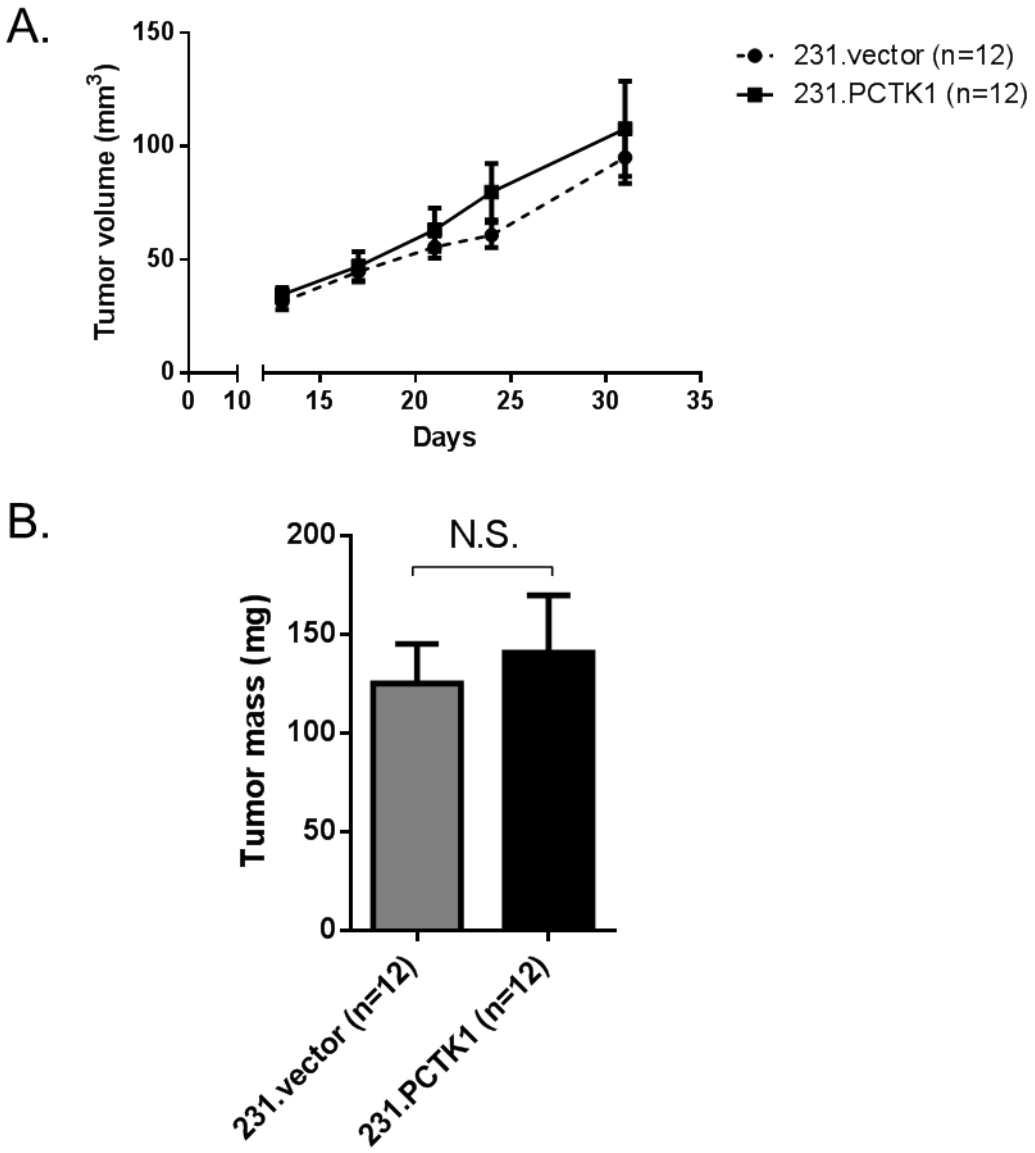

Fig 31. PCTK1 overexpression does not enhance primary mammary tumor growth. 231.PCTK1 and 231.vector were injected into the #3 mammary glands of nude mice. Injection efficiency was measured on day 1 by IVIS. Once tumors became palpable, they were regularly measured by calipers. Tumor volume estimates, calculated by the formula (L x W^2)/2 and normalized to IVIS signal on day 1, are shown in A. Tumor mass as determined at the experimental endpoint is shown in B. Unpaired t-tests, using the Holm-Sidak method to correct for multiple comparisons, revealed no significant growth differences.

To characterize the cellular mechanism by which PCTK1 enhances brain metastatic growth of MDA-MB-231 cells, basic cellular phenotypic characteristics, including proliferation, invasion, and migration were assessed *in vitro* under normal culture conditions, i.e., DMEM/F12 media supplemented with 10% FBS. The results, as shown below in Figure 32, indicated that PCTK1's dramatic pro-metastasis phenotype was not recapitulated *in vitro*.

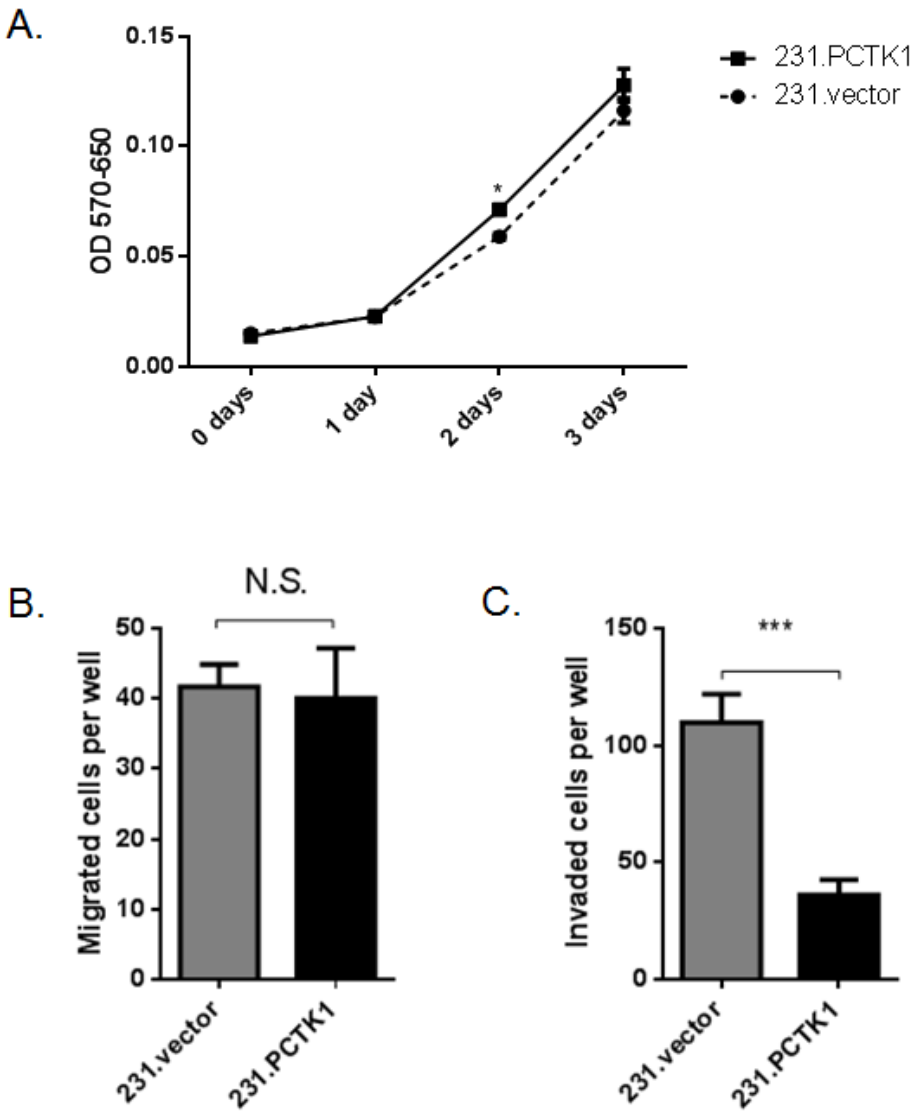

Figure 32. PCTK1 overexpression does not promote proliferation, migration, or invasion *in vitro*. (A) MTT assays demonstrated a statistically significant difference at the 2 day time point, but no dramatic biological difference was observed. (B) Transwell migration assay of

231.vector and 231.PCTK1 at 18 hours showed no significant difference. (C) Invasion through Matrigel at 24 hours was inhibited by PCTK1 overexpression. Unpaired t-tests were used to compare groups in each experiment and the results are indicated as * on graphs. In A, correction for multiple comparisons was performed.

Based on the characterization of PCTK1 as a non-canonical cyclin-dependent kinase, the fact that it provided no major growth advantage *in vitro* was unsurprising. At the same time, the strikingly rapid growth of PCTK1-overexpressing brain metastatic cells *in vivo* demanded explanation. As mentioned in Section 1.3.2, the brain represents a vastly distinct habitat compared to the primary tumor site, especially with regards to resource availability. Therefore, to examine whether growth advantage conferred by PCTK1 in brain metastasis may be related to the unique metabolic microenvironment of the brain, correlations of PCTK1 gene expression with the expression of members of the glutamine metabolism pathway were analyzed (Figure 33, A - E). Strikingly, in primary breast cancer as well as glioblastoma, PCTK1 showed strong relationships with expression of glutamine metabolizing genes, including asparagine synthetase (ASNS). These relationships were even stronger in low-grade glioma, where they extended to both forms of the classical glutamine catabolism gene glutaminase, glutaminase 1 and 2 (GLS and GLS2).

A.

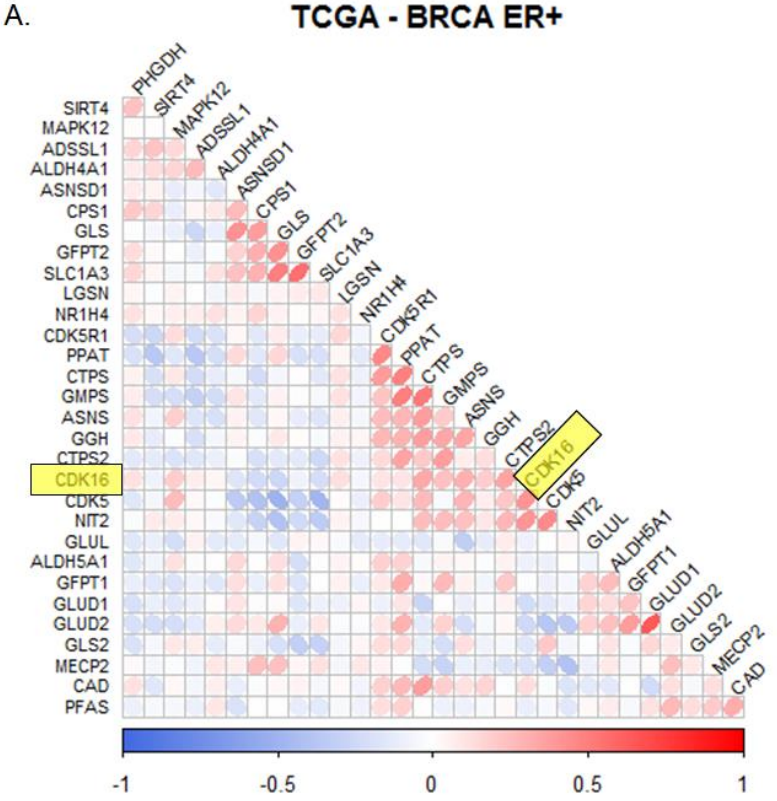
TCGA - BRCA ER+
PHGDH
SIRT4
MAPK12
ADSSL1
ALDH4A1
ASNSD1
CPS1
GLS
GFPT2
SLC1A3
LGSN
NR1H4
CDK5R1
PPAT
CTPS
GMPS
ASNS
GGH
CTPS2
CDK16
CDK5
NIT2
GLUL
ALDH5A1
GFPT1
GLUD1
GLUD2
GLS2
MECP2
CAD
PFAS
-1
-0.5
0
0.5
1

B.

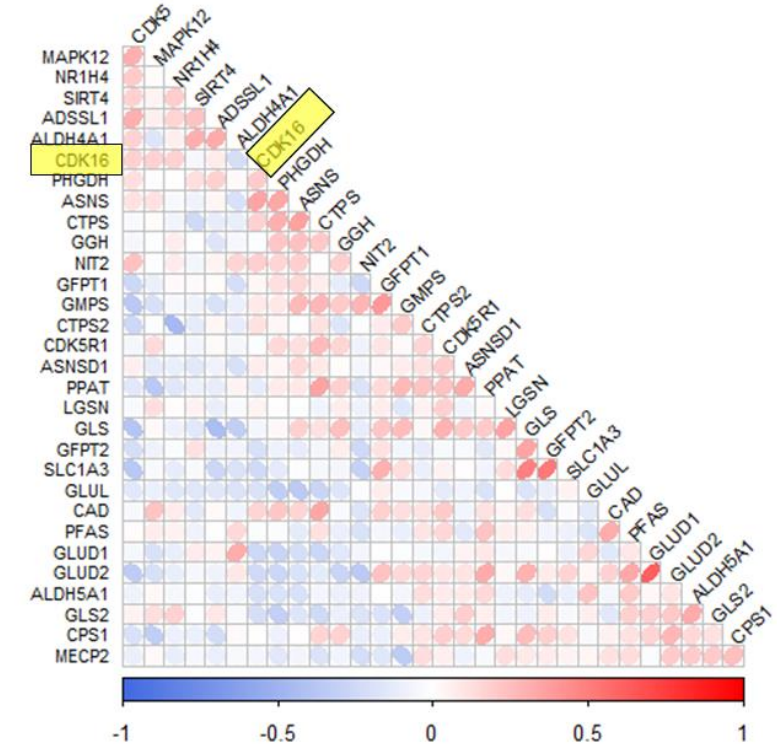
TCGA - BRCA HER2+
CDK5
MAPK12
NR1H4
SIRT4
ADSSL1
ALDH4A1
CDK16
PHGDH
ASNS
CTPS
GGH
NIT2
GFPT1
GMPS
CTPS2
CDK5R1
ASNSD1
PPAT
LGSN
GLS
GFPT2
SLC1A3
GLUL
CAD
PFAS
GLUD1
GLUD2
ALDH5A1
GLS2
CPS1
MECP2
-1
-0.5
0
0.5
1

C.

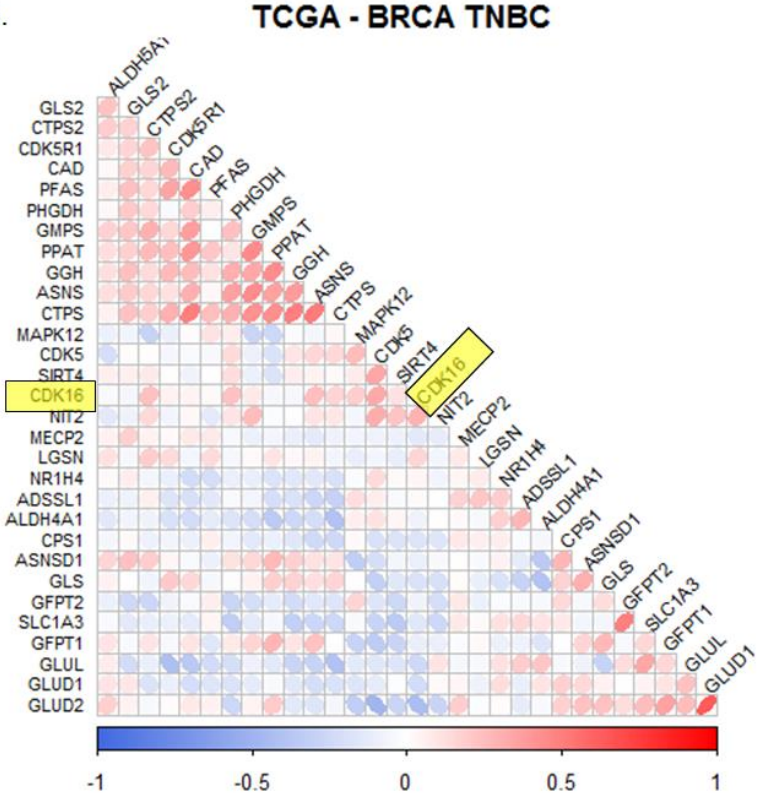
TCGA - BRCA TNBC
ALDH5A1
GLS2
CTPS2
CDK5R1
CAD
PFAS
PHGDH
GMPS
PPAT
GGH
ASNS
CTPS
MAPK12
CDK5
SIRT4
CDK16
NIT2
MECP2
LGSN
NR1H4
ADSSL1
ALDH4A1
CPS1
ASNSD1
GLS
GFPT2
SLC1A3
GFPT1
GLUL
GLUD1
GLUD2
-1
-0.5
0
0.5
1

D.

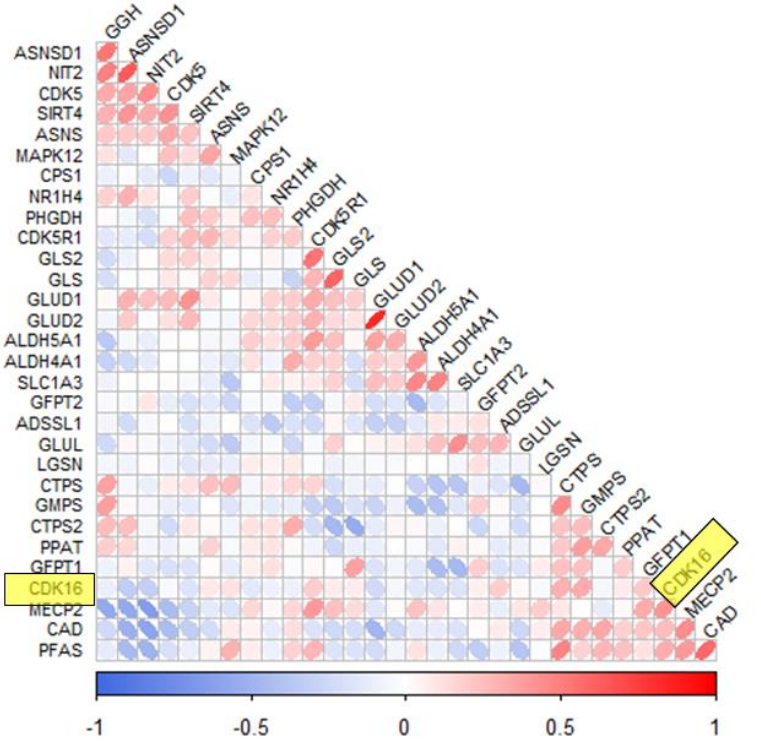
TCGA - GBM
GGH
ASNSD1
NIT2
CDK5
SIRT4
ASNS
MAPK12
CPS1
NR1H4
PHGDH
CDK5R1
GLS2
GLS
GLUD1
GLUD2
ALDH5A1
ALDH4A1
SLC1A3
GFPT2
ADSSL1
GLUL
LGSN
CTPS
GMPS
CTPS2
PPAT
GFPT1
CDK16
MECP2
CAD
PFAS
-1
-0.5
0
0.5
1

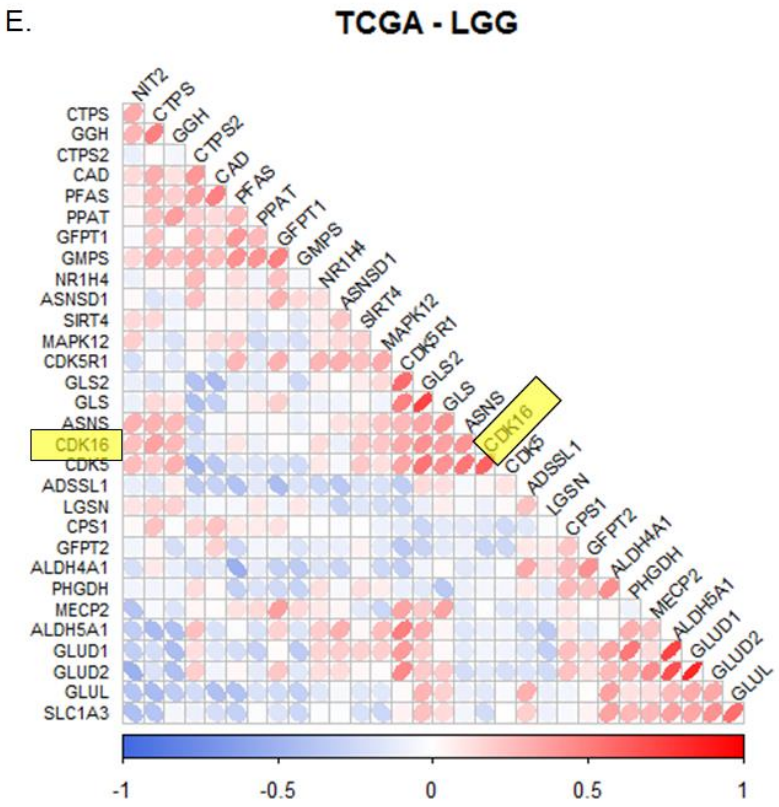

Figure 33. PCTK1 shows strong correlations with glutamine metabolism genes in TCGA data. The gene expression values of PCTK1 (CDK16) and members of the glutamine metabolic process (Gene Ontology: 0006541) family were compared within TCGA datasets of ER-positive breast cancer (A), HER2-positive breast cancer (B), TNBC (C), glioblastoma (GBM) (D), and low-grade glioma (LGG) (E). Pairwise Pearson correlation coefficient values between genes were generated and reordered using a clustering algorithm based on the similarity between genes. Genes with highly positive correlative values appear in red, those with highly negative values in blue, and those lacking correlation in white. PCTK1 is highlighted in each graph. Data matrices were generated by Dr. Patrick Zhang.

.

In consideration of this correlative relationship with glutamine metabolism, the effect of PCTK1 was functionally assayed *in vitro* in low nutrient conditions. For this purpose, Basal Medium Eagle (BME), which was developed by Harry Eagle in the 1950s for growing HeLa cells (222, 223), was selected. Basal Medium Eagle contains approximately one-third the glucose and one-fourth the amino acid content of DMEM/F12, which is more widely used in cell culture because its nutrient surplus supports a higher growth rate. Importantly, when 231.PCTK1 and 231.vector were previously compared for their proliferative abilities *in vitro*, DMEM/F12 media was used. When the assay was repeated using BME supplemented with 500 μM glutamine (representative of physiological level in the brain), PCTK1 overexpression imbued the cells with a striking growth advantage (Figure 34). This result provided an indication that PCTK1 may allow cells to better metabolize glutamine when faced with low-nutrient conditions, such as that of the brain.

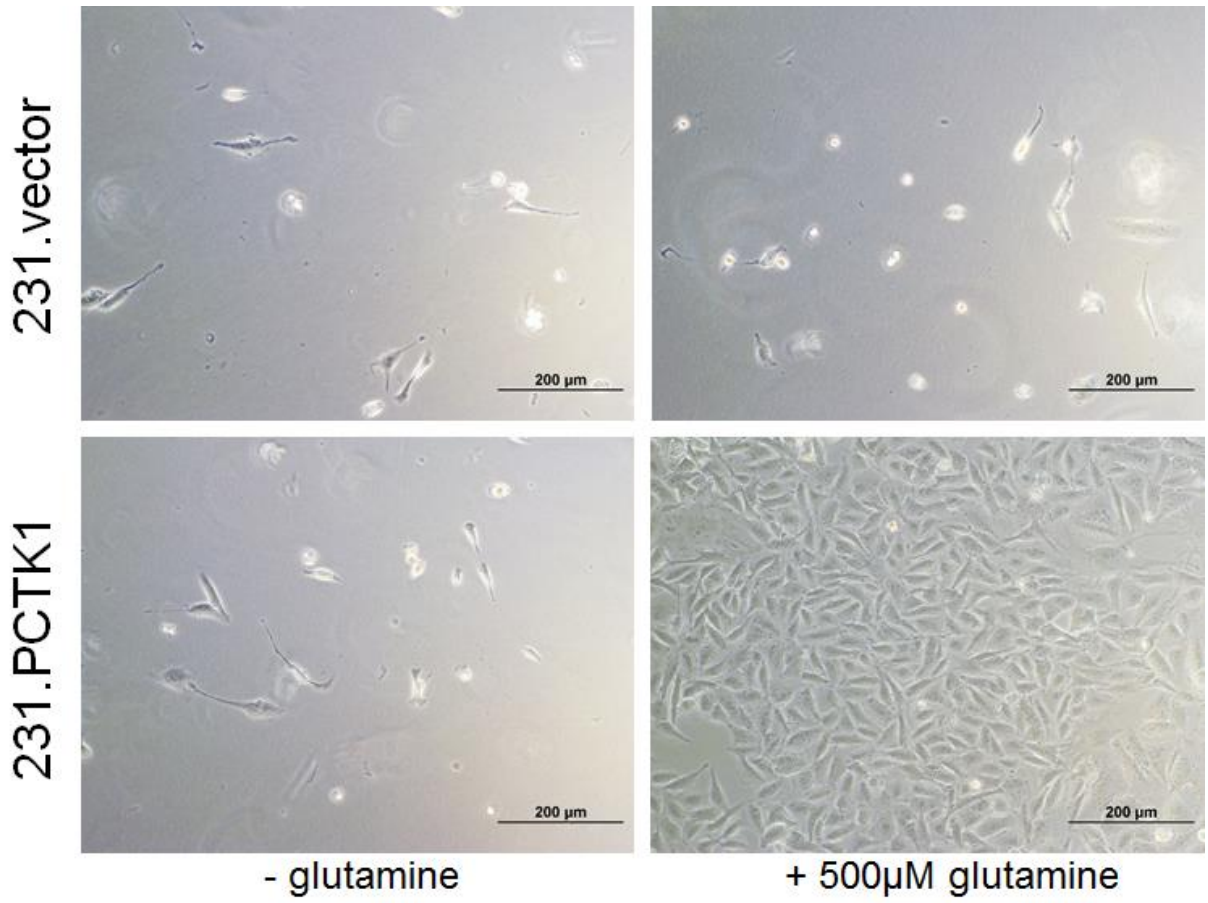

Figure 34. PCTK1-overexpressing cells have a survival advantage in low-nutrient conditions when glutamine is available 231.PCTK1 cells or 231.vector cells were plated with or without 500 µM of glutamine. After one week, cell growth was assessed by an Olympus IX70 microscope. Representative images at 10x magnification are shown.

Because the exchange of glutamine and glutamate occurs in the brain in a cyclical fashion, it was unclear whether the PCTK1-overexpressing cells were using the glutamine from the media directly, or perhaps were driven to proliferation by activation of glutamate receptors. Therefore, the relative abilities of PCTK1-overexpressing and associated vector control MDA-MB-231 cells to proliferate using similar concentrations of either glutamate or glutamine were

assayed in low-nutrient BME. While vector-expressing cells were unable to grow with either glutamate or glutamine supplementation, the PCTK1-overexpressing cells demonstrated a strong growth advantage evident at glutamine concentrations ranging from 400 μM to 2mM (Figure 35A). However, even the PCTK1-overexpressing cells were unable to grow with comparable levels of glutamate supplementation (Figure 35B). These results suggested that PCTK1-overexpressing tumor cells indeed behave similarly to neurons under limiting nutrient conditions, with an ability to use glutamine but not glutamate for survival and/or proliferation.

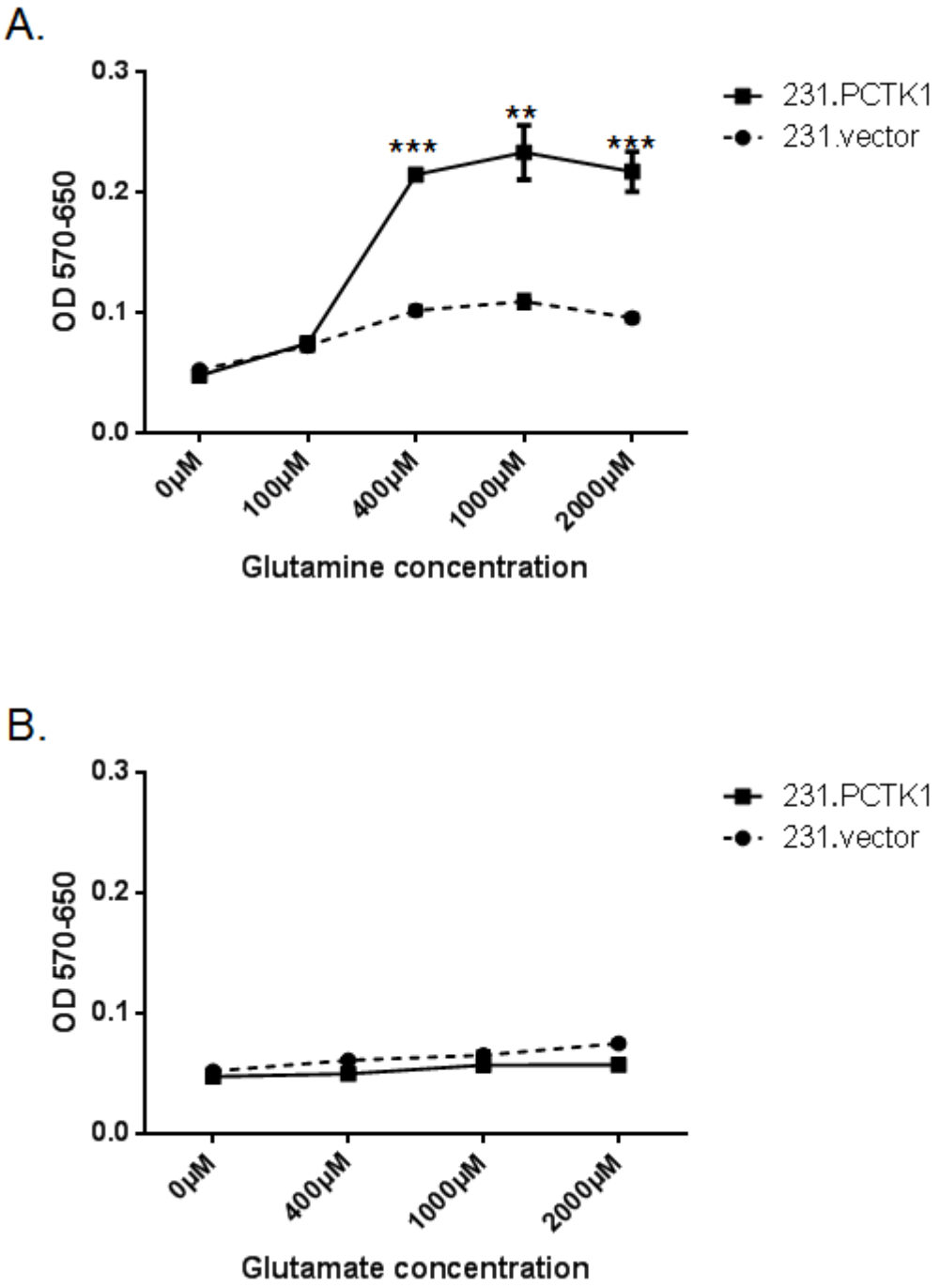

Figure 35. PCTK1-overexpressing cells have proliferative advantage in limited-nutrient media supplemented with glutamine, but not glutamate. MDA-MB-231 cells with or without PCTK1 expression were cultured in BME with the given quantities of glutamine (A) or glutamate (B) for 4 days. MTT assays were performed, and the results are shown in terms of MTT signal

at 570 nm minus the background at 650 nm (OD 570-650). T-tests were performed at each concentration, with the Holm-Sidak method used to correct for multiple comparisons.

While the previous results indicated that 231.PCTK1 cells were using glutamine in order to maintain their survival and proliferation in conditions of limited nutrients, it remained unknown whether the cells were indeed taking up more glutamine and either using it for energy or incorporation into the biomass of new cells, or simply processing the glutamine a byproduct of a homeostatic glutamine-glutamate cycle. In order to directly test these possibilities, the media of PCTK1-overexpressing and vector MDA-MB-231 cells was analyzed by mass spectrometry. In order to calculate the relative rates of substrate utilization, media was collected at the specified timepoints (0, 1.5, 3, and 6 hours) and the relative peaks of glutamine and glutamate compared. Because of the sensitivity of the experiment to environmental conditions, wells included as replicates were randomly selected from different regions of the cell culture plates (See schematic, Figure 36).

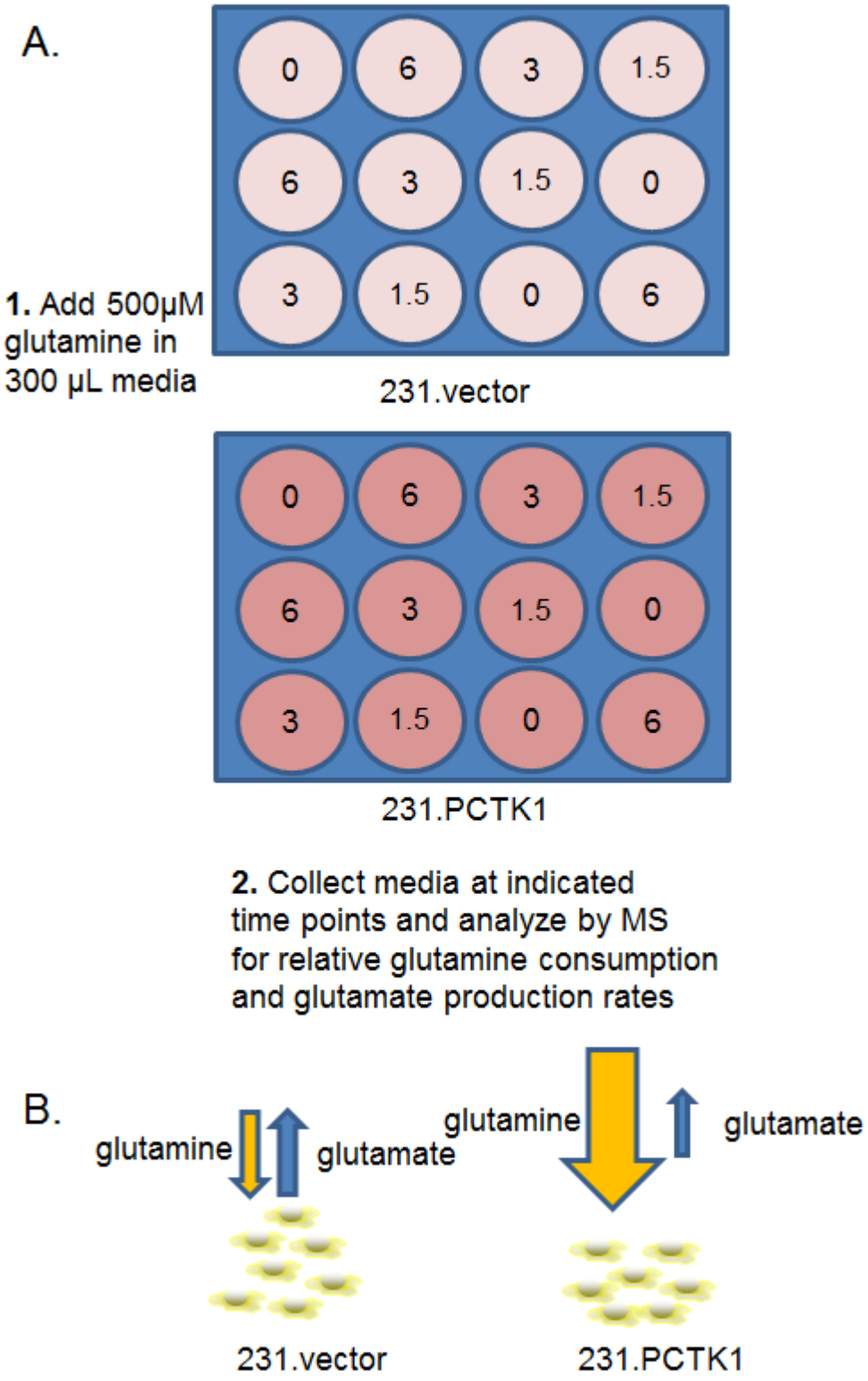

Figure 36. Schematic of MS experiment to determine relative glutamine and glutamate utilization rates in PCTK1-overexpressing cells. (A) Cells were cultured in 12-well plates in

300 µL BME with exactly 500 µM glutamine at the start of the assay. Media was collected from wells sampled from around the plate at time points indicated within circles (times are in hours) and centrifuged at 2000 x g for 5 minutes to remove cellular debris. The media from earlier time points was stored at -80°C until completion of the assay, at which time all samples were analyzed for glutamine and glutamate content by YSI Bioanalyzer. (B) Results indicated that the rate of glutamine intake rose in 231.PCTK1 cells, while at the same time the glutamate output rate actually decreased.

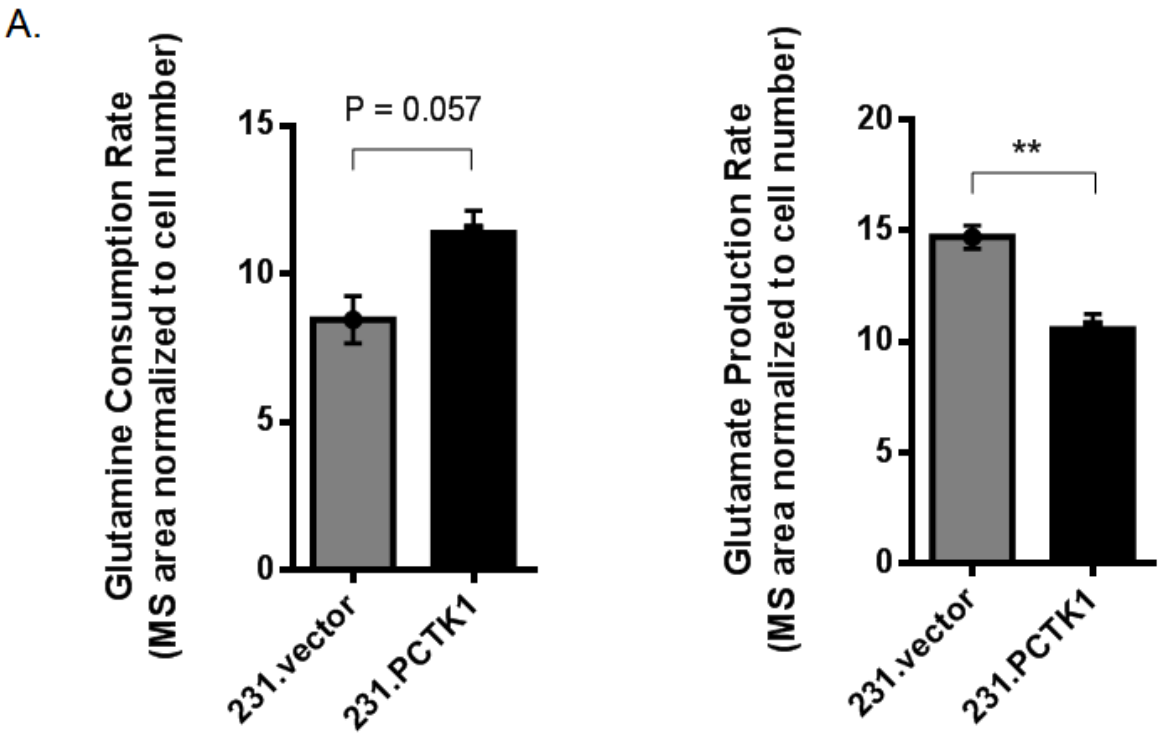

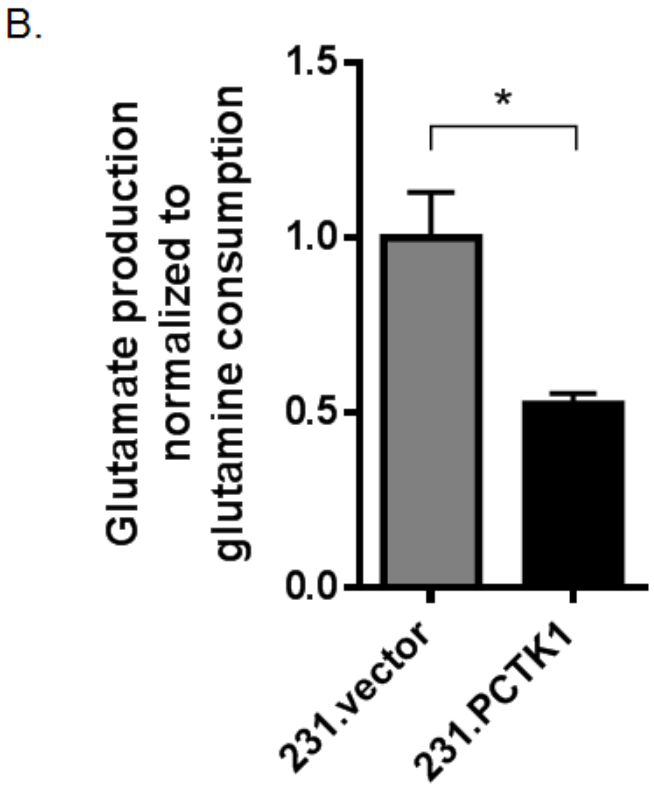

Figure 37. PCTK1 overexpression significantly enhances glutamine metabolism. (A) Left, glutamine depletion rates in the media of 231.vector and 231.PCTK1 were compared by MS. There was a trend towards increasing glutamine consumption with PCTK1 overexpression. Right, similar comparisons were made for glutamate release into the media of cultured cells. There was a significant decrease in glutamate release from PCTK1-overexpressing cells. (B) The rate of glutamate production was normalized to the rate of glutamine consumption. PCTK1 overexpression led to a deficit in glutamate production per glutamine consumed of nearly 50%. Unpaired t-tests were used to compare groups in each experiment and the results are indicated as * on graphs.

These results demonstrated several important points. First, the rates of glutamine consumption from and glutamate release into the media remained in the linear range over the time frame assayed, for simplicity the 0 hour and 6 hour time points were compared. Compared

to 231.vector cells, the PCTK1-overexpressing cells increased their uptake of glutamine from the media by 35% (Figure 37A, left). At the same time, there was a reduction in glutamate release from the PCTK1-overexpressing cells, with the relative rate falling by more than 25% (Figure 37A, right). Together, these rates meant that for every 1 unit of glutamine going into the cells, PCTK1-expressing cells were producing 48% less glutamate (Figure 37B). This deficit between expected glutamate release and actual glutamate release implies that the glutamine is staying in the cell for either energy or biomass generation.

Finally, as all of the prior experiments had been based on a gain-of-function system, loss-of-function studies were performed in order to test whether PCTK1 was necessary for brain metastasis *in vivo*. To that end, PCTK1 stable knockdown cell lines were generated from the HCC1954Br cell line (1954Br), a highly aggressive HER2-overexpressing breast cancer cell line that also possesses a high endogenous level of PCTK1. PCTK1 knockdown efficiency at the mRNA and protein levels for the 2 best clones are shown below in Figure 38. HCC1954Br shControl and HCC1954Br shPCTK1-3 were then injected into the carotid artery of nude mice. Following intracarotid injection, the mice were monitored for development of brain metastasis symptoms and sacrificed when they reached morbidity.

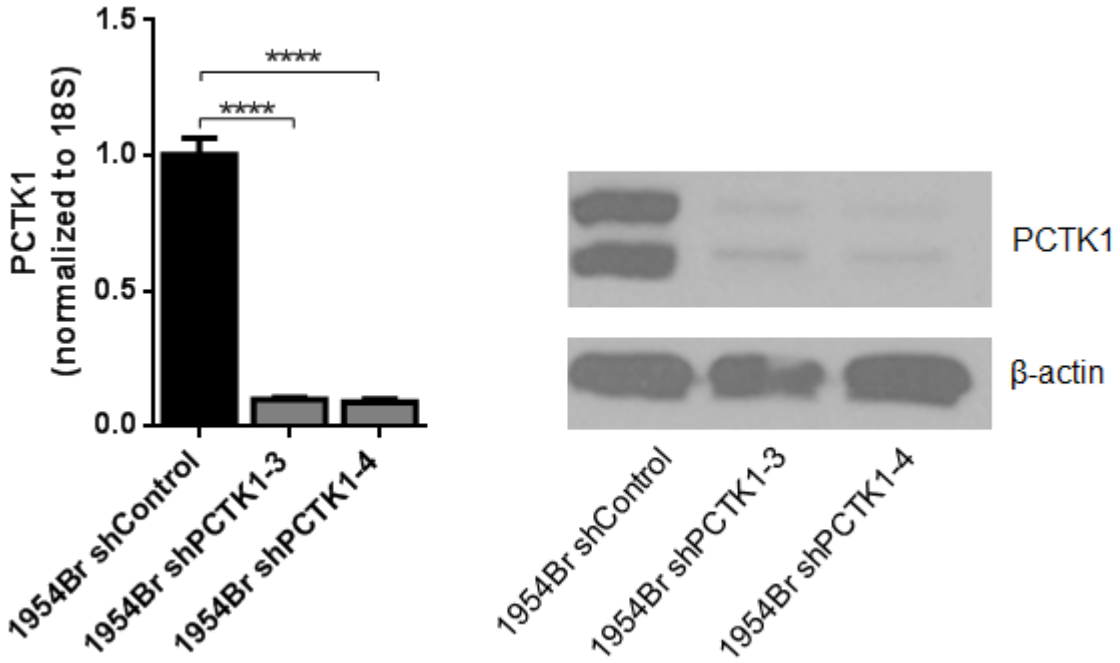

Figure 38. PCTK1 is efficiently knocked down in the HCC1954Br cell line. Left: qRT-PCR with TaqMan primers shows that *PCTK1* mRNA expression is decreased 90% in both knockdown lines compared to control line. qRT-PCR of 18S mRNA was used for normalization. The p-value was <0.0001 according to one-way ANOVA followed by Dunnett's multiple comparisons test. Right: Western blot for PCTK1 protein expression showing efficient knockdown with both shRNA clones. β-actin was used as a loading control.

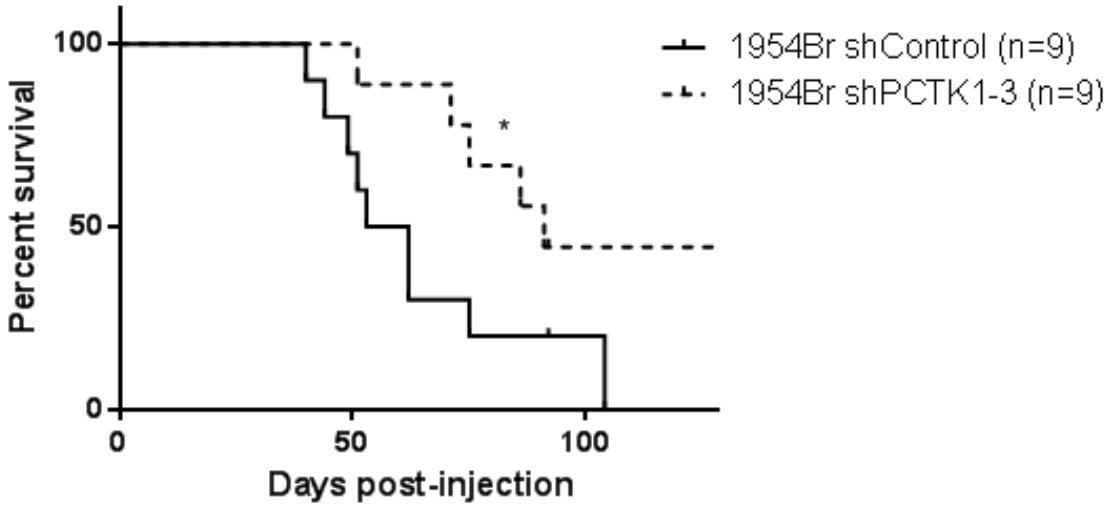

Figure 39. PCTK1 knockdown in HCC1954Br significantly extends survival of brain metastasis-bearing mice. Mice injected intracarotidly with 1954Br shControl or shPCTK1 were compared for their brain metastasis-specific survival. PCTK1 knockdown lengthened survival from a median time of 57.5 days to 91 days. Survival curves were significantly different (p=0.046) according to Mantel-Cox log-rank test.

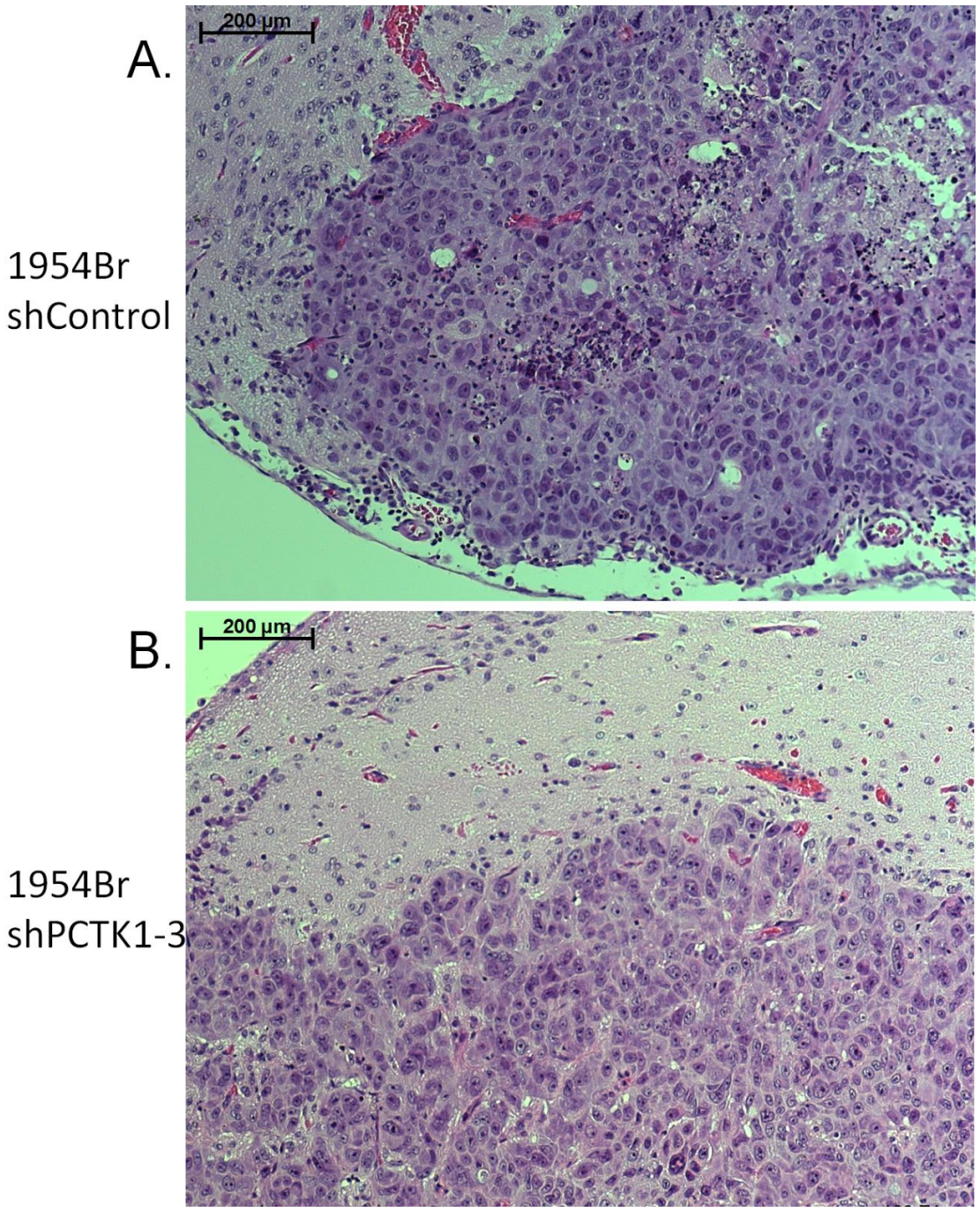

Figure 40. PCTK1 knockdown does not affect morphology of brain metastasis in HCC1954Br model. Representative H&E staining of brain metastasis formed by ICA injection of (A) HCC1954Br shControl cells on day 49 post-injection or (B) HCC1954Br shPCTK1-3 cells on day 91 post-injection. No major morphological differences were apparent between groups, with both exhibiting parenchymal growth, large volume, and abundant vasculature. All images acquired at 10x magnification; scale bars represent 200 µm.

Knockdown of PCTK1 in the 1954Br cell line significantly enhanced mouse survival relative to controls in an experimental brain metastasis model, with median survival times rising from 57.5 days in the control group to 91 days in the knockdown group (Figure 39). However, as most mice injected with PCTK1 knockdown clones eventually succumbed to brain metastases with morphology resembling the control tumors (Figure 40), knockdown of PCTK1 unsurprisingly did not seem to be a curative approach. To investigate whether the expression of PCTK1 recovered *in vivo*, either through adaptation or selection of clones with inefficient knockdown, the protein level of PCTK1 was assessed by IHC. Indeed, IHC analysis showed that PCTK1 expression can recover *in vivo* (Figure 41), indicating either that the incomplete efficiency of shRNA in eliminating protein expression or the selection of especially poor knockdown clones *in vivo*.

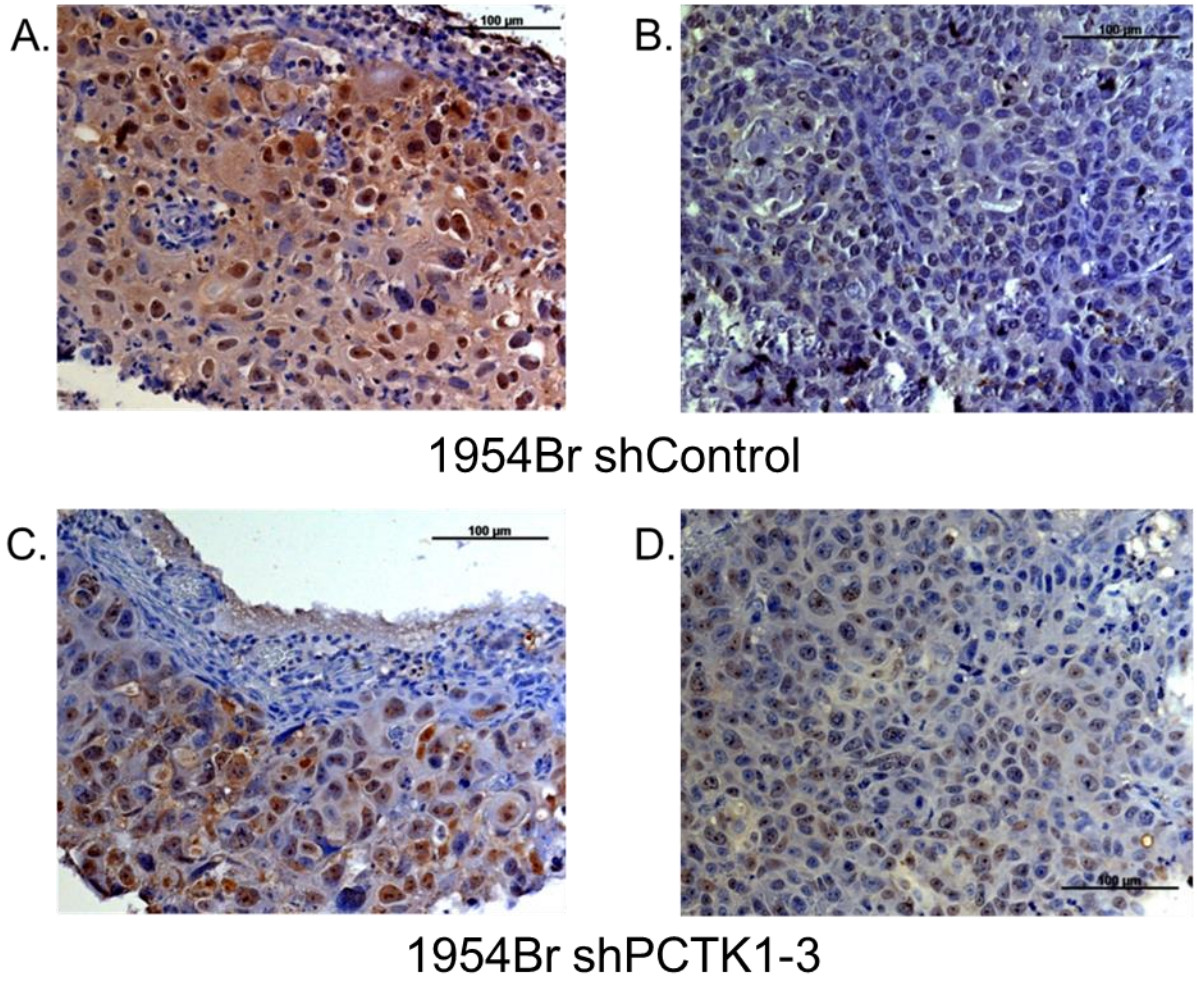

Figure 41. PCTK1 protein expression can recover *in vivo* in HCC1954Br brain metastasis with PCTK1 shRNA knockdown. Representative PCTK1 IHC staining of brain metastasis formed by ICA injection of (A & B) HCC1954Br shControl cells or (C & D) HCC1954Br shPCTK1-3 cells. Both the control and PCTK1 knockdown brain lesions show heterogeneous PCTK1 expression, with areas of almost uniform positivity and negativity both apparent. All images acquired at 20x magnification; scale bars represent 100 µm.

Chapter 5: Discussion, Conclusions, and Future Directions

Discussion

Breast cancer is one of the most common and deadly cancers among women in the United States, as almost 250,000 new cases will be diagnosed in 2016, and an expected 40,500 deaths due to breast cancer. In the past 30 years, the increase in screening and targeted therapies for breast cancer has seen the death rate fall by almost one-third from its peak in 1989. However, this improvement is almost entirely due to effects in detecting early-stage disease earlier; once cancer has metastasized, the prognosis remains bleak, as patients diagnosed with stage IV disease (distant metastasis) have only a 22% 5-year survival.

The metastasis of cancer to secondary sites is not a random process, as cancers from certain organ sites have their own preferential sites for metastasis. The 'seed and soil' principle holds that successful metastasis only occurs when the right cancer cell seed interacts with the appropriate supportive secondary organ soil. First espoused by English surgeon Stephen Paget in 1889 and validated by Isaiah Fidler in the 20th century, the seed and soil theory has stood the test of time. For breast cancer seeds, the common metastatic soils are bone, liver, lungs, and brain. While any metastatic breast cancer diagnosis is generally fatal, brain metastasis carries a brutal prognosis, with median survival of less than one year.

The especially poor prognosis for brain metastasis is not limited to the context of breast cancer. Other cancers that frequently metastasize to the brain include lung, breast, melanoma, and colorectal; once they are in the brain, all are incurable. While one explanation is the fact that brain metastases usually develop in heavily pre-treated patients, so do metastases to other organ sites that can demonstrate responses to therapy; brain metastases' therapeutic resistance is likely due to the unique biology of the brain. In either case, the clinical options for brain metastasis are only palliative; this and the fact that it is not even fully resolved as to why secondary cancers of the brain do not respond to therapy represent true failures by the clinical and biomedical research communities.

In cancer settings other than brain metastasis, molecular targeted therapies against cancer drivers, frequently kinases, have demonstrated widespread clinical efficacy. Additionally, as kinases occupy the key nodes of cancer cell signaling pathways, they are involved in many of the cellular functions and dysfunctions that represent the hallmarks of cancer. *In vitro*, kinase overexpression screens have identified previously unknown oncogenes. Finally, while genomic and transcriptomic studies comparing brain metastases to either primary cancers or non-brain metastasis have identified a number of brain-specific genes that play roles in brain metastasis, these studies are restricted to those genes whose mRNA expression remains significantly altered following the formation of brain metastasis. As the process of metastasis involves many diverse and demanding steps, genes that provide an advantage at one step may be antagonistically pleiotropic, causing their loss of expression at later stages.

Therefore, we set out to identify novel kinase drivers of brain metastasis through a functional genomic screen *in vivo*, hypothesizing that kinases previously unknown to play roles in brain metastasis may actually imbue cancer cells with growth advantages in the brain. By using the intracarotid injection method of inducing experimental brain metastasis, the cells are delivered into the capillary bed of the brain, allowing for the observation of brain metastasis, which is incredibly rare in other models. This also has the effect of focusing the interrogation of the metastatic cascade to the final few steps: extravasation, colonization, and growth at the secondary site. Because the dissemination of cancer cells throughout the body usually occurs early, understanding these steps is key to the future of therapy for metastasis. The MDA-MB-231 parental cell line was selected as the cancer cell background for the screen, because as the line is able to induce brain metastasis with high efficiency but relatively long latency, it offers a window for observing enhanced brain metastasis. One noteworthy drawback of this approach is that the use of cross-species xenografts as models of cancer and metastasis involves the growth of human cells in immunocompromised mouse hosts. In this study, nude mice were used as the hosts for metastasis experiments, as the “nude” mutation in *FOXN1* that causes

their hairlessness also leads to the absence of a thymus and deficient T cell development, thereby allowing the growth of foreign cells that would otherwise be rejected by immunocompetent animals (224). While the use of immunocompromised mice enables the interrogation of cancer cell growth dynamics in organ-specific nutrient environments much closer to approximating human disease than does *in vitro* cell culture, the artificial nature of such a system should not be understated. As cancer immunotherapy continues to lead to dramatic clinical results in cancer therapy, the immune system is obviously a key regulator in protecting against cancer and metastasis outgrowth and colonization, and the use of immunocompromised animal models downplays this factor. Studies on the importance of the immune system in curtailing brain colonization and growth by metastatic tumor cells could make use of mouse cancer cell lines such as 4T1 in a syngeneic mouse background of BALB/c, although the use of non-human cancer cell lines also raises questions of real disease relevance. As statistician George Box said, “all models are wrong; some are useful.” With this in mind, here I chose to focus on an experimental model system with certain limitations (experimental metastasis model in immunocompromised mice), in hopes of identifying some novel truths that could be validated in other systems later. While a pure brain metastasis gain-of-function screen in a spontaneous mammary fat pad tumor model or non-brain tropic cell line using a syngeneic immunocompetent mouse strain would have been much less likely to generate successful phenotypes, and was not pursued here, this approach could be taken by audacious researchers in the future.

The screen resulted in clear demonstration that kinase overexpression enhanced brain metastasis growth, as 14 of the 17 pools decreased mouse survival shorter than the 60 days seen in the parental cell line. Following this positive *in vivo* data, though, recovery of the identity of the kinases involved was non-trivial. During the screen, as the mice were euthanized, their brains were harvested; half of the metastases-bearing tissue (as estimated by GFP signal under dissecting microscope) was used for direct RNA extraction and half was dissociated and cells

were recovered from the dissociated tissue *in vitro*. The RNA from the brain metastasis lesions was isolated and used to produce cDNA, which was then subjected to RT-PCR with vector-specific primers. The resulting PCR products were then TOPO cloned and subjected to sequencing

While this methodology did yield some potentially interesting data, it was clear that there were limitations. First, it did not provide a quantitative measure of the kinases being detected. Simple identification of a kinase sequence from *in vivo* tissue did not necessarily indicate that a given kinase was enriched *in vivo*, merely that it was not completely lost from the population. More importantly, while 5 sequences were identified from pool 2, only 1 was recovered from pool 1 and 2 from pool 3, with none coming from pool 4 or 5 in spite of their increased brain metastatic growth and the fact that multiple bands were visible in gels analyzing their RT-PCR products. This was partially due to the fact that the kinase library contained 353 ORFs, but came with 409 wells of bacterial glycerol stock. The extra 56 wells, which were distributed throughout the plates of the library, contained the kinase ORF vector plasmid loaded with a "filler" DNA sequence, in many cases a segment of TGFBR2. Since these filler sequences were very short, they preferentially amplified during the PCR process and overwhelmed the true ORF sequences during the TOPO cloning process, thereby obfuscating kinase identity.

When it became clear that the TOPO cloning method was not optimal for identifying the kinases positively selected *in vivo*, the method for kinase identification was modified, instead using NGS of genetic materials isolated from recovered tumor cells compared to the pre-injection cells. Prior to performing NGS, a comparison was made between the detection capabilities of kinase library gDNA by PCR and mRNA by RT-PCR; gDNA allowed for amplification of more sequences and was thus chosen for further NGS analysis. The MiSeq NGS method allowed for the quantitative measurement of kinase enrichment *in vivo*, and was only limited by the fact that successful cell recovery was only achieved for 48/66 *in vivo* samples. As the kinase library was expressed in a retroviral vector and stably selected prior to

injection, it was possible to query the genomic DNA for kinase ORF presence without dependence on a cDNA synthesis step. This NGS analysis revealed 31 kinases that were enriched in multiple animals *in vivo*, many of which were previously unlinked to brain metastasis. Of note, 2 of the ORFs (CALM2 and PCTK1) identified by the TOPO cloning method appeared in the list of kinases enriched *in vivo*. However, the other 6 ORFs identified by that method were not enriched, demonstrating the superiority of the NGS method in determining quantitative measures of enrichment.

The overexpression of kinases in a pooled format offered the ability to survey a wider range of kinase species simultaneously. In a small pilot study in a second cell line, we attempted the screen with kinase pools of doubled size, representing approximately 40 kinases per pool. These pools appeared to be too large, as there was no minimal consistency mouse-to-mouse in terms of which kinases were enriched. However, the recovery and sequencing of this pilot study was only performed using the TOPO cloning/Sanger sequencing method. By using the MiSeq system for NGS, performing a similar screen with larger pool sizes should be possible. Results could also be made more robust by including more animals, or by direct isolation and sequencing of genomic DNA from tumor cells isolated from brain by either FACS or magnetic bead-based isolation.

Importantly, the kinome screen as performed did reveal several kinases potentially playing important roles in brain metastasis. Notably, HK2, which controls the first step of glycolysis and has previously been implicated in brain metastasis (191), was one of the top hits identified by this screen. Intriguingly, 3 other kinases enriched *in vivo* in multiple animals, phosphofructokinase-liver (PFKL), phosphofructokinase-muscle (PFKM), and phosphoenolpyruvate carboxykinase 2 (PCK2), are all associated with the utilization of glucose. As brain metastasis has been shown to be reliant upon glucose for both the glycolytic and pentose phosphate pathways (192), this serves as an indicator that the screen revealed potentially relevant hits. Indeed, the study of cancer has focused almost exclusively on the use

of glucose as an energy substrate. To wit, Otto Warburg's observations on the preference of cancer cells to obtain energy by anaerobic glycolysis serve as the basis for the Warburg hypothesis (225) and 18-FDG PET imaging relies on the preferential glucose metabolism by cancer cells as a means of differentiating them from healthy tissue (226). Intriguingly, though, while HK2, PFKL, and PFKM all are involved in glucose metabolism via glycolysis, suggestive of a Warburg effect, PCK2 plays the opposite role in glucose metabolism by its regulation of gluconeogenesis. Therefore, the seeming implication of glucose metabolism in brain metastasis might not be as simple as Warburg-driven ATP generation. While glycolysis may immediately suggest ATP generation, it can actually serve as a substrate for biomass generation as well (227). As both increased glycolysis (191) and increased use of other metabolic substrates (192) have been reported in the context of brain metastasis, it will be important to identify whether the seemingly disparate functions of glycolysis and gluconeogenesis are time- or space-dependent manifestations of metastatic response to nutrient limitations within the brain. Isotopic tracing experiments would allow the fate of these metabolic substrates to be revealed, thereby exposing which particular nutrients are limiting during the process of brain metastasis. Targeting of the salvage pathways by which brain metastases obtain limited nutrients may allow for creation of an evolutionary double bind scenario for metastasis targeting.

In addition to glucose metabolism, at least two other networks revealed themselves in the screen. The first, calcium signaling, was indicated by the presence of CALM2, CALM3, and CAMK4. Calcium signaling is critical for brain function. It is involved in astrocyte-neuron communication (228), synaptic glutamate receptor activation leads to an influx of Ca^{2+} into neurons, which can trigger transcriptional changes (229), and ionic calcium entry into neuronal mitochondria stimulates oxidative phosphorylation (230) and is coupled to synaptic vesicle release (231). In the context of cancer, calcium signaling has been shown to be activated in prostate cancer following stimulation with bone ECM (232); calcium may also stimulate cell migration (233). Interestingly, in the context of brain metastasis, transport of calcium from

cancer cells to astrocytes has been shown to be chemoprotective to cancer cells (234). Lastly, brain metastatic breast cancer cells have been shown to express GABAergic neuronal features (235). It is plausible that they could also express glutaminergic neuronal receptors, thus enabling enhanced calcium influx and calcium-mediated signaling. Though not yet validated, the fact that several calcium signaling proteins were enriched in brain metastasis *in vivo* suggests an important role for calcium signaling in brain metastasis.

Another interesting pathway revealed by the screen is the CDK5/CDK5R1/PCTK1 axis. CDK5 and PCTK1 are both non-canonical CDKs, and CDK5R1 is a specific regulator of CDK5. The three proteins are expressed in the brain and have been shown to interact *in vitro* and *in vivo* (213); phosphorylation of PCTK1 by the CDK5/CDK5R1 complex at S95 enhances its activity. In a screen of over 350 kinases that yielded 31 hits, the odds of three members of the same complex being enriched accidentally are small.

However, in regards to which kinase ought to have been pursued further, the screen results alone were not sufficiently informative. For example, which putative hit would have been better to investigate, the one that is enriched 10-fold in two animals, or the one enriched 1.5-fold in all mice of a group? While a larger sample size per group may have allowed for purely quantitative measurements, including differential weighting of positive and negative selection, this analysis was simple: if the average expression of a kinase in brain metastases of a group was greater than the input cells, and if at least two animals in the group had expression >1 relative to input cells, the kinase was deemed a hit. Therefore, to further functionally rank the putative hits, a secondary screen was performed assaying single kinase-overexpressing MDA-MB-231 cells for growth in hard agar (209). This assay simultaneously measures both the tumor-initiating capacity and invasive phenotype, both characteristics important for brain metastasis growth. Most kinases were able to enhance the hard agar colony formation relative to vector cells, some more than 100-fold, thus further prioritizing the hits.

In spite of the notable relationships existing within the putative hit kinases and their enhanced hard agar colony-forming ability, the kinome screen was built upon the principle of functional artificial heterogeneity: kinases were overexpressed in a cell line and queried for their potential to enhance brain metastasis growth without regard for whether or not they are actually expressed in brain metastasis. Therefore, prior to fully committing to a certain path, it was necessary to confirm that the putative hits were actually expressed in brain metastasis and not mere artifacts of this artificial heterogeneity approach. While NGS data on human brain metastasis is incredibly rare, an Australian group recently published NGS data on 36 human brain metastases, including 10 cases from breast cancer (205). Through a collaboration, the kinase hits identified in the screen were analyzed in their data. The results showed that all but 2 of the kinome screen hits are expressed in human brain metastases, and are therefore not simply screen artifacts. Provocatively, the top 7 genes, whose expression exceeded the upper outlier threshold of [Q3+1.5 x IQR], included CALM2, CALM3, HK2, PFKL, and PCTK1. Based on the rank-sum score of the kinase hits in hard agar colony formation and human brain metastasis, PCTK1 was selected for validation.

PCTK1 overexpression in the MDA-MB-231 cell line indeed enhanced brain metastasis growth and decreased mouse survival in the experimental brain metastasis setting. The resulting metastases included large lesions in the ventricles and leptomeninges of the mouse brain, with long invasive extensions into the brain parenchyma. The corresponding vector cells exclusively formed smaller ventricular and leptomeningeal metastases, with only sparse micrometastases observed in the parenchyma. Because these observations were made using the H&E stained brain sections harvested from mice that had become moribund, they represent different time points and are not directly comparable; a repeat of the experiment could be performed with all animals sacrificed at a set time point. Likewise, as this data represents overt brain metastases, a repeated experiment could include the sacrifice groups of mice at early times post-injection to investigate whether PCTK1 is more important for cancer cell survival at

the early stages of dissemination, extravasation, and colonization or only once the tumors are actively growing in the brain.

Out of curiosity as to whether PCTK1's effect on brain metastasis was brain-specific or common to all tumor growth *in vivo*, the relative abilities of 231.PCTK1 and 231.vector to form primary mammary tumors in nude mice was assayed. While the experiment is still ongoing, as of this writing there are no significant differences in primary tumor formation due to PCTK1 overexpression, suggesting its pro-growth effect may be metastasis-specific. However, in order to test whether the phenotype is brain metastasis-specific, additional *in vivo* experimental metastasis assays would be required to test whether PCTK1 enhances lung, bone, or even liver metastasis in the MDA-MB-231 model.

When PCTK1 failed to show growth advantages *in vitro*, it was unsurprising due to its status as a non-canonical CDK. However, it also failed to enhance migration, which is one of its commonly reported phenotypes in myoblasts and neurons (212, 236, 237). Interestingly, PCTK1 overexpression significantly reduced invasion of MDA-MB-231 cells through Matrigel, which is especially striking in light of its enhancement of invasion through hard agar. Matrigel, which is produced by a specialized line of mouse sarcoma cells, consists of a variety of basement membrane proteins including laminin and Type IV collagen (238). The fact that PCTK1 overexpression actually decreases invasion through Matrigel could simply be an *in vitro* artifact due to the specific composition of Matrigel; after all, the same cells actually have a growth advantage in the stiff matrix of hard agar and extend projections into the brain parenchyma from the meninges *in vivo*. Alternatively, it may indicate antagonistic pleiotropy of PCTK1 expression: if expressed in the primary tumor, it may actually decrease invasion through the basement membrane and extravasation. This would be suggestive of the fact that PCTK1's functional benefit to metastases is limited to growth and survival at the metastatic site. Experiments involving the modulation of PCTK1 in a spontaneous brain metastasis system

such as HIM (239) or BBM (235) could be helpful in identifying whether PCTK1 truly inhibits invasion and intravasation *in vivo*.

Because of the brain's abundant supply of glutamine relative to other amino acids (194) and the literature reports of brain metastatic tumor cells metabolizing glutamine to obtain ATP and biomass (200), TCGA data was examined for potential correlations of PCTK1 expression with glutamine metabolism. Since no large-scale datasets of brain metastasis are available, PCTK1 expressional correlations were examined in primary breast cancer as well as primary brain tumors, with the rationale that the brain environment represents a set of constraints, and all tumors, both primary and metastatic, are subject to these rules. While there were some correlations of PCTK1 with glutamine metabolism in all 3 subtypes of primary breast cancer (with ASNS) and in glioblastoma (with glucosamine-fructose-6-phosphate transaminase 1, GFPT1). The majority of the strong correlations observed were in low-grade glioma, where correlations existed between PCTK1, ASNS, GLS, and GLS2, as well and PCTK1, CDK5, and CDK5R1. It is established that the BBB is intact in LGG (240), while the vascular permeability of GBM renders the BBB functionally irrelevant (241). Therefore, the presence of these underlying relationships in LGG is highly suggestive of the fact that glutamine metabolism is important for cancer cell survival in the unique nutrient environment of the brain, but once the BBB functional barrier is lost, the nutrient restriction is lifted and PCTK1 may no longer provide a growth advantage.

The strength of the correlations between PCTK1 and the glutamine metabolism pathway were intriguing enough to demand functional examination. Using BME, low glucose, low amino acid-containing media, the PCTK1-overexpressing cells and their controls were compared for their relative growth ability. The answer was clear: with PCTK1 overexpression, cells can survive in glutamine-supplemented BME; without either glutamine presence of PCTK1 expression, the cells died. Attempts to grow the cells in similar concentrations of glutamate instead of glutamine did not enable cell proliferation or survival, suggesting that if the cancer

cells in the brain are involved in a glutamate-glutamine cycle, it is unlikely to be autocrine in nature. Since one of the crucial functions of astrocytes in the brain is to scavenge glutamate from the synapse, process it into glutamine, and deliver glutamine to neurons (242), the potential exists that cancer cells, which are known to interact with astrocytes, use this same pathway to obtain glutamine.

While the proliferative advantage enjoyed by PCTK1-overexpressing cells cultured in glutamine pointed to the cells' utilization of glutamine for energy or biomass generation, it could simply be donating its amino group for purine biosynthesis and leaving the cell as glutamate (243). Thus it was necessary to test whether there was a difference in glutamine and glutamate uptake and release from cell culture media by cancer cells. Indeed, MS analysis showed that although not statistically significant, glutamine uptake is slightly enhanced by PCTK1 overexpression. At the same time, net glutamate release into the media is actually lower in PCTK1-overexpressing cells. The combined increase in glutamine uptake and decrease in net glutamate release implies that the glutamine is being used as a fuel or mass substrate, although further MS experiments tracing the fate of glutamine's carbons and nitrogens are necessary are necessary to confirm whether they are being used for energy or building blocks.

In order to test whether there was a functional requirement for PCTK1 in brain metastasis, the HCC1954Br cell line was selected. A HER2-overexpressing line, 1954Br forms large parenchymal brain metastasis lesions in nude mice. Furthermore, of all of the *in vivo* brain-selected cell lines in the lab, it had the highest endogenous expression of PCTK1. Therefore, when knockdown of PCTK1 extended the median survival of 1954Br-bearing mice by nearly 60%, it was quite striking. The fact that the brain H&E sections of 1954Br controls and PCTK1-knockdown cells appeared to be morphologically very similar, in spite of their differences in survival time, could indicate two possibilities. Either the PCTK1 expression recovered *in vivo*, either through loss of the shRNA plasmid or selection for a clone that had inefficient knockdown, or PCTK1 provides a growth advantage at the early stage of brain

colonization but is dispensable later. While IHC analysis of the same slides for PCTK1 expression did reveal that PCTK1 expression can recover *in vivo* in the shRNA knockdown group, the expression of PCTK1 in all samples was heterogeneous. Therefore, the possibility still remains that there is spatiotemporal variability in the requirement for PCTK1 during the process of brain metastasis. To resolve the absolute necessity of PCTK1 and whether it is important only at certain stages of the brain metastatic process, experiments utilizing CRISPR-Cas9-based knockout of PCTK1 of inducible shRNA against PCTK1 can be performed *in vivo*.

Conclusions and future directions

Brain metastasis is a common and deadly malignancy for which the biomedical research has little in the way of understanding and even less in terms of treatment options. This study, an in vivo functional genomics screen aimed at identification of novel kinases driving brain metastasis, sought to better elucidate the biology of brain metastasis. The screen was successful in identifying 31 potential drivers of brain metastasis, most of which are indeed expressed in human brain metastases. The screen identified several hits related to glucose utilization in the brain, a pathway already identified in brain metastasis that serves as a positive control that this study's underlying methodology was sound. Other interconnected networks identified by the screen included calcium signaling, which is of great importance to neural function but whose function in brain metastasis remains unclear, and the non-canonical CDK axis of CDK5R1-CDK5-PCTK1. I validated the functional importance of PCTK1 in enhancing brain metastasis growth by overexpression in the MDA-MB-231 model, and went on to show that PCTK1's brain metastasis growth enhancement does not extend to primary tumors in the same model. Additionally, while PCTK1 did not convey proliferative or survival advantages *in vitro* under normal culture conditions, it did dramatically enhance these phenotypes in a glutamine-dependent manner when grown in a glucose and amino acid-limited medium that was supplemented with glutamine to mimic the nutrient environment of the brain. Finally, I

showed that stable knockdown of PCTK1 in a different breast cancer cell line delayed the mortality due to brain metastasis by nearly 60%.

Future directions of this study will aim at identification of the molecular mechanism by which PCTK1 enables the enhanced utilization of glutamine. By performing MS tracing analysis of metabolites generated from isotopically labeled glutamine, it will be possible to identify exactly how brain metastatic cells may be utilizing glutamine, whether it be for fuel or biomolecule generation. Identification of metabolites will guide the search for a direct phosphorylation target of PCTK1, and identification of that PCTK1 substrate and its phosphorylation site, followed by validation of the pathway's activation in clinical brain metastasis, could allow for the development of PCTK1-targeted therapy. Further studies involving inducible knockdowns of PCTK1 can also be performed to investigate the timing of PCTK1's growth advantage in brain metastasis, and whether it is limited to the early colonization steps or throughout brain metastatic growth. Additionally, CRISPR-based knockout of PCTK1 will allow observation of whether PCTK1 is necessary for brain metastasis growth, as it would remove the possibility of selection for metastatic clones with inefficient knockdown of PCTK1.

Furthermore, there are 30 additional unvalidated targets that have been identified by this study. While PCTK1 demonstrated a dramatic pro-brain metastasis phenotype, there could be several other, potentially more important kinases and pathways to investigate in brain metastasis. By using functional genomics, it was possible to identify the key barriers that cancer cells have to overcome for growth in the brain. The potential exists that re-establishing these barriers and forcing brain metastases into an evolutionary double bind could result in therapeutic efficacy heretofore unseen in this disease setting.

Chapter 6: References

1. Society AC. Cancer Statistics Center 2016 [cited 2016 March 23, 2016]. Available from: https://cancerstatisticscenter.cancer.org/.

2. Parker-Pope T. A Grim Breast Cancer Milestone for Black Women New York Times2015 [cited 2016 March 23]. Available from: http://well.blogs.nytimes.com/2015/10/29/a-grim-breast-cancer-milestone-for-black-women/?_r=1.

3. Institute NC. About Cancer 2016 [cited 2016 March 23]. Available from: http://www.cancer.gov/about-cancer.

4. Siegel RL, Miller KD, Jemal A. Cancer statistics, 2015. CA: a cancer journal for clinicians. 2015 Jan-Feb;65(1):5-29. PubMed PMID: 25559415.

5. Berry DA, Cronin KA, Plevritis SK, Fryback DG, Clarke L, Zelen M, Mandelblatt JS, Yakovlev AY, Habbema JD, Feuer EJ, Cancer I, Surveillance Modeling Network C. Effect of screening and adjuvant therapy on mortality from breast cancer. The New England journal of medicine. 2005 Oct 27;353(17):1784-92. PubMed PMID: 16251534.

6. Oeffinger KC, Fontham ET, Etzioni R, Herzig A, Michaelson JS, Shih YC, Walter LC, Church TR, Flowers CR, LaMonte SJ, Wolf AM, DeSantis C, Lortet-Tieulent J, Andrews K, Manassaram-Baptiste D, Saslow D, Smith RA, Brawley OW, Wender R, American Cancer S. Breast Cancer Screening for Women at Average Risk: 2015 Guideline Update From the American Cancer Society. Jama. 2015 Oct 20;314(15):1599-614. PubMed PMID: 26501536.

7. Force USPST. Screening for breast cancer: U.S. Preventive Services Task Force recommendation statement. Annals of internal medicine. 2009 Nov 17;151(10):716-26, W-236. PubMed PMID: 19920272.

8. Schnitt SJ. Classification and prognosis of invasive breast cancer: from morphology to molecular taxonomy. Modern pathology : an official journal of the United States and Canadian Academy of Pathology, Inc. 2010 May;23 Suppl 2:S60-4. PubMed PMID: 20436504.

9. Cancer Genome Atlas N. Comprehensive molecular portraits of human breast tumours. Nature. 2012 Oct 4;490(7418):61-70. PubMed PMID: 23000897. Pubmed Central PMCID: 3465532.

10. Curtis C, Shah SP, Chin SF, Turashvili G, Rueda OM, Dunning MJ, Speed D, Lynch AG, Samarajiwa S, Yuan Y, Graf S, Ha G, Haffari G, Bashashati A, Russell R, McKinney S, Group M, Langerod A, Green A, Provenzano E, Wishart G, Pinder S, Watson P, Markowetz F, Murphy L, Ellis I, Purushotham A, Borresen-Dale AL, Brenton JD, Tavare S, Caldas C, Aparicio S. The genomic and transcriptomic architecture of 2,000 breast tumours reveals novel subgroups. Nature. 2012 Jun 21;486(7403):346-52. PubMed PMID: 22522925. Pubmed Central PMCID: 3440846.

11. Lim E, Vaillant F, Wu D, Forrest NC, Pal B, Hart AH, Asselin-Labat ML, Gyorki DE, Ward T, Partanen A, Feleppa F, Huschtscha LI, Thorne HJ, kConFab, Fox SB, Yan M, French JD, Brown MA, Smyth GK, Visvader JE, Lindeman GJ. Aberrant luminal progenitors as the candidate target population for basal tumor development in BRCA1 mutation carriers. Nature medicine. 2009 Aug;15(8):907-13. PubMed PMID: 19648928.

12. Prat A, Perou CM. Mammary development meets cancer genomics. Nature medicine. 2009 Aug;15(8):842-4. PubMed PMID: 19661985.

13. Prat A, Parker JS, Karginova O, Fan C, Livasy C, Herschkowitz JI, He X, Perou CM. Phenotypic and molecular characterization of the claudin-low intrinsic subtype of breast cancer. Breast cancer research : BCR. 2010;12(5):R68. PubMed PMID: 20813035. Pubmed Central PMCID: 3096954.

14. Nofech-Mozes S, Trudeau M, Kahn HK, Dent R, Rawlinson E, Sun P, Narod SA, Hanna WM. Patterns of recurrence in the basal and non-basal subtypes of triple-negative breast cancers. Breast cancer research and treatment. 2009 Nov;118(1):131-7. PubMed PMID: 19189211.

15. Prat A, Pineda E, Adamo B, Galvan P, Fernandez A, Gaba L, Diez M, Viladot M, Arance A, Munoz M. Clinical implications of the intrinsic molecular subtypes of breast cancer. Breast. 2015 Nov;24 Suppl 2:S26-35. PubMed PMID: 26253814.

16. Turner NC, Ro J, Andre F, Loi S, Verma S, Iwata H, Harbeck N, Loibl S, Huang Bartlett C, Zhang K, Giorgetti C, Randolph S, Koehler M, Cristofanilli M, Group PS. Palbociclib in Hormone-Receptor-Positive Advanced Breast Cancer. The New England journal of medicine. 2015 Jul 16;373(3):209-19. PubMed PMID: 26030518.

17. von Minckwitz G, Martin M. Neoadjuvant treatments for triple-negative breast cancer (TNBC). Annals of oncology : official journal of the European Society for Medical Oncology / ESMO. 2012 Aug;23 Suppl 6:vi35-9. PubMed PMID: 23012300.

18. von Minckwitz G, Untch M, Nuesch E, Loibl S, Kaufmann M, Kummel S, Fasching PA, Eiermann W, Blohmer JU, Costa SD, Mehta K, Hilfrich J, Jackisch C, Gerber B, du Bois A, Huober J, Hanusch C, Konecny G, Fett W, Stickeler E, Harbeck N, Muller V, Juni P. Impact of treatment characteristics on response of different breast cancer phenotypes: pooled analysis of the German neo-adjuvant chemotherapy trials. Breast cancer research and treatment. 2011 Jan;125(1):145-56. PubMed PMID: 21042932.

19. Sikov WM, Dizon DS, Strenger R, Legare RD, Theall KP, Graves TA, Gass JS, Kennedy TA, Fenton MA. Frequent pathologic complete responses in aggressive stages II to III breast cancers with every-4-week carboplatin and weekly paclitaxel with or without trastuzumab: a Brown University Oncology Group Study. Journal of clinical oncology : official journal of the American Society of Clinical Oncology. 2009 Oct 1;27(28):4693-700. PubMed PMID: 19720916.

20. Kern P, Kalisch A, Kolberg HC, Kimmig R, Otterbach F, von Minckwitz G, Sikov WM, Pott D, Kurbacher C. Neoadjuvant, anthracycline-free chemotherapy with carboplatin and docetaxel in triple-negative, early-stage breast cancer: a multicentric analysis of feasibility and

rates of pathologic complete response. Chemotherapy. 2013;59(5):387-94. PubMed PMID: 24852315.

21. Dent RA, Lindeman GJ, Clemons M, Wildiers H, Chan A, McCarthy NJ, Singer CF, Lowe ES, Watkins CL, Carmichael J. Phase I trial of the oral PARP inhibitor olaparib in combination with paclitaxel for first- or second-line treatment of patients with metastatic triple-negative breast cancer. Breast cancer research : BCR. 2013;15(5):R88. PubMed PMID: 24063698. Pubmed Central PMCID: 3979135.

22. Matulonis UA, Penson RT, Domchek SM, Kaufman B, Shapira-Frommer R, Audeh MW, Kaye S, Molife LR, Gelmon KA, Robertson JD, Mann H, Ho TW, Coleman RL. Olaparib monotherapy in patients with advanced relapsed ovarian cancer and a germline BRCA1/2 mutation: a multi-study analysis of response rates and safety. Annals of oncology : official journal of the European Society for Medical Oncology / ESMO. 2016 Mar 8. PubMed PMID: 26961146.

23. Sleeman J, Steeg PS. Cancer metastasis as a therapeutic target. European journal of cancer. 2010 May;46(7):1177-80. PubMed PMID: 20307970.

24. Mehlen P, Puisieux A. Metastasis: a question of life or death. Nature reviews Cancer. 2006 Jun;6(6):449-58. PubMed PMID: 16723991.

25. Kitchen H. HolleyKitchenCancerLife Facebook2016 [cited 2016 March 23]. Available from: www.facebook.com/HolleyKitchenCancerLifer/.

26. Pfizer. A Story Half Told: Meet Holley Kitchen 2015 [cited 2016 March 23]. Available from: http://www.storyhalftold.com/meet-holley-kitchen.

27. Early Breast Cancer Trialists' Collaborative G, Coleman R, Powles T, Paterson A, Gnant M, Anderson S, Diel I, Gralow J, von Minckwitz G, Moebus V, Bergh J, Pritchard KI, Bliss J, Cameron D, Evans V, Pan H, Peto R, Bradley R, Gray R. Adjuvant bisphosphonate treatment in early breast cancer: meta-analyses of individual patient data from randomised trials. Lancet. 2015 Oct 3;386(10001):1353-61. PubMed PMID: 26211824.

28. Erdi AK, Erdi YE, Yorke ED, Wessels BW. Treatment planning for radio-immunotherapy. Physics in medicine and biology. 1996 Oct;41(10):2009-26. PubMed PMID: 8912377.

29. Erdi YE. Limits of Tumor Detectability in Nuclear Medicine and PET. Molecular imaging and radionuclide therapy. 2012 Apr;21(1):23-8. PubMed PMID: 23486256. Pubmed Central PMCID: 3590963.

30. Del Monte U. Does the cell number 10(9) still really fit one gram of tumor tissue? Cell cycle. 2009 Feb 1;8(3):505-6. PubMed PMID: 19176997.

31. Coleman RE, Smith P, Rubens RD. Clinical course and prognostic factors following bone recurrence from breast cancer. British journal of cancer. 1998;77(2):336-40. PubMed PMID: 9461007. Pubmed Central PMCID: 2151240.

32. Coleman RE. Skeletal complications of malignancy. Cancer. 1997 Oct 15;80(8 Suppl):1588-94. PubMed PMID: 9362426.

33. Connolly JE, Jr., Erasmus JJ, Patz EF, Jr. Thoracic manifestations of breast carcinoma: metastatic disease and complications of treatment. Clinical radiology. 1999 Aug;54(8):487-94. PubMed PMID: 10484214.

34. Parham DM, Robertson AJ. A retrospective study of breast carcinoma: causes of death and pattern of metastases. British journal of cancer. 1989 Sep;60(3):394-6. PubMed PMID: 2789949. Pubmed Central PMCID: 2247170.

35. Kreisman H, Wolkove N, Finkelstein HS, Cohen C, Margolese R, Frank H. Breast cancer and thoracic metastases: review of 119 patients. Thorax. 1983 Mar;38(3):175-9. PubMed PMID: 6857580. Pubmed Central PMCID: 459514.

36. Miyaaki H, Ichikawa T, Taura N, Yamashima M, Arai H, Obata Y, Furusu A, Hayashi H, Kohno S, Nakao K. Diffuse liver metastasis of small cell lung cancer causing marked hepatomegaly and fulminant hepatic failure. Internal medicine. 2010;49(14):1383-6. PubMed PMID: 20647652.

37. Helling TS, Martin M. Cause of death from liver metastases in colorectal cancer. Annals of surgical oncology. 2014 Feb;21(2):501-6. PubMed PMID: 24081807.

38. Sawaya R. Considerations in the diagnosis and management of brain metastases. Oncology. 2001 Sep;15(9):1144-54, 57-8; discussion 58, 63-5. PubMed PMID: 11589063.

39. Lassman AB, DeAngelis LM. Brain metastases. Neurologic clinics. 2003 Feb;21(1):1-23, vii. PubMed PMID: 12690643.

40. Paget S. The distribution of secondary growths in cancer of the breast. 1889. Cancer metastasis reviews. 1989 Aug;8(2):98-101. PubMed PMID: 2673568.

41. Fidler IJ, Kripke ML. Metastasis results from preexisting variant cells within a malignant tumor. Science. 1977 Aug 26;197(4306):893-5. PubMed PMID: 887927.

42. Fidler IJ. Metastasis: quantitative analysis of distribution and fate of tumor emboli labeled with 125 I-5-iodo-2'-deoxyuridine. Journal of the National Cancer Institute. 1970 Oct;45(4):773-82. PubMed PMID: 5513503.

43. Hart IR, Fidler IJ. Role of organ selectivity in the determination of metastatic patterns of B16 melanoma. Cancer research. 1980 Jul;40(7):2281-7. PubMed PMID: 7388794.

44. Talmadge JE, Fidler IJ. AACR centennial series: the biology of cancer metastasis: historical perspective. Cancer research. 2010 Jul 15;70(14):5649-69. PubMed PMID: 20610625. Pubmed Central PMCID: 4037932.

45. Hanahan D, Weinberg RA. Hallmarks of cancer: the next generation. Cell. 2011 Mar 4;144(5):646-74. PubMed PMID: 21376230.

46. Helmlinger G, Yuan F, Dellian M, Jain RK. Interstitial pH and pO2 gradients in solid tumors in vivo: high-resolution measurements reveal a lack of correlation. Nature medicine. 1997 Feb;3(2):177-82. PubMed PMID: 9018236.

47. Gimbrone MA, Jr., Aster RH, Cotran RS, Corkery J, Jandl JH, Folkman J. Preservation of vascular integrity in organs perfused in vitro with a platelet-rich medium. Nature. 1969 Apr 5;222(5188):33-6. PubMed PMID: 5775827.

48. Thomlinson RH, Gray LH. The histological structure of some human lung cancers and the possible implications for radiotherapy. British journal of cancer. 1955 Dec;9(4):539-49. PubMed PMID: 13304213. Pubmed Central PMCID: 2073776.

49. Tannock IF. The relation between cell proliferation and the vascular system in a transplanted mouse mammary tumour. British journal of cancer. 1968 Jun;22(2):258-73. PubMed PMID: 5660132. Pubmed Central PMCID: PMC2008239. Epub 1968/06/01. eng.

50. Folkman J. Tumor angiogenesis: therapeutic implications. The New England journal of medicine. 1971 Nov 18;285(21):1182-6. PubMed PMID: 4938153.

51. Donnem T, Hu J, Ferguson M, Adighibe O, Snell C, Harris AL, Gatter KC, Pezzella F. Vessel co-option in primary human tumors and metastases: an obstacle to effective anti-angiogenic treatment? Cancer medicine. 2013 Aug;2(4):427-36. PubMed PMID: 24156015. Pubmed Central PMCID: 3799277.

52. Soda Y, Marumoto T, Friedmann-Morvinski D, Soda M, Liu F, Michiue H, Pastorino S, Yang M, Hoffman RM, Kesari S, Verma IM. Transdifferentiation of glioblastoma cells into vascular endothelial cells. Proceedings of the National Academy of Sciences of the United States of America. 2011 Mar 15;108(11):4274-80. PubMed PMID: 21262804. Pubmed Central PMCID: 3060261.

53. Clark WH. Tumour progression and the nature of cancer. British journal of cancer. 1991 Oct;64(4):631-44. PubMed PMID: 1911211. Pubmed Central PMCID: 1977704.

54. Piepmeier J, Baehring JM. Surgical resection for patients with benign primary brain tumors and low grade gliomas. Journal of neuro-oncology. 2004 Aug-Sep;69(1-3):55-65. PubMed PMID: 15527080.

55. Liotta LA, Abe S, Robey PG, Martin GR. Preferential digestion of basement membrane collagen by an enzyme derived from a metastatic murine tumor. Proceedings of the National Academy of Sciences of the United States of America. 1979 May;76(5):2268-72. PubMed PMID: 221920. Pubmed Central PMCID: 383580.

56. Zeng ZS, Cohen AM, Guillem JG. Loss of basement membrane type IV collagen is associated with increased expression of metalloproteinases 2 and 9 (MMP-2 and MMP-9) during human colorectal tumorigenesis. Carcinogenesis. 1999 May;20(5):749-55. PubMed PMID: 10334190.

57. Fearon ER, Vogelstein B. A genetic model for colorectal tumorigenesis. Cell. 1990 Jun 1;61(5):759-67. PubMed PMID: 2188735.

58. Francis A, Thomas J, Fallowfield L, Wallis M, Bartlett JM, Brookes C, Roberts T, Pirrie S, Gaunt C, Young J, Billingham L, Dodwell D, Hanby A, Pinder SE, Evans A, Reed M, Jenkins V, Matthews L, Wilcox M, Fairbrother P, Bowden S, Rea D. Addressing overtreatment of screen detected DCIS; the LORIS trial. European journal of cancer. 2015 Nov;51(16):2296-303. PubMed PMID: 26296293.

59. Psaila B, Lyden D. The metastatic niche: adapting the foreign soil. Nature reviews Cancer. 2009 Apr;9(4):285-93. PubMed PMID: 19308068. Pubmed Central PMCID: 3682494.

60. Klotz L. Prostate cancer overdiagnosis and overtreatment. Current opinion in endocrinology, diabetes, and obesity. 2013 Jun;20(3):204-9. PubMed PMID: 23609043.

61. Tomasetti C, Vogelstein B. Cancer etiology. Variation in cancer risk among tissues can be explained by the number of stem cell divisions. Science. 2015 Jan 2;347(6217):78-81. PubMed PMID: 25554788. Pubmed Central PMCID: 4446723.

62. Janni WJ, Rack B, Terstappen LW, Pierga JY, Taran FA, Fehm T, Hall C, de Groot MR, Bidard FC, Friedl TW, Fasching PA, Brucker SY, Pantel K, Lucci A. Pooled Analysis of the Prognostic Relevance of Circulating Tumor Cells in Primary Breast Cancer. Clinical cancer research : an official journal of the American Association for Cancer Research. 2016 Jan 5. PubMed PMID: 26733614.

63. Cui L, Kwong J, Wang CC. Prognostic value of circulating tumor cells and disseminated tumor cells in patients with ovarian cancer: a systematic review and meta-

analysis. Journal of ovarian research. 2015;8:38. PubMed PMID: 26077676. Pubmed Central PMCID: 4479068.

64. Tarin D, Price JE, Kettlewell MG, Souter RG, Vass AC, Crossley B. Mechanisms of human tumor metastasis studied in patients with peritoneovenous shunts. Cancer research. 1984 Aug;44(8):3584-92. PubMed PMID: 6744281.

65. Liotta LA, Kohn E. Anoikis: cancer and the homeless cell. Nature. 2004 Aug 26;430(7003):973-4. PubMed PMID: 15329701.

66. Bates RC, Buret A, van Helden DF, Horton MA, Burns GF. Apoptosis induced by inhibition of intercellular contact. The Journal of cell biology. 1994 Apr;125(2):403-15. PubMed PMID: 8163556. Pubmed Central PMCID: 2120042.

67. Fidler IJ. The pathogenesis of cancer metastasis: the 'seed and soil' hypothesis revisited. Nature reviews Cancer. 2003 Jun;3(6):453-8. PubMed PMID: 12778135.

68. Chivukula VK, Krog BL, Nauseef JT, Henry MD, Vigmostad SC. Alterations in cancer cell mechanical properties after fluid shear stress exposure: a micropipette aspiration study. Cell health and cytoskeleton. 2015 Jan 9;7:25-35. PubMed PMID: 25908902. Pubmed Central PMCID: 4405123.

69. Fidler IJ. The relationship of embolic homogeneity, number, size and viability to the incidence of experimental metastasis. European journal of cancer. 1973 Mar;9(3):223-7. PubMed PMID: 4787857.

70. Liotta LA, Saidel MG, Kleinerman J. The significance of hematogenous tumor cell clumps in the metastatic process. Cancer research. 1976 Mar;36(3):889-94. PubMed PMID: 1253177.

71. Molnar B, Ladanyi A, Tanko L, Sreter L, Tulassay Z. Circulating tumor cell clusters in the peripheral blood of colorectal cancer patients. Clinical cancer research : an official journal of the American Association for Cancer Research. 2001 Dec;7(12):4080-5. PubMed PMID: 11751505.

72. Cho EH, Wendel M, Luttgen M, Yoshioka C, Marrinucci D, Lazar D, Schram E, Nieva J, Bazhenova L, Morgan A, Ko AH, Korn WM, Kolatkar A, Bethel K, Kuhn P. Characterization of circulating tumor cell aggregates identified in patients with epithelial tumors. Physical biology. 2012 Feb;9(1):016001. PubMed PMID: 22306705. Pubmed Central PMCID: 3387999.

73. Aceto N, Bardia A, Miyamoto DT, Donaldson MC, Wittner BS, Spencer JA, Yu M, Pely A, Engstrom A, Zhu H, Brannigan BW, Kapur R, Stott SL, Shioda T, Ramaswamy S, Ting DT, Lin CP, Toner M, Haber DA, Maheswaran S. Circulating tumor cell clusters are oligoclonal precursors of breast cancer metastasis. Cell. 2014 Aug 28;158(5):1110-22. PubMed PMID: 25171411. Pubmed Central PMCID: 4149753.

74. Wirtz D, Konstantopoulos K, Searson PC. The physics of cancer: the role of physical interactions and mechanical forces in metastasis. Nature reviews Cancer. 2011 Jul;11(7):512-22. PubMed PMID: 21701513. Pubmed Central PMCID: 3262453.

75. Kienast Y, von Baumgarten L, Fuhrmann M, Klinkert WE, Goldbrunner R, Herms J, Winkler F. Real-time imaging reveals the single steps of brain metastasis formation. Nature medicine. 2010 Jan;16(1):116-22. PubMed PMID: 20023634.

76. Geng Y, Marshall JR, King MR. Glycomechanics of the metastatic cascade: tumor cell-endothelial cell interactions in the circulation. Annals of biomedical engineering. 2012 Apr;40(4):790-805. PubMed PMID: 22101756.

77. Ku DN. Blood Flow in Arteries. Annual Review of Fluid Mechanics. 1997 January 1997;29:399-434.

78. Miles FL, Pruitt FL, van Golen KL, Cooper CR. Stepping out of the flow: capillary extravasation in cancer metastasis. Clinical & experimental metastasis. 2008;25(4):305-24. PubMed PMID: 17906932.

79. Bos PD, Zhang XH, Nadal C, Shu W, Gomis RR, Nguyen DX, Minn AJ, van de Vijver MJ, Gerald WL, Foekens JA, Massague J. Genes that mediate breast cancer metastasis to

the brain. Nature. 2009 Jun 18;459(7249):1005-9. PubMed PMID: 19421193. Pubmed Central PMCID: 2698953.

80. Gasic GJ, Gasic TB, Stewart CC. Antimetastatic effects associated with platelet reduction. Proceedings of the National Academy of Sciences of the United States of America. 1968 Sep;61(1):46-52. PubMed PMID: 5246932. Pubmed Central PMCID: 285903.

81. Camerer E, Qazi AA, Duong DN, Cornelissen I, Advincula R, Coughlin SR. Platelets, protease-activated receptors, and fibrinogen in hematogenous metastasis. Blood. 2004 Jul 15;104(2):397-401. PubMed PMID: 15031212.

82. Karpatkin S, Pearlstein E, Ambrogio C, Coller BS. Role of adhesive proteins in platelet tumor interaction in vitro and metastasis formation in vivo. The Journal of clinical investigation. 1988 Apr;81(4):1012-9. PubMed PMID: 3280598. Pubmed Central PMCID: 329625.

83. Roussos ET, Condeelis JS, Patsialou A. Chemotaxis in cancer. Nature reviews Cancer. 2011 Aug;11(8):573-87. PubMed PMID: 21779009. Pubmed Central PMCID: 4030706.

84. New JY, Li B, Koh WP, Ng HK, Tan SY, Yap EH, Chan SH, Hu HZ. T cell infiltration and chemokine expression: relevance to the disease localization in murine graft-versus-host disease. Bone marrow transplantation. 2002 Jun;29(12):979-86. PubMed PMID: 12098066.

85. Carman CV, Springer TA. A transmigratory cup in leukocyte diapedesis both through individual vascular endothelial cells and between them. The Journal of cell biology. 2004 Oct 25;167(2):377-88. PubMed PMID: 15504916. Pubmed Central PMCID: 2172560.

86. Leong HS, Robertson AE, Stoletov K, Leith SJ, Chin CA, Chien AE, Hague MN, Ablack A, Carmine-Simmen K, McPherson VA, Postenka CO, Turley EA, Courtneidge SA, Chambers AF, Lewis JD. Invadopodia are required for cancer cell extravasation and are a therapeutic target for metastasis. Cell reports. 2014 Sep 11;8(5):1558-70. PubMed PMID: 25176655.

87. Boecke A, Carstens AC, Neacsu CD, Baschuk N, Haubert D, Kashkar H, Utermohlen O, Pongratz C, Kronke M. TNF-receptor-1 adaptor protein FAN mediates TNF-induced B16 melanoma motility and invasion. British journal of cancer. 2013 Jul 23;109(2):422-32. PubMed PMID: 23674089. Pubmed Central PMCID: 3721409.

88. Lucas JT, Jr., Salimath BP, Slomiany MG, Rosenzweig SA. Regulation of invasive behavior by vascular endothelial growth factor is HEF1-dependent. Oncogene. 2010 Aug 5;29(31):4449-59. PubMed PMID: 20498643. Pubmed Central PMCID: 2921319.

89. Suzuki M, Mose ES, Montel V, Tarin D. Dormant cancer cells retrieved from metastasis-free organs regain tumorigenic and metastatic potency. The American journal of pathology. 2006 Aug;169(2):673-81. PubMed PMID: 16877365. Pubmed Central PMCID: 1698784.

90. Aguirre-Ghiso JA. Models, mechanisms and clinical evidence for cancer dormancy. Nature reviews Cancer. 2007 Nov;7(11):834-46. PubMed PMID: 17957189. Pubmed Central PMCID: 2519109.

91. Klein CA, Holzel D. Systemic cancer progression and tumor dormancy: mathematical models meet single cell genomics. Cell cycle. 2006 Aug;5(16):1788-98. PubMed PMID: 16929175.

92. Karrison TG, Ferguson DJ, Meier P. Dormancy of mammary carcinoma after mastectomy. Journal of the National Cancer Institute. 1999 Jan 6;91(1):80-5. PubMed PMID: 9890174.

93. Demicheli R, Biganzoli E, Boracchi P, Greco M, Retsky MW. Recurrence dynamics does not depend on the recurrence site. Breast cancer research : BCR. 2008;10(5):R83. PubMed PMID: 18844974. Pubmed Central PMCID: 2614518.

94. Early Breast Cancer Trialists' Collaborative G. Effects of chemotherapy and hormonal therapy for early breast cancer on recurrence and 15-year survival: an overview of the randomised trials. Lancet. 2005 May 14-20;365(9472):1687-717. PubMed PMID: 15894097.

95. Demicheli R, Abbattista A, Miceli R, Valagussa P, Bonadonna G. Time distribution of the recurrence risk for breast cancer patients undergoing mastectomy: further support about the concept of tumor dormancy. Breast cancer research and treatment. 1996;41(2):177-85. PubMed PMID: 8944336.

96. Menczer J, Schreiber L, Peled O, Levy T. Very late recurrence (after more than 20 years) of epithelial ovarian carcinoma: case report and literature review. Archives of gynecology and obstetrics. 2015 Jun;291(6):1199-203. PubMed PMID: 25524538.

97. Tincani AJ, Martins AS, Lage Hde T, Souza LS. Melanoma ganglionic metastasis 30 years after treatment of the primary tumor--a case report. Sao Paulo medical journal = Revista paulista de medicina. 1996 Mar-Apr;114(2):1131-3. PubMed PMID: 9077023.

98. Stephens JK, Everson GT, Elliott CL, Kam I, Wachs M, Haney J, Bartlett ST, Franklin WA. Fatal transfer of malignant melanoma from multiorgan donor to four allograft recipients. Transplantation. 2000 Jul 15;70(1):232-6. PubMed PMID: 10919612.

99. Morris-Stiff G, Steel A, Savage P, Devlin J, Griffiths D, Portman B, Mason M, Jurewicz WA, Welsh Transplantation Research G. Transmission of donor melanoma to multiple organ transplant recipients. American journal of transplantation : official journal of the American Society of Transplantation and the American Society of Transplant Surgeons. 2004 Mar;4(3):444-6. PubMed PMID: 14962000.

100. Lipshutz GS, Mihara N, Wong R, Wallace WD, Allen-Auerbach M, Dorigo O, Rao PN, Pham PC, Pham PT. Death from metastatic donor-derived ovarian cancer in a male kidney transplant recipient. American journal of transplantation : official journal of the American Society of Transplantation and the American Society of Transplant Surgeons. 2009 Feb;9(2):428-32. PubMed PMID: 19178417.

101. Quail DF, Joyce JA. Microenvironmental regulation of tumor progression and metastasis. Nature medicine. 2013 Nov;19(11):1423-37. PubMed PMID: 24202395. Pubmed Central PMCID: 3954707.

102. Talmadge JE, Wolman SR, Fidler IJ. Evidence for the clonal origin of spontaneous metastases. Science. 1982 Jul 23;217(4557):361-3. PubMed PMID: 6953592.

103. Yamamoto N, Yang M, Jiang P, Xu M, Tsuchiya H, Tomita K, Moossa AR, Hoffman RM. Determination of clonality of metastasis by cell-specific color-coded fluorescent-protein imaging. Cancer research. 2003 Nov 15;63(22):7785-90. PubMed PMID: 14633704.

104. Montel V, Mose ES, Tarin D. Tumor-stromal interactions reciprocally modulate gene expression patterns during carcinogenesis and metastasis. International journal of cancer. 2006 Jul 15;119(2):251-63. PubMed PMID: 16482564.

105. Park ES, Kim SJ, Kim SW, Yoon SL, Leem SH, Kim SB, Kim SM, Park YY, Cheong JH, Woo HG, Mills GB, Fidler IJ, Lee JS. Cross-species hybridization of microarrays for studying tumor transcriptome of brain metastasis. Proceedings of the National Academy of Sciences of the United States of America. 2011 Oct 18;108(42):17456-61. PubMed PMID: 21987811. Pubmed Central PMCID: 3198333.

106. Minn AJ, Gupta GP, Siegel PM, Bos PD, Shu W, Giri DD, Viale A, Olshen AB, Gerald WL, Massague J. Genes that mediate breast cancer metastasis to lung. Nature. 2005 Jul 28;436(7050):518-24. PubMed PMID: 16049480. Pubmed Central PMCID: 1283098.

107. Lee YC, Lin SC, Yu G, Cheng CJ, Liu B, Liu HC, Hawke DH, Parikh NU, Varkaris A, Corn P, Logothetis C, Satcher RL, Yu-Lee LY, Gallick GE, Lin SH. Identification of Bone-Derived Factors Conferring De Novo Therapeutic Resistance in Metastatic Prostate Cancer. Cancer research. 2015 Nov 15;75(22):4949-59. PubMed PMID: 26530902. Pubmed Central PMCID: 4651787.

108. Kerbel RS, Kobayashi H, Graham CH. Intrinsic or acquired drug resistance and metastasis: are they linked phenotypes? Journal of cellular biochemistry. 1994 Sep;56(1):37-47. PubMed PMID: 7806590.

109. Cunningham JJ, Brown JS, Vincent TL, Gatenby RA. Divergent and convergent evolution in metastases suggest treatment strategies based on specific metastatic sites.

Evolution, medicine, and public health. 2015;2015(1):76-87. PubMed PMID: 25794501. Pubmed Central PMCID: 4404930.

110. Gottesman MM, Fojo T, Bates SE. Multidrug resistance in cancer: role of ATP-dependent transporters. Nature reviews Cancer. 2002 Jan;2(1):48-58. PubMed PMID: 11902585.

111. Fidler IJ. Critical determinants of cancer metastasis: rationale for therapy. Cancer chemotherapy and pharmacology. 1999;43 Suppl:S3-10. PubMed PMID: 10357552.

112. Kim SW, Choi HJ, Lee HJ, He J, Wu Q, Langley RR, Fidler IJ, Kim SJ. Role of the endothelin axis in astrocyte- and endothelial cell-mediated chemoprotection of cancer cells. Neuro-oncology. 2014 Dec;16(12):1585-98. PubMed PMID: 25008093. Pubmed Central PMCID: 4232084.

113. Patel LR, Camacho DF, Shiozawa Y, Pienta KJ, Taichman RS. Mechanisms of cancer cell metastasis to the bone: a multistep process. Future oncology. 2011 Nov;7(11):1285-97. PubMed PMID: 22044203. Pubmed Central PMCID: 3258525.

114. Prideaux M, Findlay DM, Atkins GJ. Osteocytes: The master cells in bone remodelling. Current opinion in pharmacology. 2016 Feb 26;28:24-30. PubMed PMID: 26927500.

115. Fornier MN. Denosumab: second chapter in controlling bone metastases or a new book? Journal of clinical oncology : official journal of the American Society of Clinical Oncology. 2010 Dec 10;28(35):5127-31. PubMed PMID: 21060038.

116. Bednarz-Knoll N, Efstathiou A, Gotzhein F, Wikman H, Mueller V, Kang Y, Pantel K. Potential Involvement of Jagged1 in Metastatic Progression of Human Breast Carcinomas. Clinical chemistry. 2016 Feb;62(2):378-86. PubMed PMID: 26721293.

117. Hynes RO. Metastatic potential: generic predisposition of the primary tumor or rare, metastatic variants-or both? Cell. 2003 Jun 27;113(7):821-3. PubMed PMID: 12837240.

118. Klein E. Gradual transformation of solid into ascites tumors; evidence favoring the mutation-selection theory. Experimental cell research. 1955 Feb;8(1):188-212. PubMed PMID: 14353117.

119. Cifone MA, Fidler IJ. Increasing metastatic potential is associated with increasing genetic instability of clones isolated from murine neoplasms. Proceedings of the National Academy of Sciences of the United States of America. 1981 Nov;78(11):6949-52. PubMed PMID: 6947269. Pubmed Central PMCID: 349170.

120. Welch DR, Neri A, Nicolson GL. Comparison of 'spontaneous' and 'experimental' metastasis using rat 13762 mammary adenocarcinoma metastatic cell clones. Invasion & metastasis. 1983;3(2):65-80. PubMed PMID: 6677622.

121. Caldas C. Cancer sequencing unravels clonal evolution. Nature biotechnology. 2012 May;30(5):408-10. PubMed PMID: 22565966.

122. Wang Y, Waters J, Leung ML, Unruh A, Roh W, Shi X, Chen K, Scheet P, Vattathil S, Liang H, Multani A, Zhang H, Zhao R, Michor F, Meric-Bernstam F, Navin NE. Clonal evolution in breast cancer revealed by single nucleus genome sequencing. Nature. 2014 Aug 14;512(7513):155-60. PubMed PMID: 25079324. Pubmed Central PMCID: 4158312.

123. Navin N, Kendall J, Troge J, Andrews P, Rodgers L, McIndoo J, Cook K, Stepansky A, Levy D, Esposito D, Muthuswamy L, Krasnitz A, McCombie WR, Hicks J, Wigler M. Tumour evolution inferred by single-cell sequencing. Nature. 2011 Apr 7;472(7341):90-4. PubMed PMID: 21399628. Pubmed Central PMCID: 4504184.

124. Klein CA. Parallel progression of primary tumours and metastases. Nature reviews Cancer. 2009 Apr;9(4):302-12. PubMed PMID: 19308069.

125. Hanrahan EO, Gonzalez-Angulo AM, Giordano SH, Rouzier R, Broglio KR, Hortobagyi GN, Valero V. Overall survival and cause-specific mortality of patients with stage T1a,bN0M0 breast carcinoma. Journal of clinical oncology : official journal of the American Society of Clinical Oncology. 2007 Nov 1;25(31):4952-60. PubMed PMID: 17971593.

126. Rosen PP, Groshen S, Saigo PE, Kinne DW, Hellman S. Pathological prognostic factors in stage I (T1N0M0) and stage II (T1N1M0) breast carcinoma: a study of 644 patients with median follow-up of 18 years. Journal of clinical oncology : official journal of the American Society of Clinical Oncology. 1989 Sep;7(9):1239-51. PubMed PMID: 2549203.

127. Haeno H, Gonen M, Davis MB, Herman JM, Iacobuzio-Donahue CA, Michor F. Computational modeling of pancreatic cancer reveals kinetics of metastasis suggesting optimum treatment strategies. Cell. 2012 Jan 20;148(1-2):362-75. PubMed PMID: 22265421. Pubmed Central PMCID: 3289413.

128. Rhim AD, Mirek ET, Aiello NM, Maitra A, Bailey JM, McAllister F, Reichert M, Beatty GL, Rustgi AK, Vonderheide RH, Leach SD, Stanger BZ. EMT and dissemination precede pancreatic tumor formation. Cell. 2012 Jan 20;148(1-2):349-61. PubMed PMID: 22265420. Pubmed Central PMCID: 3266542.

129. Varadhachary GR. Carcinoma of unknown primary origin. Gastrointestinal cancer research : GCR. 2007 Nov;1(6):229-35. PubMed PMID: 19262901. Pubmed Central PMCID: 2631214.

130. Talmadge JE. Clonal selection of metastasis within the life history of a tumor. Cancer research. 2007 Dec 15;67(24):11471-5. PubMed PMID: 18089772.

131. Ware JL, Lieberman AP, Webb KS. Metastatic phenotype of human prostate tumor cells in athymic nude mice: alteration by exposure to ethyl methanesulfonate and "reversion" by 5-azacytidine. Cancer immunology, immunotherapy : CII. 1986;21(1):58-62. PubMed PMID: 2417701.

132. Zhang L, Zhang S, Yao J, Lowery FJ, Zhang Q, Huang WC, Li P, Li M, Wang X, Zhang C, Wang H, Ellis K, Cheerathodi M, McCarty JH, Palmieri D, Saunus J, Lakhani S, Huang S, Sahin AA, Aldape KD, Steeg PS, Yu D. Microenvironment-induced PTEN loss by exosomal microRNA primes brain metastasis outgrowth. Nature. 2015 Nov 5;527(7576):100-4. PubMed PMID: 26479035.

133. Darwin C. On the origin of species by means of natural selection. London,: J. Murray; 1859. ix, 1 , 502 p. p.

134. Nowell PC. The clonal evolution of tumor cell populations. Science. 1976 Oct 1;194(4260):23-8. PubMed PMID: 959840.

135. Valster A, Tran NL, Nakada M, Berens ME, Chan AY, Symons M. Cell migration and invasion assays. Methods. 2005 Oct;37(2):208-15. PubMed PMID: 16288884.

136. Goodwin AM. In vitro assays of angiogenesis for assessment of angiogenic and anti-angiogenic agents. Microvascular research. 2007 Sep-Nov;74(2-3):172-83. PubMed PMID: 17631914. Pubmed Central PMCID: 2692317.

137. Hayden EC. Technology: The $1,000 genome. Nature. 2014 Mar 20;507(7492):294-5. PubMed PMID: 24646979.

138. Lawson DA, Bhakta NR, Kessenbrock K, Prummel KD, Yu Y, Takai K, Zhou A, Eyob H, Balakrishnan S, Wang CY, Yaswen P, Goga A, Werb Z. Single-cell analysis reveals a stem-cell program in human metastatic breast cancer cells. Nature. 2015 Oct 1;526(7571):131-5. PubMed PMID: 26416748. Pubmed Central PMCID: 4648562.

139. Robinson DR, Wu YM, Vats P, Su F, Lonigro RJ, Cao X, Kalyana-Sundaram S, Wang R, Ning Y, Hodges L, Gursky A, Siddiqui J, Tomlins SA, Roychowdhury S, Pienta KJ, Kim SY, Roberts JS, Rae JM, Van Poznak CH, Hayes DF, Chugh R, Kunju LP, Talpaz M, Schott AF, Chinnaiyan AM. Activating ESR1 mutations in hormone-resistant metastatic breast cancer. Nature genetics. 2013 Dec;45(12):1446-51. PubMed PMID: 24185510. Pubmed Central PMCID: 4009946.

140. Kobayashi S, Boggon TJ, Dayaram T, Janne PA, Kocher O, Meyerson M, Johnson BE, Eck MJ, Tenen DG, Halmos B. EGFR mutation and resistance of non-small-cell lung cancer to gefitinib. The New England journal of medicine. 2005 Feb 24;352(8):786-92. PubMed PMID: 15728811.

141. Gorre ME, Mohammed M, Ellwood K, Hsu N, Paquette R, Rao PN, Sawyers CL. Clinical resistance to STI-571 cancer therapy caused by BCR-ABL gene mutation or amplification. Science. 2001 Aug 3;293(5531):876-80. PubMed PMID: 11423618.

142. Wang TL, Diaz LA, Jr., Romans K, Bardelli A, Saha S, Galizia G, Choti M, Donehower R, Parmigiani G, Shih Ie M, Iacobuzio-Donahue C, Kinzler KW, Vogelstein B, Lengauer C, Velculescu VE. Digital karyotyping identifies thymidylate synthase amplification as a mechanism of resistance to 5-fluorouracil in metastatic colorectal cancer patients. Proceedings of the National Academy of Sciences of the United States of America. 2004 Mar 2;101(9):3089-94. PubMed PMID: 14970324. Pubmed Central PMCID: 420348.

143. Broxterman HJ, Pinedo HM, Kuiper CM, Kaptein LC, Schuurhuis GJ, Lankelma J. Induction by verapamil of a rapid increase in ATP consumption in multidrug-resistant tumor cells. FASEB journal : official publication of the Federation of American Societies for Experimental Biology. 1988 Apr;2(7):2278-82. PubMed PMID: 3350243.

144. Gatenby RA, Brown J, Vincent T. Lessons from applied ecology: cancer control using an evolutionary double bind. Cancer research. 2009 Oct 1;69(19):7499-502. PubMed PMID: 19752088.

145. Basanta D, Gatenby RA, Anderson AR. Exploiting evolution to treat drug resistance: combination therapy and the double bind. Molecular pharmaceutics. 2012 Apr 2;9(4):914-21. PubMed PMID: 22369188. Pubmed Central PMCID: 3325107.

146. Enriquez-Navas PM, Wojtkowiak JW, Gatenby RA. Application of Evolutionary Principles to Cancer Therapy. Cancer research. 2015 Nov 15;75(22):4675-80. PubMed PMID: 26527288. Pubmed Central PMCID: 4693617.

147. Davis FG, Dolecek TA, McCarthy BJ, Villano JL. Toward determining the lifetime occurrence of metastatic brain tumors estimated from 2007 United States cancer incidence data. Neuro-oncology. 2012 Sep;14(9):1171-7. PubMed PMID: 22898372. Pubmed Central PMCID: 3424213.

148. Nathoo N, Chahlavi A, Barnett GH, Toms SA. Pathobiology of brain metastases. Journal of clinical pathology. 2005 Mar;58(3):237-42. PubMed PMID: 15735152. Pubmed Central PMCID: 1770599.

149. Nayak L, Lee EQ, Wen PY. Epidemiology of brain metastases. Current oncology reports. 2012 Feb;14(1):48-54. PubMed PMID: 22012633.

150. Fink KR, Fink JR. Imaging of brain metastases. Surgical neurology international. 2013;4(Suppl 4):S209-19. PubMed PMID: 23717792. Pubmed Central PMCID: 3656556.

151. Patchell RA. The management of brain metastases. Cancer treatment reviews. 2003 Dec;29(6):533-40. PubMed PMID: 14585263.

152. Markesbery WR, Brooks WH, Gupta GD, Young AB. Treatment for patients with cerebral metastases. Archives of neurology. 1978 Nov;35(11):754-6. PubMed PMID: 718475.

153. Freilich RJ, Seidman AD, DeAngelis LM. Central nervous system progression of metastatic breast cancer in patients treated with paclitaxel. Cancer. 1995 Jul 15;76(2):232-6. PubMed PMID: 8625097.

154. Patchell RA, Tibbs PA, Regine WF, Dempsey RJ, Mohiuddin M, Kryscio RJ, Markesbery WR, Foon KA, Young B. Postoperative radiotherapy in the treatment of single metastases to the brain: a randomized trial. Jama. 1998 Nov 4;280(17):1485-9. PubMed PMID: 9809728.

155. Ammannagari N, Ahmed S, Patel A, Bravin EN. Radiological response of brain metastases to novel tyrosine kinase inhibitor lapatinib. QJM : monthly journal of the Association of Physicians. 2013 Sep;106(9):869-70. PubMed PMID: 23596263.

156. Peak S, Abrey LE. Chemotherapy and the treatment of brain metastases. Hematology/oncology clinics of North America. 2006 Dec;20(6):1287-95. PubMed PMID: 17113463.

157. Fabi A, Felici A, Metro G, Mirri A, Bria E, Telera S, Moscetti L, Russillo M, Lanzetta G, Mansueto G, Pace A, Maschio M, Vidiri A, Sperduti I, Cognetti F, Carapella CM. Brain

metastases from solid tumors: disease outcome according to type of treatment and therapeutic resources of the treating center. Journal of experimental & clinical cancer research : CR. 2011;30:10. PubMed PMID: 21244695. Pubmed Central PMCID: 3033846.

158. Lin NU. Targeted therapies in brain metastases. Current treatment options in neurology. 2014 Jan;16(1):276. PubMed PMID: 24353011. Pubmed Central PMCID: 3895218.

159. Fokas E, Steinbach JP, Rodel C. Biology of brain metastases and novel targeted therapies: time to translate the research. Biochimica et biophysica acta. 2013 Jan;1835(1):61-75. PubMed PMID: 23142311.

160. Steeg PS, Camphausen KA, Smith QR. Brain metastases as preventive and therapeutic targets. Nature reviews Cancer. 2011 May;11(5):352-63. PubMed PMID: 21472002.

161. Abbott NJ. Dynamics of CNS barriers: evolution, differentiation, and modulation. Cellular and molecular neurobiology. 2005 Feb;25(1):5-23. PubMed PMID: 15962506.

162. Wolburg H, Lippoldt A. Tight junctions of the blood-brain barrier: development, composition and regulation. Vascular pharmacology. 2002 Jun;38(6):323-37. PubMed PMID: 12529927.

163. Butt AM, Jones HC, Abbott NJ. Electrical resistance across the blood-brain barrier in anaesthetized rats: a developmental study. The Journal of physiology. 1990 Oct;429:47-62. PubMed PMID: 2277354. Pubmed Central PMCID: 1181686.

164. Fakhrejahani E, Toi M. Tumor angiogenesis: pericytes and maturation are not to be ignored. Journal of oncology. 2012;2012:261750. PubMed PMID: 22007214. Pubmed Central PMCID: 3191787.

165. Cabezas R, Avila M, Gonzalez J, El-Bacha RS, Baez E, Garcia-Segura LM, Jurado Coronel JC, Capani F, Cardona-Gomez GP, Barreto GE. Astrocytic modulation of blood brain

barrier: perspectives on Parkinson's disease. Frontiers in cellular neuroscience. 2014;8:211. PubMed PMID: 25136294. Pubmed Central PMCID: 4120694.

166. Carreau A, El Hafny-Rahbi B, Matejuk A, Grillon C, Kieda C. Why is the partial oxygen pressure of human tissues a crucial parameter? Small molecules and hypoxia. Journal of cellular and molecular medicine. 2011 Jun;15(6):1239-53. PubMed PMID: 21251211. Pubmed Central PMCID: 4373326.

167. Smith QR. Transport of glutamate and other amino acids at the blood-brain barrier. The Journal of nutrition. 2000 Apr;130(4S Suppl):1016S-22S. PubMed PMID: 10736373.

168. Strell C, Entschladen F. Extravasation of leukocytes in comparison to tumor cells. Cell communication and signaling : CCS. 2008;6:10. PubMed PMID: 19055814. Pubmed Central PMCID: 2627905.

169. Feng S, Cen J, Huang Y, Shen H, Yao L, Wang Y, Chen Z. Matrix metalloproteinase-2 and -9 secreted by leukemic cells increase the permeability of blood-brain barrier by disrupting tight junction proteins. PloS one. 2011;6(8):e20599. PubMed PMID: 21857898. Pubmed Central PMCID: 3157343.

170. Stamatovic SM, Keep RF, Andjelkovic AV. Brain endothelial cell-cell junctions: how to "open" the blood brain barrier. Current neuropharmacology. 2008 Sep;6(3):179-92. PubMed PMID: 19506719. Pubmed Central PMCID: 2687937.

171. Sevenich L, Joyce JA. Pericellular proteolysis in cancer. Genes & development. 2014 Nov 1;28(21):2331-47. PubMed PMID: 25367033. Pubmed Central PMCID: 4215179.

172. Huchzermeyer C, Berndt N, Holzhutter HG, Kann O. Oxygen consumption rates during three different neuronal activity states in the hippocampal CA3 network. Journal of cerebral blood flow and metabolism : official journal of the International Society of Cerebral Blood Flow and Metabolism. 2013 Feb;33(2):263-71. PubMed PMID: 23168532. Pubmed Central PMCID: 3564197.

173. Lockman PR, Mittapalli RK, Taskar KS, Rudraraju V, Gril B, Bohn KA, Adkins CE, Roberts A, Thorsheim HR, Gaasch JA, Huang S, Palmieri D, Steeg PS, Smith QR. Heterogeneous blood-tumor barrier permeability determines drug efficacy in experimental brain metastases of breast cancer. Clinical cancer research : an official journal of the American Association for Cancer Research. 2010 Dec 1;16(23):5664-78. PubMed PMID: 20829328. Pubmed Central PMCID: 2999649.

174. Schackert G, Simmons RD, Buzbee TM, Hume DA, Fidler IJ. Macrophage infiltration into experimental brain metastases: occurrence through an intact blood-brain barrier. Journal of the National Cancer Institute. 1988 Sep 7;80(13):1027-34. PubMed PMID: 3261801.

175. Zhang RD, Price JE, Fujimaki T, Bucana CD, Fidler IJ. Differential permeability of the blood-brain barrier in experimental brain metastases produced by human neoplasms implanted into nude mice. The American journal of pathology. 1992 Nov;141(5):1115-24. PubMed PMID: 1443046. Pubmed Central PMCID: 1886664.

176. Carbonell WS, Ansorge O, Sibson N, Muschel R. The vascular basement membrane as "soil" in brain metastasis. PloS one. 2009;4(6):e5857. PubMed PMID: 19516901. Pubmed Central PMCID: 2689678.

177. Jacus MO, Daryani VM, Harstead KE, Patel YT, Throm SL, Stewart CF. Pharmacokinetic Properties of Anticancer Agents for the Treatment of Central Nervous System Tumors: Update of the Literature. Clinical pharmacokinetics. 2016 Mar;55(3):297-311. PubMed PMID: 26293618. Pubmed Central PMCID: 4761278.

178. Gee JR, Keller JN. Astrocytes: regulation of brain homeostasis via apolipoprotein E. The international journal of biochemistry & cell biology. 2005 Jun;37(6):1145-50. PubMed PMID: 15778078.

179. Abbott NJ, Ronnback L, Hansson E. Astrocyte-endothelial interactions at the blood-brain barrier. Nature reviews Neuroscience. 2006 Jan;7(1):41-53. PubMed PMID: 16371949.

180. Pellerin L, Pellegri G, Bittar PG, Charnay Y, Bouras C, Martin JL, Stella N, Magistretti PJ. Evidence supporting the existence of an activity-dependent astrocyte-neuron lactate shuttle. Developmental neuroscience. 1998;20(4-5):291-9. PubMed PMID: 9778565.

181. Valiente M, Obenauf AC, Jin X, Chen Q, Zhang XH, Lee DJ, Chaft JE, Kris MG, Huse JT, Brogi E, Massague J. Serpins promote cancer cell survival and vascular co-option in brain metastasis. Cell. 2014 Feb 27;156(5):1002-16. PubMed PMID: 24581498. Pubmed Central PMCID: 3988473.

182. Kim SJ, Kim JS, Park ES, Lee JS, Lin Q, Langley RR, Maya M, He J, Kim SW, Weihua Z, Balasubramanian K, Fan D, Mills GB, Hung MC, Fidler IJ. Astrocytes upregulate survival genes in tumor cells and induce protection from chemotherapy. Neoplasia. 2011 Mar;13(3):286-98. PubMed PMID: 21390191. Pubmed Central PMCID: 3050871.

183. Lee HJ, Hanibuchi M, Kim SJ, Yu H, Kim MS, He J, Langley RR, Lehembre F, Regenass U, Fidler IJ. Treatment of experimental human breast cancer and lung cancer brain metastases in mice by macitentan, a dual antagonist of endothelin receptors, combined with paclitaxel. Neuro-oncology. 2016 Apr;18(4):486-96. PubMed PMID: 26995790. Pubmed Central PMCID: 4799693.

184. Xing F, Kobayashi A, Okuda H, Watabe M, Pai SK, Pandey PR, Hirota S, Wilber A, Mo YY, Moore BE, Liu W, Fukuda K, Iiizumi M, Sharma S, Liu Y, Wu K, Peralta E, Watabe K. Reactive astrocytes promote the metastatic growth of breast cancer stem-like cells by activating Notch signalling in brain. EMBO molecular medicine. 2013 Mar;5(3):384-96. PubMed PMID: 23495140. Pubmed Central PMCID: 3598079.

185. Neman J, Choy C, Kowolik CM, Anderson A, Duenas VJ, Waliany S, Chen BT, Chen MY, Jandial R. Co-evolution of breast-to-brain metastasis and neural progenitor cells. Clinical & experimental metastasis. 2013 Aug;30(6):753-68. PubMed PMID: 23456474. Pubmed Central PMCID: 3808473.

186. Pardridge WM. Brain metabolism: a perspective from the blood-brain barrier. Physiological reviews. 1983 Oct;63(4):1481-535. PubMed PMID: 6361813.

187. Raichle ME, Gusnard DA. Appraising the brain's energy budget. Proceedings of the National Academy of Sciences of the United States of America. 2002 Aug 6;99(16):10237-9. PubMed PMID: 12149485. Pubmed Central PMCID: 124895.

188. Huang Z, Zuo C, Guan Y, Zhang Z, Liu P, Xue F, Lin X. Misdiagnoses of 11C-choline combined with 18F-FDG PET imaging in brain tumours. Nuclear medicine communications. 2008 Apr;29(4):354-8. PubMed PMID: 18317300.

189. Simpson IA, Carruthers A, Vannucci SJ. Supply and demand in cerebral energy metabolism: the role of nutrient transporters. Journal of cerebral blood flow and metabolism : official journal of the International Society of Cerebral Blood Flow and Metabolism. 2007 Nov;27(11):1766-91. PubMed PMID: 17579656. Pubmed Central PMCID: 2094104.

190. Mergenthaler P, Lindauer U, Dienel GA, Meisel A. Sugar for the brain: the role of glucose in physiological and pathological brain function. Trends in neurosciences. 2013 Oct;36(10):587-97. PubMed PMID: 23968694. Pubmed Central PMCID: 3900881.

191. Palmieri D, Fitzgerald D, Shreeve SM, Hua E, Bronder JL, Weil RJ, Davis S, Stark AM, Merino MJ, Kurek R, Mehdorn HM, Davis G, Steinberg SM, Meltzer PS, Aldape K, Steeg PS. Analyses of resected human brain metastases of breast cancer reveal the association between up-regulation of hexokinase 2 and poor prognosis. Molecular cancer research : MCR. 2009 Sep;7(9):1438-45. PubMed PMID: 19723875. Pubmed Central PMCID: 2746883.

192. Chen EI, Hewel J, Krueger JS, Tiraby C, Weber MR, Kralli A, Becker K, Yates JR, 3rd, Felding-Habermann B. Adaptation of energy metabolism in breast cancer brain metastases. Cancer research. 2007 Feb 15;67(4):1472-86. PubMed PMID: 17308085.

193. O'Kane RL, Hawkins RA. Na+-dependent transport of large neutral amino acids occurs at the abluminal membrane of the blood-brain barrier. American journal of physiology Endocrinology and metabolism. 2003 Dec;285(6):E1167-73. PubMed PMID: 12933350.

194. Basun H, Forssell LG, Almkvist O, Cowburn RF, Eklof R, Winblad B, Wetterberg L. Amino-Acid-Concentrations in Cerebrospinal-Fluid and Plasma in Alzheimers-Disease and Healthy Control Subjects. J Neural Transm-Park. 1990;2(4):295-304. PubMed PMID: WOS:A1990EQ73400006. English.

195. Seidlitz EP, Sharma MK, Saikali Z, Ghert M, Singh G. Cancer cell lines release glutamate into the extracellular environment. Clinical & experimental metastasis. 2009;26(7):781-7. PubMed PMID: 19526315.

196. Carrascosa JM, Martinez P, Nunez de Castro I. Nitrogen movement between host and tumor in mice inoculated with Ehrlich ascitic tumor cells. Cancer research. 1984 Sep;44(9):3831-5. PubMed PMID: 6146402.

197. Takano T, Lin JH, Arcuino G, Gao Q, Yang J, Nedergaard M. Glutamate release promotes growth of malignant gliomas. Nature medicine. 2001 Sep;7(9):1010-5. PubMed PMID: 11533703.

198. Ye ZC, Sontheimer H. Glioma cells release excitotoxic concentrations of glutamate. Cancer research. 1999 Sep 1;59(17):4383-91. PubMed PMID: 10485487.

199. Venneti S, Dunphy MP, Zhang H, Pitter KL, Zanzonico P, Campos C, Carlin SD, La Rocca G, Lyashchenko S, Ploessl K, Rohle D, Omuro AM, Cross JR, Brennan CW, Weber WA, Holland EC, Mellinghoff IK, Kung HF, Lewis JS, Thompson CB. Glutamine-based PET imaging facilitates enhanced metabolic evaluation of gliomas in vivo. Science translational medicine. 2015 Feb 11;7(274):274ra17. PubMed PMID: 25673762. Pubmed Central PMCID: 4431550.

200. Chen J, Lee HJ, Wu X, Huo L, Kim SJ, Xu L, Wang Y, He J, Bollu LR, Gao G, Su F, Briggs J, Liu X, Melman T, Asara JM, Fidler IJ, Cantley LC, Locasale JW, Weihua Z. Gain of glucose-independent growth upon metastasis of breast cancer cells to the brain. Cancer research. 2015 Feb 1;75(3):554-65. PubMed PMID: 25511375. Pubmed Central PMCID: 4315743.

201. Wise DR, Thompson CB. Glutamine addiction: a new therapeutic target in cancer. Trends in biochemical sciences. 2010 Aug;35(8):427-33. PubMed PMID: 20570523. Pubmed Central PMCID: 2917518.

202. Tardito S, Oudin A, Ahmed SU, Fack F, Keunen O, Zheng L, Miletic H, Sakariassen PO, Weinstock A, Wagner A, Lindsay SL, Hock AK, Barnett SC, Ruppin E, Morkve SH, Lund-Johansen M, Chalmers AJ, Bjerkvig R, Niclou SP, Gottlieb E. Glutamine synthetase activity fuels nucleotide biosynthesis and supports growth of glutamine-restricted glioblastoma. Nature cell biology. 2015 Dec;17(12):1556-68. PubMed PMID: 26595383. Pubmed Central PMCID: 4663685.

203. Boehm JS, Zhao JJ, Yao J, Kim SY, Firestein R, Dunn IF, Sjostrom SK, Garraway LA, Weremowicz S, Richardson AL, Greulich H, Stewart CJ, Mulvey LA, Shen RR, Ambrogio L, Hirozane-Kishikawa T, Hill DE, Vidal M, Meyerson M, Grenier JK, Hinkle G, Root DE, Roberts TM, Lander ES, Polyak K, Hahn WC. Integrative genomic approaches identify IKBKE as a breast cancer oncogene. Cell. 2007 Jun 15;129(6):1065-79. PubMed PMID: 17574021.

204. Pear WS, Nolan GP, Scott ML, Baltimore D. Production of high-titer helper-free retroviruses by transient transfection. Proceedings of the National Academy of Sciences of the United States of America. 1993 Sep 15;90(18):8392-6. PubMed PMID: 7690960. Pubmed Central PMCID: 47362.

205. Saunus JM, Quinn MC, Patch AM, Pearson JV, Bailey PJ, Nones K, McCart Reed AE, Miller D, Wilson PJ, Al-Ejeh F, Mariasegaram M, Lau Q, Withers T, Jeffree RL, Reid LE, Da Silva L, Matsika A, Niland CM, Cummings MC, Bruxner TJ, Christ AN, Harliwong I, Idrisoglu S, Manning S, Nourse C, Nourbakhsh E, Wani S, Anderson MJ, Fink JL, Holmes O, Kazakoff S, Leonard C, Newell F, Taylor D, Waddell N, Wood S, Xu Q, Kassahn KS, Narayanan V, Taib NA, Teo SH, Chow YP, kConFab, Jat PS, Brandner S, Flanagan AM, Khanna KK, Chenevix-Trench G, Grimmond SM, Simpson PT, Waddell N, Lakhani SR. Integrated genomic and transcriptomic analysis of human brain metastases identifies alterations of

potential clinical significance. The Journal of pathology. 2015 Nov;237(3):363-78. PubMed PMID: 26172396.

206. Xia Y, Song X, Li D, Ye T, Xu Y, Lin H, Meng N, Li G, Deng S, Zhang S, Liu L, Zhu Y, Zeng J, Lei Q, Pan Y, Wei Y, Zhao Y, Yu L. YLT192, a novel, orally active bioavailable inhibitor of VEGFR2 signaling with potent antiangiogenic activity and antitumor efficacy in preclinical models. Scientific reports. 2014;4:6031. PubMed PMID: 25112436. Pubmed Central PMCID: 4129416.

207. Shaner NC, Campbell RE, Steinbach PA, Giepmans BN, Palmer AE, Tsien RY. Improved monomeric red, orange and yellow fluorescent proteins derived from Discosoma sp. red fluorescent protein. Nature biotechnology. 2004 Dec;22(12):1567-72. PubMed PMID: 15558047.

208. Saldana SM, Lee HH, Lowery FJ, Khotskaya YB, Xia W, Zhang C, Chang SS, Chou CK, Steeg PS, Yu D, Hung MC. Inhibition of type I insulin-like growth factor receptor signaling attenuates the development of breast cancer brain metastasis. PloS one. 2013;8(9):e73406. PubMed PMID: 24039934. Pubmed Central PMCID: 3764163.

209. Guo L, Fan D, Zhang F, Price JE, Lee JS, Marchetti D, Fidler IJ, Langley RR. Selection of brain metastasis-initiating breast cancer cells determined by growth on hard agar. The American journal of pathology. 2011 May;178(5):2357-66. PubMed PMID: 21514446. Pubmed Central PMCID: 3081177.

210. Okuda T, Cleveland JL, Downing JR. PCTAIRE-1 and PCTAIRE-3, two members of a novel cdc2/CDC28-related protein kinase gene family. Oncogene. 1992 Nov;7(11):2249-58. PubMed PMID: 1437147.

211. Mikolcevic P, Sigl R, Rauch V, Hess MW, Pfaller K, Barisic M, Pelliniemi LJ, Boesl M, Geley S. Cyclin-dependent kinase 16/PCTAIRE kinase 1 is activated by cyclin Y and is essential for spermatogenesis. Molecular and cellular biology. 2012 Feb;32(4):868-79. PubMed PMID: 22184064. Pubmed Central PMCID: 3272973.

212. Graeser R, Gannon J, Poon RY, Dubois T, Aitken A, Hunt T. Regulation of the CDK-related protein kinase PCTAIRE-1 and its possible role in neurite outgrowth in Neuro-2A cells. Journal of cell science. 2002 Sep 1;115(Pt 17):3479-90. PubMed PMID: 12154078.

213. Cheng K, Li Z, Fu WY, Wang JH, Fu AK, Ip NY. Pctaire1 interacts with p35 and is a novel substrate for Cdk5/p35. The Journal of biological chemistry. 2002 Aug 30;277(35):31988-93. PubMed PMID: 12084709.

214. Fu WY, Cheng K, Fu AK, Ip NY. Cyclin-dependent kinase 5-dependent phosphorylation of Pctaire1 regulates dendrite development. Neuroscience. 2011 Apr 28;180:353-9. PubMed PMID: 21335063.

215. Liu Y, Cheng K, Gong K, Fu AK, Ip NY. Pctaire1 phosphorylates N-ethylmaleimide-sensitive fusion protein: implications in the regulation of its hexamerization and exocytosis. The Journal of biological chemistry. 2006 Apr 14;281(15):9852-8. PubMed PMID: 16461345.

216. Iwano S, Satou A, Matsumura S, Sugiyama N, Ishihama Y, Toyoshima F. PCTK1 regulates integrin-dependent spindle orientation via protein kinase A regulatory subunit KAP0 and myosin X. Molecular and cellular biology. 2015 Apr;35(7):1197-208. PubMed PMID: 25605337. Pubmed Central PMCID: 4355539.

217. Shehata SN, Deak M, Morrice NA, Ohta E, Hunter RW, Kalscheuer VM, Sakamoto K. Cyclin Y phosphorylation- and 14-3-3-binding-dependent activation of PCTAIRE-1/CDK16. The Biochemical journal. 2015 Aug 1;469(3):409-20. PubMed PMID: 26205494. Pubmed Central PMCID: 4613515.

218. Shehata SN, Hunter RW, Ohta E, Peggie MW, Lou HJ, Sicheri F, Zeqiraj E, Turk BE, Sakamoto K. Analysis of substrate specificity and cyclin Y binding of PCTAIRE-1 kinase. Cellular signalling. 2012 Nov;24(11):2085-94. PubMed PMID: 22796189. Pubmed Central PMCID: 3590450.

219. Zi Z, Zhang Z, Li Q, An W, Zeng L, Gao D, Yang Y, Zhu X, Zeng R, Shum WW, Wu J. CCNYL1, but Not CCNY, Cooperates with CDK16 to Regulate Spermatogenesis in Mouse.

PLoS genetics. 2015 Aug;11(8):e1005485. PubMed PMID: 26305884. Pubmed Central PMCID: 4549061.

220. Yanagi T, Shi R, Aza-Blanc P, Reed JC, Matsuzawa S. PCTAIRE1-knockdown sensitizes cancer cells to TNF family cytokines. PloS one. 2015;10(3):e0119404. PubMed PMID: 25790448. Pubmed Central PMCID: 4366397.

221. Yanagi T, Krajewska M, Matsuzawa S, Reed JC. PCTAIRE1 phosphorylates p27 and regulates mitosis in cancer cells. Cancer research. 2014 Oct 15;74(20):5795-807. PubMed PMID: 25205104. Pubmed Central PMCID: 4199897.

222. Eagle H. Nutrition needs of mammalian cells in tissue culture. Science. 1955 Sep 16;122(3168):501-14. PubMed PMID: 13255879.

223. Eagle H. Amino acid metabolism in mammalian cell cultures. Science. 1959 Aug 21;130(3373):432-7. PubMed PMID: 13675766.

224. Morton CL, Houghton PJ. Establishment of human tumor xenografts in immunodeficient mice. Nature protocols. 2007;2(2):247-50. PubMed PMID: 17406581.

225. Warburg O. On the origin of cancer cells. Science. 1956 Feb 24;123(3191):309-14. PubMed PMID: 13298683.

226. Ben-Haim S, Ell P. 18F-FDG PET and PET/CT in the evaluation of cancer treatment response. Journal of nuclear medicine : official publication, Society of Nuclear Medicine. 2009 Jan;50(1):88-99. PubMed PMID: 19139187.

227. Vander Heiden MG, Cantley LC, Thompson CB. Understanding the Warburg effect: the metabolic requirements of cell proliferation. Science. 2009 May 22;324(5930):1029-33. PubMed PMID: 19460998. Pubmed Central PMCID: 2849637.

228. Fellin T, Sul JY, D'Ascenzo M, Takano H, Pascual O, Haydon PG. Bidirectional astrocyte-neuron communication: the many roles of glutamate and ATP. Novartis Foundation symposium. 2006;276:208-17; discussion 17-21, 33-7, 75-81. PubMed PMID: 16805432.

229. Xia Z, Dudek H, Miranti CK, Greenberg ME. Calcium influx via the NMDA receptor induces immediate early gene transcription by a MAP kinase/ERK-dependent mechanism. The Journal of neuroscience : the official journal of the Society for Neuroscience. 1996 Sep 1;16(17):5425-36. PubMed PMID: 8757255.

230. Ivannikov MV, Macleod GT. Mitochondrial free Ca(2)(+) levels and their effects on energy metabolism in Drosophila motor nerve terminals. Biophysical journal. 2013 Jun 4;104(11):2353-61. PubMed PMID: 23746507. Pubmed Central PMCID: 3672877.

231. Ivannikov MV, Sugimori M, Llinas RR. Synaptic vesicle exocytosis in hippocampal synaptosomes correlates directly with total mitochondrial volume. Journal of molecular neuroscience : MN. 2013 Jan;49(1):223-30. PubMed PMID: 22772899. Pubmed Central PMCID: 3488359.

232. Lecrone V, Li W, Devoll RE, Logothetis C, Farach-Carson MC. Calcium signals in prostate cancer cells: specific activation by bone-matrix proteins. Cell calcium. 2000 Jan;27(1):35-42. PubMed PMID: 10726209.

233. Agle KA, Vongsa RA, Dwinell MB. Calcium mobilization triggered by the chemokine CXCL12 regulates migration in wounded intestinal epithelial monolayers. The Journal of biological chemistry. 2010 May 21;285(21):16066-75. PubMed PMID: 20348095. Pubmed Central PMCID: 2871475.

234. Lin Q, Balasubramanian K, Fan D, Kim SJ, Guo L, Wang H, Bar-Eli M, Aldape KD, Fidler IJ. Reactive astrocytes protect melanoma cells from chemotherapy by sequestering intracellular calcium through gap junction communication channels. Neoplasia. 2010 Sep;12(9):748-54. PubMed PMID: 20824051. Pubmed Central PMCID: 2933695.

235. Neman J, Termini J, Wilczynski S, Vaidehi N, Choy C, Kowolik CM, Li H, Hambrecht AC, Roberts E, Jandial R. Human breast cancer metastases to the brain display GABAergic properties in the neural niche. Proceedings of the National Academy of Sciences of the

United States of America. 2014 Jan 21;111(3):984-9. PubMed PMID: 24395782. Pubmed Central PMCID: 3903266.

236. Shimizu K, Uematsu A, Imai Y, Sawasaki T. Pctaire1/Cdk16 promotes skeletal myogenesis by inducing myoblast migration and fusion. FEBS letters. 2014 Aug 25;588(17):3030-7. PubMed PMID: 24931367.

237. Mokalled MH, Johnson A, Kim Y, Oh J, Olson EN. Myocardin-related transcription factors regulate the Cdk5/Pctaire1 kinase cascade to control neurite outgrowth, neuronal migration and brain development. Development. 2010 Jul;137(14):2365-74. PubMed PMID: 20534669. Pubmed Central PMCID: 2889604.

238. Kleinman HK, Martin GR. Matrigel: basement membrane matrix with biological activity. Seminars in cancer biology. 2005 Oct;15(5):378-86. PubMed PMID: 15975825.

239. Ma CX, Cai S, Li S, Ryan CE, Guo Z, Schaiff WT, Lin L, Hoog J, Goiffon RJ, Prat A, Aft RL, Ellis MJ, Piwnica-Worms H. Targeting Chk1 in p53-deficient triple-negative breast cancer is therapeutically beneficial in human-in-mouse tumor models. The Journal of clinical investigation. 2012 Apr;122(4):1541-52. PubMed PMID: 22446188. Pubmed Central PMCID: 3314455.

240. Machein MR, Kullmer J, Fiebich BL, Plate KH, Warnke PC. Vascular endothelial growth factor expression, vascular volume, and, capillary permeability in human brain tumors. Neurosurgery. 1999 Apr;44(4):732-40; discussion 40-1. PubMed PMID: 10201297.

241. Dhermain FG, Hau P, Lanfermann H, Jacobs AH, van den Bent MJ. Advanced MRI and PET imaging for assessment of treatment response in patients with gliomas. The Lancet Neurology. 2010 Sep;9(9):906-20. PubMed PMID: 20705518.

242. De Pitta M, Volman V, Berry H, Ben-Jacob E. A tale of two stories: astrocyte regulation of synaptic depression and facilitation. PLoS computational biology. 2011 Dec;7(12):e1002293. PubMed PMID: 22162957. Pubmed Central PMCID: 3228793.

243. Brosnan JT. Interorgan amino acid transport and its regulation. The Journal of nutrition. 2003 Jun;133(6 Suppl 1):2068S-72S. PubMed PMID: 12771367.

Vitae

Frank Joseph Lowery III was born in Honolulu, HI on October 16, 1987, the son of the late Michele Marie Lowery and Frank Joseph Michael Lowery. After graduating from St. Bernard High School in Uncasville, CT in 2005, he enrolled at Duke University in Durham, NC. He graduated from Duke in May 2009 with a Bachelor's of Science in Biology, with a concentration in Pharmacology, minoring in History and Chemistry. In September of 2009 he entered The University of Texas Graduate School of Biomedical Sciences at Houston.

Permanent address:

2925 Beaverwood Lane

Silver Spring, MD 20906